Functional Characterisation of the Centrosomal Protein Cep170

Dissertation

zur Erlangung des Doktorgrades der Naturwissenschaften

der Fakultät für Biologie der Ludwig-Maximilians-Universität

München

Vorgelegt von

Stefan Lamla

München, 2008

Dissertation eingereicht am:
03. November 2008

Tag der mündlichen Prüfung:
22. Januar 2009

Erstgutachter: Prof. E.A. Nigg
Zweitgutachter: PD Dr. A. Böttger

Hiermit erkläre ich, dass ich die vorliegende Dissertation selbständig und ohne unerlaubte Hilfe angefertigt habe. Sämtliche Experimente wurden von mir selbst durchgeführt, soweit nicht explizit auf Dritte verwiesen wird. Ich habe weder an anderer Stelle versucht eine Dissertation oder Teile einer solchen einzureichen bzw. einer Prüfungskommission vorzulegen, noch eine Doktorprüfung zu absolvieren.

München, den

1 Zusammenfassung

Zentrosomen erfüllen zwei Funktionen: 1) Sie organisieren die Mikrotubuli (MT) und 2) sie stellen eine Vorlage für den Bau primärer Zilien (PZ) zu Verfügung. Zentrosomen bestehen aus zwei Zentriolen, der Mutter- und Tochterzentriole. Die Mutterzentriole ist durch subdistale und distale Anhängsel charakterisiert, die für die Erfüllung beider Funktionen benötigt werden.

Die Verankerung der MT wird von dem subdistalen Anhängselprotein Ninein vermittelt. Es war jedoch unbekannt, ob Ninein alleine oder im Verbund mit anderen Proteinen zusammen wirkt. Hier konnten wir zeigen, dass Ninein mit Cep170 interagiert, und dass Cep170 an MT bindet. Verminderung der Konzentration oder Fehllokalisation von Cep170 verursachte Defekte bei der Verankerung der MT. Zusätzlich bündelte Cep170 die MT in der Zelle, wodurch sie stabiler als ungebündelte MT wurden. Daraus folgt, dass Cep170 ein Schlüsselprotein für die Verankerung der MT an den subdistalen Anhängsel der Mutterzentriole ist. Zusätzlich fanden wir heraus, dass die Lokalisation von Cep170 in der Mitose durch die Kinase Cdk1-Zyklin B reguliert wird. Die Phosphorylierung von Cep170 führt zu dessen Freisetzung von den subdistalen Anhängsel und ermöglicht vielleicht dadurch die Bildung der mitotischen Spindel, die durch wenig fest verankerte MT charakterisiert ist.

Im zweiten Teil der Doktorarbeit, beschreiben wir die Entdeckung zweier neuer Interaktoren von Cep170, IFT81 und PRAX-1. IFT81 ist eine wichtige strukturelle Komponente der intraflagellaren Transportpartikel (IFT-Partikel). IFT ermöglicht sowohl den Aufbau, als auch den Abbau des PZ, indem IFT-Partikel Proteine innerhalb des PZ transportieren. Hier zeigten wir, dass IFT81 ein Anhänselprotein der Mutterzentriole ist, welches hierfür mit Cep170 interagiert. Verminderung der IFT81 Proteinkonzentration durch siRNA behinderte den Aufbau der PZ. Überraschenderweise inhibierte die Verminderung der Cep170 Konzentration nur den Abbau des PZ. Dies lässt sich dadurch erklären, dass Cep170 IFT81 während des PZ Abbaus zurück zu den Anhängsel bringt. Dadurch wird der IFT stark verlangsamt, wodurch das PZ destabilisiert wird. Deshalb ist Cep170 auch ein Schlüsselprotein bei der Regulation des Abbaus des PZ.

2 Summary

Centrosomes have to main functions: 1) They organise the microtubules (MTs) and 2) they also provide a template for the formation of the primary cilium (PC). Centrosomes consist of two centrioles, the mother and the daughter centriole. The mother centriole is characterised by subdistal and distal appendages which are required for both functions of the centrosome.

Anchoring of MTs is mediated by the subdistal appendage protein Ninein. However, it was unknown whether Ninein acts alone or in association with other proteins. Here we demonstrated that Ninein interacts with Cep170 and that Cep170 binds MTs. Depletion or mislocalisation of Cep170 caused MT anchoring defects. Conversely, Cep170 bundled MT within the cell which kept them more stable than unbundled MT. Thus, Cep170 is a key protein for the anchoring of MTs at the subdistal appendages of the mother centriole. Additionally we found that, localisation of Cep170 is regulated by the kinase Cdk1-cyclin B during mitosis. Phosphorylation of Cep170 lead to its release from the subdistal appendages and may allow the formation of the mitotic spindle, which is characterised by less strongly anchored MTs.

In the second part of this thesis, we describe the discovery of two new interactors of Cep170, IFT81 and PRAX-1. IFT81 is an important structural component of the intraflagellar transport (IFT) particles. IFT allows the formation and the diasassembly of the PC through transporting different precursors within the PC. Here we demonstrated that IFT81 is an appendage protein of the mother centriole which therefore interacts with Cep170. Depletion of IFT81 by siRNA impaired PC formation. Somewhat surprisingly, depletion of Cep170 only supressed PZ disassembly and not the formation. We thus propose that Cep170 retargets IFT81 back to the appendages during PC disassembly, resulting in a slowdown of IFT which then destabilises the PC. So, Cep170 is also a key protein for the regulation of PC disassembly.

3 Introduction

3.1 The centrosome

Since the discovery of the centrosome by Boveri over a century ago, cell biologist are still fascinated by its structure and function. The centrosome is a tiny organelle in close proximity to the nucleus. It organises the MTs and, when cells enter G0, the primary cilium (PC). Deregulation of centriole duplication can be found in several cancers (Carroll et al. 1999; Nigg 2002) and defects in ciliogenesis cause kidney diseases, infertility and developmental disorders (Bisgrove and Yost 2006; Fliegauf et al. 2007; Marshall 2008).

MT nucleation activity of the centrosome is relatively well understood (Zheng et al. 1991; Job et al. 2003). However, centrosomes further organise MT by anchoring and bundling them to allow the formation of a radial MT array (Dammermann et al. 2003). The mechanisms underlying MT anchoring and bundling remain to be elucidated.

The role of the centrosome in ciliogenesis has gained renewed interest, because recent findings highlightened the importance of this organelle in several diseases. The PC was long considered as rudimentary, in spite of its presence on almost every cell in the human body. However, recently it became more and more clear that cilia control signalling pathways that are critical in development (Singla and Reiter 2006; Ainsworth 2007).

Below the structure and the function of centrosomes will be reviewed. I will focus on MT anchoring and bundling and the formation of the PC: The centrosome consists of a pair of centrioles and a surrounding protein matrix, the pericentriolar material (PCM). It is a non-membranous organelle, approximately 1 μm^3 in size, and often found in proximity to the nucleus (Doxsey 2001; Bettencourt-Dias and Glover 2007). Nine MT triplets are arranged like a barrel to form one centriole. Centrioles are characterised by their orthogonal orientation. As most polymers, the centriolar MTs are polar, with an unstable minus end and a more stable plus end. The plus end of the MTs forms the distal end of the centriole whereas the minus end forms the proximal end. The MTs of the centriole are stabilised by posttranslational modifications such as polyglutamylation and acetylation (Piperno et al. 1987; Bobinnec et al. 1998; Bobinnec et al. 1998). The lumen of the centriole contains several proteins, in particular δ-tubulin, centrin-2 and –3, hSas-6, CPAP, Cep135 and Plk4

(Salisbury et al. 2002; Kleylein-Sohn et al. 2007). These proteins regulate the duplication of the centriole during S phase of the cell cycle and are assembled in a sequential manner. (Habedanck et al. 2005; Kleylein-Sohn et al. 2007). In particular, Plk4 is a key regulator of centriole biogenesis and overexpression of Plk4 results in supernumerary centrioles (Habedanck et al. 2005; Kleylein-Sohn et al. 2007). Not surprisingly, the centrosome cycle and cell cycle are closely linked with each other and the uncoupling of these cycles can be found in many types of cancer.

The two centrioles within each centrosome are not identical. The older centriole, known as the mother centriole, harbours appendages at its distal and subdistal end. Several lines of evidence support the idea that the subdistal appendages are the main site for MT anchoring (Luders and Stearns 2007). Injection of antibodies against subdistal appendage proteins like Ninein or Cep110 disrupts the ability of the centrosome to organise MTs (Ou et al. 2002). Similar results can be seen in experiments using anti-Nlp or anti-ε–tubulin antibodies (Casenghi et al. 2003; Chang et al. 2003). Typically, at the onset of mitosis the subdistal appendage proteins disappear from the mother centriole and reappear at the end of mitosis. This includes the retargeting of Cep170, Ninein, Nlp, ODF2 and ε–tubulin to the centriole (Lange and Gull 1995; Chang and Stearns 2000; Mogensen et al. 2000; Chang et al. 2003; Guarguaglini et al. 2005).

The predominant function of the distal appendages is the coordination of PC formation (Graser et al. 2007). Cep164, the only known distal appendage protein, shows a severe cilia phenotype when depleted (Graser et al. 2007).

The protein ODF2 seems to be a component of both appendages. Odf2-/- mouse cells lack distal and subdistal appendages and they can not assemble a PC (Nakagawa et al. 2001; Ishikawa et al. 2005).

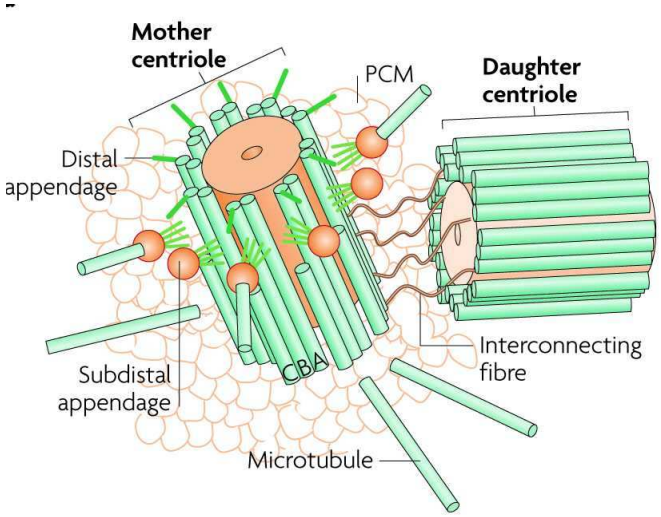

Figure 1. Structure of the centrosome. Schematic diagram depicting the centrosome consisting of the centrioles and the surrounding PCM. In each triplet, the most internal tubule is called the A-tubule; the one following it is the B-tubule; and this is followed by the most external one, the C-tubule. The mother centriole is characterised by distal and subdistal appendages. (Bettencourt-Dias and Glover, 2007).

The PCM surrounds the centrioles and harbours the main sites for MT nucleation. The MT nucleation complex comprises γ-tubulin, γ-tubulin complex proteins 2-6 (GCP2-6) and GCP-WD (Luders and Stearns 2007; Raynaud-Messina and Merdes 2007). This complex is anchored in the PCM by interaction with AKAP450 and pericentrin/kendrin (Dictenberg et al. 1998; Takahashi et al. 2002). During the cell cycle the PCM undergoes structural alterations and compositional changes (Doxsey 2001). It is built predominantly by coiled–coil proteins, which were identified in a proteomic screen (Andersen et al. 2003). In total, around 100 proteins build the PCM. Interestingly, the PCM is required for centriole duplication and depletion of the PCM component SPD-2 inhibits centriole duplication (Dammermann et al. 2004; Leidel and Gonczy 2005).

3.2 The centrosome cycle

The centrosome cycle can be divided into four steps. 1) centrosome duplication, 2) centrosome maturation, 3) centrosome separation and 4) centriole disengagement (Tsou and Stearns 2006; Nigg 2007).

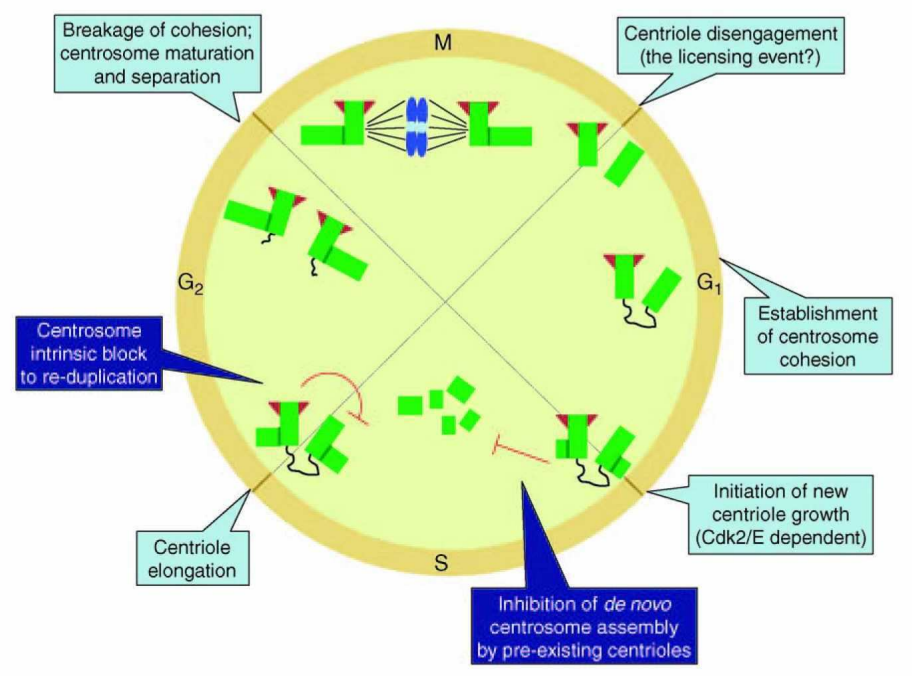

Figure 2. The centrosome duplication cycle. Centrioles (green), centriole appendages that mark the distal end of mature centrioles (red), and chromosomes (blue) are shown (adapted from Tsou and Stearns, 2006a).

Duplication of the centrosome starts at the G1-S phase transition and finishes in G2. During centriole duplication one new procentriole buds adjacent to the proximal end of each centriole. Thus, the two parental centrioles bud two procentrioles, so that a G2 cell harbours two centrosomes each consisting of two attached “engaged” centrioles. Key regulators are the protein kinases Cdk2-cyclin A/E and Plk4 (Meraldi et al. 1999; Bettencourt-Dias et al. 2005; Habedanck et al. 2005). Overexpression or depletion/inhibition of one of these kinases promotes or inhibits centrosome duplication, respectively. At present, little is known about the target proteins which are phosphorylated by these kinases. Meraldi et al. suggested an involvement of the Rb/E2F pathway in the regulation of the centrosome duplication by Cdk2-cyclin A (Meraldi et al. 1999). New insights into the role of Plk4 came from studies using *C. elegans*, *Drosophila*, as well as from a human cell line overexpressing Plk4 (Leidel and Gonczy 2003; Bettencourt-Dias et al. 2005; Leidel and Gonczy 2005; Pelletier et al. 2006; Kleylein-Sohn et al. 2007).

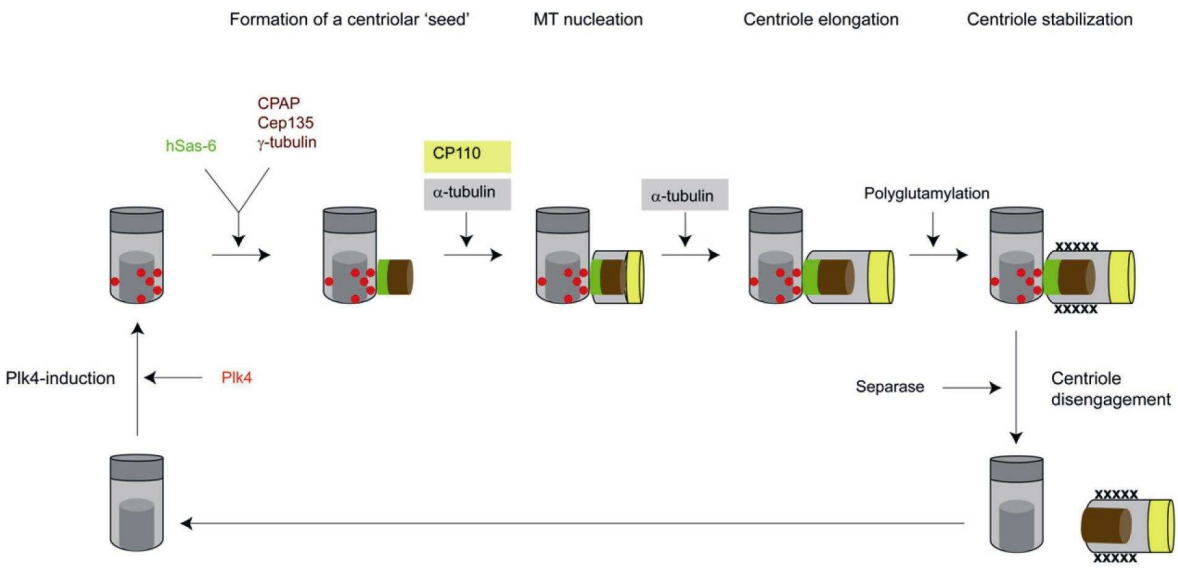

Figure 3. Model for the centriole assembly in human cells. Nascent procentriolar structures are depicted coding Plk4 in red; hSas-6 in green, CPAP, Cep135, and γ-tubulin in brown, α-tubulin in grey; and CP110 in yellow (adapted from Kleylein-Sohn 2007).

Overexpression of Plk4 induced centrosome over duplication in human cells and contributed to cancer formation in *Drosophila* (Habedanck et al. 2005; Basto et al. 2008). Depletion of Plk4 by siRNA blocked centriole biogenesis, suggesting that Plk4 is a key regulator of centriole duplication (Bettencourt-Dias et al. 2005; Habedanck et al. 2005).

Plk4 localises to the centrosomes and recruits essential factors for centriole duplication. After activation of Plk4, the initiation factor hSas-6 is recruited to the proximal end of the centriole followed by the recruitment of CPAP, Cep135 and γ–tubulin (Figure 3) (Kleylein-Sohn et al. 2007). These proteins form a seed for assembling the procentriole. CP110 caps the plus end of the centriolar MTs to restrict the size of the centriole. Tsang and colleagues showed that depletion of CP110 causes the formation of MT extensions (Tsang et al. 2008). Interestingly, CPAP could be a positive regulator of centriole elongation. Overexpression of CPAP in fact results in extended centrioles (LeClech M., personal communication). So a balance of CP110 and CPAP may control the size of the centrioles.

Interestingly, CP110 is also relevant to PC assembly. During ciliogenesis the MTs of the mother centriole are extended in a process that involves intraflagellar transport (IFT). Se-

lective removal of the CP110 cap from the mother centriole seems to be required for the formation of a PC (Tsang et al. 2008).

At the onset of mitosis the centrosome turns into a spindle pole. At this time, the centrosome acquires additional MT nucleation sites, allowing the rapid nucleation of new MTs during mitosis (Palazzo et al. 2000; Meraldi and Nigg 2002). Similar to centriole duplication, centrosome maturation is regulated by kinases (Meraldi and Nigg 2002). Plk1, which is recruited to the centrosome in late G2, is one key player (Barr et al. 2004). Injection of anti-Plk1 antibodies into humans cells results in small centrosomes with reduced amounts of γ–tubulin (Lane and Nigg 1996).

Aurora A also plays a key role in centrosome maturation. Aurora A localises to the centrosome and both activity and amount peaks during the G2-M transition (Meraldi and Nigg 2002; Bahe et al. 2005). Depletion of the *C. elegans* homolog of Aurora A by siRNA in embryos disrupts the recruitment of γ-tubulin (Hannak et al. 2001) to the centrosome. These embryonic cells are not able to form mitotic spindles (Hannak et al. 2001). Terada and colleagues could show that Aurora A interacted with centrosomin and that this interaction was required for γ–tubulin recruitment (Terada et al. 2003). Similar results suggest an interaction of Aurora A with TACC or TPX2 (Giet et al. 2002; Kufer et al. 2002).

Centrosome maturation is followed by the separation of the duplicated centrosomes into two spindle poles. Centrosome separation starts with the disruption of cohesion between the two parental centrioles (Meraldi and Nigg 2002; Bahe et al. 2005). Some electron microscopic studies suggested a linker region between the parental centrioles (Bornens et al. 1987). This linker region is thought to be formed by a fibrous structure which contains the proteins C-Nap1, rootletin and Cep68 (Bahe et al. 2005; Graser et al. 2007). Localisation of C-Nap1 is regulated by phosphorylation through the kinase Nek2 (Fry et al. 1998; Mayor et al. 2002). At the onset of mitosis, C-Nap1 is phosphorylated, which leads to the disassembly of the linker region. Injection of anti-C-Nap1 antibodies into cells results in centrosome splitting (Mayor et al. 2002), comparable to results seen in cells that were treated with siRNA depleting rootletin and Cep68 (Bahe et al. 2005). The two latter proteins form fibrous fibres when transiently expressed and both localise to the linker region (Graser et al. 2007). These data support the idea that C-Nap1, rootletin and Cep68 build a

dynamic linker between the parental centrioles and that Nek2 regulates the disassembly of the linker during mitosis.

Late in mitosis the two centrioles disengage, meaning that they lose their orthogonal orientation (Tsou and Stearns 2006; Nigg 2007). Centriole disengagement is required for centriole duplication. It is now thought to be regulated by separase, a protease known to control sister chromatid separation (Nagao and Yanagida 2002; Nasmyth 2002). Using *Xenopus* egg extract Tsou and colleagues showed that engaged S phase centrioles became disengaged after addition to mitotic extract. Interestingly, disengagement could be blocked by the addition of a peptide inhibiting the ubiquitin ligase APC/C or by the addition of securin, a inhibitor of separase (Tsou and Stearns 2006). These results suggest an involvement of the ubiquitin ligase APC/C and of the protease separase in centriole disengagement. Recently, Wang et al. suggested that Shugoshin 1 is the glue between the centrioles (Tsang and Dynlacht 2008; Wang et al. 2008). However it remains unclear whether these proteins act directly on the centrosome or indirectly by supporting progression through mitosis

In late mitosis the spindle poles must become again G1 centrosomes. The centrosomes lose their additional nucleation sites, the linker between both centrioles is formed again and the subdistal appendages reassemble (Casenghi et al. 2003; Guarguaglini et al. 2005). The amount of γ–tubulin, pericentrin and other proteins required for the organisation of the mitotic spindle is reduced. The amount of γ–TuRCs within the PCM is diminished to normal contents and Aurora A and Plk1 are lost from the centrosome. In contrast, the linker structure between both centrioles reforms by the recruitment of C-Nap1, Cep68 and rootletin (Bahe et al. 2005; Graser et al. 2007). It is thought that phosphatases like Cdc14 remove the phosphates from Cdk1 targets to revert the phosphorylation state of many proteins (Torres-Rosell et al. 2005).

3.3 Function of the centrosome

The centrosome has two main functions: First it organises the MTs and second it forms a template for the formation of the cilium (Doxsey 2001; Bettencourt-Dias and Glover 2007).

During cell cycle, the centrosome organises two different MT arrays: in interphase a stable MT network and in mitosis the highly dynamic spindle (Dammermann et al. 2003; Varmark 2004).

The cilium is a projection of the cell surface required for chemo- and mechanosensation (Singla and Reiter 2006). During ciliogenesis, the A tubule and B tubule of the mother centriole is extended to form an axoneme. Motile cilia in epithelial cells are needed for the transport processes in the respiratory tract or in the fallopian tube. Some cilia are found in sensory cells and are specialised for sensing light or odorant (Fliegauf et al. 2007). In contrast to motile or sensory cilia, the immotile PC can be found on almost every cell of the organism (Ainsworth 2007). Primary cilia are now thought to act as antennae to sense the environment (Singla and Reiter 2006). In tissue culture some cells form a PC in the absence of growth stimulation. Interestingly, there is a striking correlation between entry in G0 and formation of the PC (Quarmby and Parker 2005).

3.4 Centrosomes, organisers of the MTs

To allow the organisation of a MT array, MTs have to be nucleated, anchored and bundled at different structures at the centrosome.

The PCM for instance, contains the nucleation sites for the MTs (Wiese and Zheng 2006). After nucleation the MTs are anchored at the subdistal appendages of the mother centriole (Mogensen et al. 2000; Luders and Stearns 2007).

MTs are polar cylindrical polymers consisting of thirteen protofilaments of α– and β–tubulin dimers. The β-tubulin subunits point towards the plus end and the α-tubulin towards the minus end of the MT. MTs attach with their minus (slow growing) end at the centrosomes and are oriented outward with their plus (fast growing) ends (Wiese and Zheng 2006). The minus end is capped by the γ–tubulin ring complexes (γ–TuRCs), allowing the nucleation of the MTs. γ–tubulin forms a complex with the gamma complex proteins 2-6 (GCP2-6) and with GCP-WD (Luders and Stearns 2007; Raynaud-Messina and Merdes 2007). Depletion experiments showed, that each GCP protein is required for the assembly of the γ–TuRC (Gunawardane et al. 2000; Verollet et al. 2006).

Several observations led to the notion that the γ–TuRC is the MT nucleator *in vivo*: (1) γ–TuRC could be seen in the PCM of purified centrosomes using electron tomography (Moritz et al. 1995; Moritz et al. 2000) (2) purified γ–TuRC nucleates more than 30 times more efficient than other complexes (Oegema et al. 1999) (3) purified γ–TuRC remains associated with the minus end of the MT (Gunawardane et al. 2000; Moritz et al. 2000) and (4) all subunits of the γ–TuRC are concentrated at the centrosome.

Structural studies suggest that γ–tubulin forms a ring on top of a GCP complex, allowing the stabilisation of the minus end of a MT. The γ–TuRCs function as a template, mimicking the MT end. This template model is supported by X-ray crystallography which shows adjacent subunits of γ–tubulin (Aldaz et al. 2005).

After nucleation, MTs need to be anchored at the centrosome. Takashi and colleagues demonstrated that the amino-terminal regions of AKAP450 and kendrin interact with GCP2 and GCP3 (Takahashi et al. 2002). This allows the stable binding of γ–TuRC to the PCM. Addition of anti-kendrin- or anti AKAP450 antibodies blocks the nucleation activity of isolated centrosomes. Similar results could be observed in experiments evaluating the function of pericentrin B, CAP350 and FOP (Doxsey et al. 1994; Dictenberg et al. 1998; Yan et al. 2006).

The subdistal appendages of the mother centriole appear to be the major sites for MT anchoring (Mogensen et al. 2000; Luders and Stearns 2007). The mother centriole is located at the centre of the MT array, although both centrioles are associated with γ–tubulin. Additionally, the MTs are often seen to terminate on the subdistal appendages of the mother centriole (Gorgidze and Vorobjev 1995). Interestingly, both centrioles nucleate almost similar numbers of MT, but only the mother centriole is able to maintain a radial array after nocodazole treatment (Mogensen et al. 2000).

The subdistal appendages consist of Ninein, centriolin, ε–tubulin, cenexin/ODF2, Cep170 and Nlp (Lange and Gull 1995; Chang and Stearns 2000; Mogensen et al. 2000; Casenghi et al. 2003; Gromley et al. 2003; Guarguaglini et al. 2005). All of these proteins are implicated in MT organisation. For instance, Nlp was shown to organise MTs by targeting

γ–TuRC to the appendages (Casenghi et al. 2003) and injection of anti-Cep110 antibodies abolishes MT organisation (Chang and Stearns 2000; Chang et al. 2003).

Along the above proteins Ninein is the best studied appendage protein (Bouckson-Castaing et al. 1996; Mogensen et al. 2000; Abal et al. 2002; Delgehyr et al. 2005; Moss et al. 2007). Ninein is concentrated at both the minus end of the MT and at the subdistal appendages and is required for MT anchoring (Mogensen et al. 2000; Delgehyr et al. 2005).

Delgehayr and colleagues transiently transfected cells with different Ninein constructs to show that Ninein anchors MTs at the subdistal appendages. They found that a fragment comprising the C-terminus (aa 1874-2113) of Ninein localised to centrioles and displaced endogenous Ninein and γ–tubulin. They also observed that transiently expression induced a delay in MT regrowth and prevented the anchoring of the MTs. They explained this fact by a reduction of centriolar Ninein and γ–tubulin because other proteins implicated in anchoring, Nlp, pericentrin and AKAP450, were not influenced (Delgehyr et al. 2005). However, a fusion protein containing the N-terminus (aa 1-373) and the C-terminus of Ninein localised to one centriole and displaced only endogenous Ninein and only affected MT anchoring. The anchoring phenotype could also be confirmed in expression and depletion studies (Abal et al. 2002; Dammermann and Merdes 2002)

3.5 Centrioles as templates for PC formation

The PC is a projection of the plasma membrane and contains a barrel shaped MT network, the axoneme (Figure 4). The axoneme continues the A and B MTs of the basal body and thus consists of nine doublets of MTs varying in length from 3-30 µm. It is surrounded by a membrane and can comprise an additional centrally located doublet of MT, forming the 9+2 cilia. This type of cilium is motile, in contrast to the non-motile PC which has no additional doublet of MT within the axoneme (Eggenschwiler and Anderson 2007; Fliegauf et al. 2007).

The zone between the basal body and the axoneme is called transition zone. It is characterised by a fibrous protein structure. This structure might form a selective barrier regulating the shuttling of ciliary proteins (Singla and Reiter 2006).

The cilium is built in a process called intraflagellar transport (IFT). A specialised machinery moves proteins, precursor particles and vesicles bi-directionally along the axoneme. The anterograde transport is done by kinesin-II, the retrograde transport by cytoplasmic dyneins. Both motor proteins interact with adapter proteins of the IFT family to transport several different target proteins (Rosenbaum and Witman 2002; Scholey 2008).

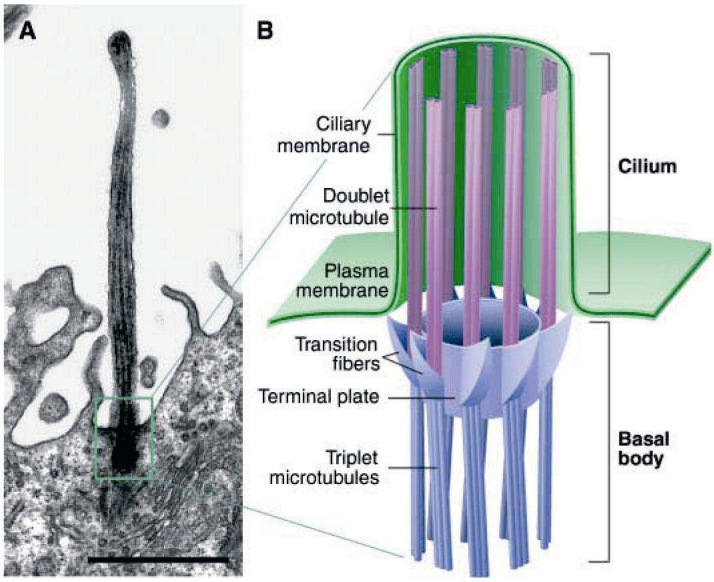

Figure 4. The PC. (A) Electron micrograph of the PC of a canary brain radial glia. (B) Schematic showing structure of the basal body and PC (adapted from Reiter, 2006).

For a long time the PC was considered as a rudimentary organelle without any function. However, recently it became apparent that some severe diseases are linked to ciliary defects (Fliegauf et al. 2007; Marshall 2008). Most prominent are diseases of the kidney. An autosomal recessive disease is caused by mutations of genes coding for the mechanosensitive Ca^{2+}-channels polycystin-1 and polycystin-2. Both proteins localise to the PC and allow the influx of Ca^{2+}-ions into the cell when the cilium is bended (Praetorius and Spring 2001; Praetorius et al. 2003). This signal seems to be required for proper development of the kidney and mutations in polycystin-1 and –2 are linked to polycystic kidney disease. Nowadays, many of additional ciliopathies are known, including Bardet-Biedl and Alström syndrome. Patients with these syndromes suffer from obesity, cystic kidneys and retinal degeneration. Similarly, Oral-facial-digital syndrome patients show polydactyly,

infertility and cystic kidneys. Recently, it was shown that the Jeune-syndrome can be caused by mutations in the genes encoding for ciliary IFT80 (Beales et al. 2007). Some of these phenotypes can be explained by defects in specialized cilia in the respiratory tract (bronchitis), in the fallopian tube or in the sperm (infertility), in the eye (retinal degeneration) or in the pancreatic duct cilia (diabetes). Developmental disorders like polydactyly or small limbs can be explained by defects in the Hedgehog or Wnt signalling. Thus, the PC is now considered as a cell´s antenna, which senses mechano- or chemo signals and regulates the development of embryos (Singla and Reiter 2006; Fliegauf et al. 2007).

3.6 The life cycle of the PC

The life cycle of the cilium comprises four steps:

1) Transport of the centrosome to the plasma membrane
2) Initiation of cilium assembly
3) Elongation of the cilium
4) Disassembly of the cilium

The formation of a PC starts when cells enter G0 (Snell et al. 2004). First, the centrosome is brought to the plasma membrane to attach the mother centriole to the plasma membrane. Until now little is known about which proteins transport the centrosome to the plasma membrane, or how this program is regulated. However, there are some structural changes within the centrosome that characterise this process. The transition fibres are formed which connect the tip of the mother centriole to the plasma membrane to build a selective barrier. Most likely, the tips of the transition fibres fuse with some vesicles during the transport to the plasma membrane (Barr 2008). Therefore, a close proximity to the Golgi apparatus is needed (Poole et al. 1997). Interestingly, IFT20 is both a Golgi protein and a ciliary protein (Follit et al. 2006), and depletion of IFT20 inhibits cilium formation. Additionally, some proteins implicated in vesicular trafficking, membrane fusion and membrane cytoskeleton interaction were shown to be required for cilium formation (Nachury et al. 2007; Yoshimura et al. 2007). Yoshimura and colleagues showed that the Rab proteins Rab8a, Rab17 and Rab23 and their GTPase activating proteins (GAP) XM037557, TBC1D7 and

EVI5like are required for ciliogenesis. Overexpression of these GAPs efficiently suppressed cilium formation (Yoshimura et al. 2007). Surprisingly, Rab8 interacts with the appendage protein ODF2 and localises to the PC when transiently expressed. This suggests that the appendage protein ODF2 might catalyse the first interaction of vesicles with the transition fibres.

Interesting lessons could be learned on the transcriptional program controlling the cilia formation by using the algae *Chlamydomonas*. This organism starts a reassembly program when the flagella were removed (Stolc et al. 2005). Stolc and colleagues could identify a set of transcripts which are highly upregulated after 30 min of flagellum removal. Besides typical flagellar proteins, such as IFT proteins or dynein, tubulin folding factors, molecular chaperons and the two nuclear proteins reptin and pontin were highly upregulated (Stolc et al. 2005).

After the attachment of the mother centriole to the plasma membrane the A tubule and B tubule of the centriole are extended. This requires the removal of proteins which normally restrict the extension of the centriolar MT. In some regards, the formation of the axoneme is comparable to the biogenesis of the centriole and it should thus not be surprising that some proteins are needed for both processes. Specifically, CP110 and Cep97 were identified as two proteins that limit MT assembly. Their removal, by siRNA, resulted in extended centrioles (Tsang et al. 2008). Interestingly, depletion of Cep290 suppressed the extended centrioles seen in CP110 depleted cells, suggesting that Cep290 counteract CP110 (Tsang et al. 2008).

After removal of capping proteins from the plus end of centriolar MTs the axoneme is assembled. The cilium is built by a process called intraflagellar transport (IFT) (Rosenbaum and Witman 2002; Scholey 2008). The IFT proteins form two complexes A and B (IFT-A, IFT-B) and act as adapters for the transport of precursor particles and vesicles. B subcomplex proteins mainly drive anterograde transport, whereas IFT-A is required for retrograde transport (Rosenbaum and Witman 2002). During IFT α-and β–tubulin dimers, tubulin chaperones, radial spoke arms, matrix and membrane proteins are transported to the growing tip of the PC (Qin et al. 2004). The IFT particles are assembled in the cell body and then accumulate in the transition zone of the basal body (Rosenbaum and Witman 2002).

Depletion of any component of the IFT complex B disrupts the formation of the cilium. This is also true for both motor proteins. The anterograde transport is done by the motor-protein kinesin-II, a heterodimer of Kif3a and Kif2a and the accessory subunit KAP (kinesin associated protein) (Cole et al. 1998; Signor et al. 1999), whereas cytoplasmic dyneins transport proteins back from the tip to the base of the cilium (Pazour and Witman 2003). Thanks to this bi-directional transport machinery, the IFT particles function like constantly moving molecular trucks on a closed loop (Snell et al. 2004). The movement does not cease when the cilium reaches full length, implying that the length of the axoneme is kept by a steady state equilibrium, characterised by constant levels of addition and removal of tubulin subunits (Qin et al. 2004). When IFT particles reach the tip, kinesin II is inactivated and cytoplasmic dynein is activated. Studies in *Chlamydomonas* could identify some proteins which control the length of the flagellum including a member of the MAP kinase family (Berman et al. 2003).

Basically, the cilium is a MT cylinder surrounded by the plasma membrane. Not surprisingly, ciliogenesis and maintenance requires the transport of membranes and the regulation of membrane MT contact (Follit et al. 2006; Barr 2008). Several proteins have been implicated in this process. Some proteins which regulate membrane fusion are also targeted to the PC. IFT27, a Rab like GTPase, is required for ciliogenesis (Qin et al. 2007). Yoshimura et al. could identified several Rab proteins and their corresponding GTPase activating factors (GAP), all of them required for ciliogenesis (Yoshimura et al. 2007). Generally, GTPases of the Rab family facilitate vesicular trafficking by promoting the docking and fusion of transport vesicles to their target compartments. Rab8 was recently found to interact with proteins of the BBS family (Nachury et al. 2007). Mutations in genes coding for the twelve BBS proteins cause the Bardet-Biedl syndrome, a pleiotropic disease characterised by obesity, retinal degeneration, kidney malfunctions and olfactory deficits (Badano et al. 2006). The underlying molecular mechanism remains poorly understood. Nachury and colleagues identified a core complex of BBS proteins co localizing with PCM-1 in the centrosomal periphery. They could show that seven proteins of the BBS family form a core complex. This complex (termed Bbsome), consisting of BBS1,2,4,5.7,8,9, interacts with membranes or vesicles in the PC through BBS5. Interestingly, BBS1 interacts with Rabin, a GEF protein which stabilizes the GTP form of Rab8. Depletion or inhibition of Rabin

prevents the formation of the PC, suggesting that Rab8 GTP and Rabin8 are required for cilium biogenesis (Nachury et al. 2007).

According to the current a model IFT20 transports vesicles from the Golgi apparatus to the periphery of the basal body. Here they associate with Rabin, Rab8GTP and the BBSome. Stabilized Rab8GTP allows the transport of vesicles from the basal body to the tip of the axoneme. The vesicles might pass the transition zone by the interaction of Rab8 with ODF2. This fact might explain why ODF2 depletion causes primary cilia defects (Ishikawa et al. 2005). After passing the transition zone the fusion of the vesicles with the ciliary membrane would then be controlled by the Rab8-GAP XM037557 (Nachury et al. 2007).

These results demonstrate that not only the prolongation of the MTs is regulated, but the enlargement of the ciliary membrane is also tightly regulated by a balance of Rab8 activating proteins (GAPs) and inhibiting proteins (GEFs).

At the end of its life cycle the cilium has to be absorbed. Usually, disassembly of the cilium is linked to re-entry of the cell into S phase. Recently, the process was found to be regulated by Aurora kinases. This was shown first in *Chlamydomonas* and subsequently in human cells (Pan et al. 2004; Pugacheva et al. 2007). Pan et al. reported that the Aurora kinase family member CALK regulates flagellar disassembly in *Chlamydomonas*. Using siRNA these authors could show that CALK is essential for disassembly of the flagellum. Additionally, they showed that CALK is phosphorylated when the flagellum disassembles (Pan et al. 2004). These findings were extended by a report indicating that activated and phosphorylated Aurora A controls the disassembly of the PC in human cells (Pugacheva et al. 2007). According to their data, Aurora A interacts with HEF1 at the basal body to activate the tubulin deacetylase HDAC6. A few hours after serum addition the levels of HEF1 increased, which activated Aurora A. This resulted in an accumulation of the phosphorylated and activated form of Aurora A at the basal body. Both depletion of Aurora A and inhibition of kinase activity blocked the disassembly of the cilium. Similarly, depletion of the tubulin deacetylase HDAC6 or HEF1 and inhibited the resorption of the cilium (Pugacheva et al. 2007).

There are still some open questions. For example, which kinase phosphorylates Aurora A and which proteins bind the phosphorylated Aurora A at the centrosome? A MAP kinase or a cyclin dependent kinase could be candidates for phosphorylating Aurora A. In *Chlamydomonas* a MAP kinase and a cyclin dependent kinase in fact control the length of the flagellum and mutations of the corresponding genes cause extended flagella (Berman et al. 2003; Tam et al. 2007).

IFT proteins:

IFT was first described by Kozminski and colleagues in 1993 in *Chlamydomonas* (Kozminski et al. 1993). Theses authors saw particles moving from the base to the tip of the flagellum and back again when they examined flagella. These particles moved relatively fast, with an speed of about 2-4 µm/s (Kozminski et al. 1993). In total, at least 17 proteins assemble the two subcomplexes. Complex A contains at least six subunits, whereas complex B contains at least eleven subunits (Cole et al. 1998; Piperno et al. 1998; Cole 2003). Mutation of either one of the kinesin 2 subunits or one of the B subunits abolishes cilium formation (Cole et al. 1998; Pazour et al. 2000; Huangfu et al. 2003; Sun et al. 2004).

Subcomplex B consists of the core components IFT88, IFT81, IFT74/72, IFT52, IFT46 and IFT27 (Figure 5, Figure 6). The core complex binds to the peripheral components IFT80, IFT172, IFT57 and IFT20 (Lucker et al. 2005). The two core proteins IFT81 and IFT74/IFT72 can assemble tetrameric complexes. Two IFT81 proteins interact with a heterodimer of IFT74/IFT72 to form a scaffold for the formation of the subcomplex B (Lucker et al. 2005). Deletion mutants of IFT88, IFT172, IFT52 in *Chlamydomonas* were completely unable to form a flagellum (Pazour et al. 2000; Brazelton et al. 2001; Cole 2003). The more peripheral subcomplex B component IFT57 only caused stunted flagella when mutated, suggesting that it is involved in length control (Cole 2003). The other peripheral IFT B protein IFT172 interacts with EB1 at the tip of the flagellum and might be involved in the switch from anterograde to retrograde movement (Pedersen et al. 2003; Pedersen et al. 2005).

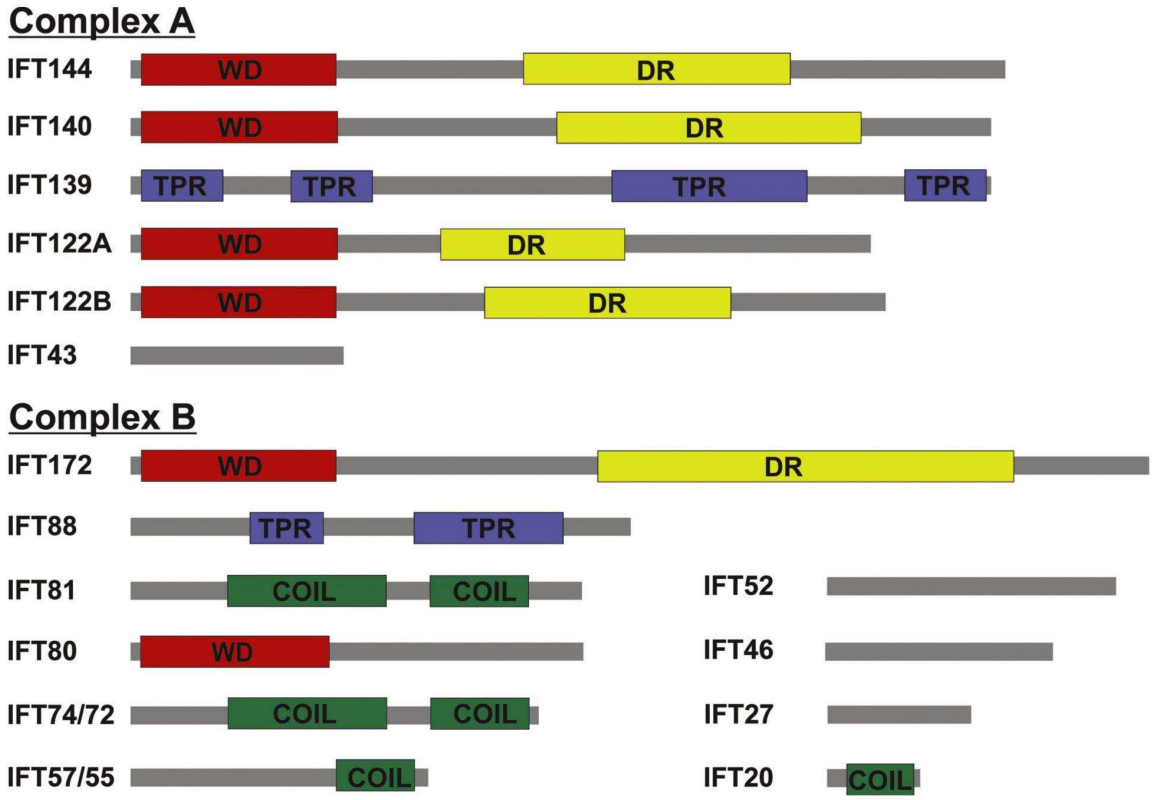

Figure 5. Intraflagellar transport (IFT) particle composition in *Chlamydomonas*. Putative protein-protein binding motifs have been identified through sequence analysis. WD40: WD repeat; DR: degenerate repeats; TPR: tetratricopeptide repeats; COIL: coiled-coil (Cole, 2003).

The subcomplex A contains the IFT proteins IFT144, IFT140, IFT139, IFT122A, IFT122B and possibly IFT43 (Lucker et al. 2005). IFT122A and B, IFT140 and IFT144 contain putative WD repeats and degenerated repeats (DR). WD repeats often serve as sites for transient protein-protein interactions. In contrast, coiled-coil domains form more permanent protein–protein interactions. Likely the permanent interaction between the coiled coil domains of IFT81 and IFT74/IFT72 keeps the core complexes of subcomplex A and B tightly together (Lucker et al. 2005).

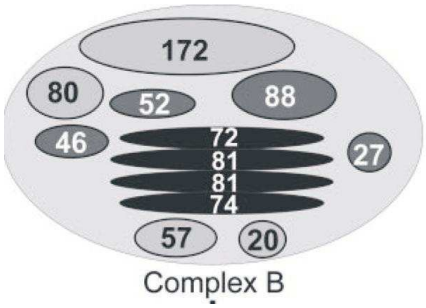

Figure 6. IFT complex B core model. The *Chlamydomonas* IFT complex B reveals a core complex containing IFT88, IFT81, IFT74, IFT72, IFT52, IFT46 and IFT172. IFT81 forms an oligomer with IFT74 and IFT72 (Cole, 2005).

A genetic screen in the zebrafish identified several IFT proteins to be involved in the development of cystic kidneys (Sun et al. 2004). Mutagenesis of the IFT-B components IFT 81, IFT57 and IFT172 caused kidney cyst in the developing embryo (Sun et al. 2004). Another interesting finding on the role of IFT proteins was the discovery that some mice carrying mutations in IFT proteins show a similar phenotype as mice mutated in Hedgehog (Hh). Murine embryos with mutations in the genes coding for IFT88 (polaris, Tg737) and IFT152 showed similar phenotypes as Hh mutants (Pazour et al. 2000). Below, we shall address the question how this phenotype can be explained.

3.7 PC in signalling

Recently, it became apparent that some important signalling pathways are regulated by the PC, most prominently Hedgehog signalling, Wnt signalling, Ca^{2+} signalling and PDGF $\alpha\alpha$ signalling.

Hh signalling plays pivotal roles in development and tissue maintenance. In addition, Hh signalling is required for stem cell differentiation and is also relevant in cancer. Constitutively active Smoothened (Smo), an important protein within the Hh pathway (see below), can act as a proto-oncogene and mutations can be frequently found in basal cell carcinomas (BCC) (Epstein 2008).

As illustrated in Fig. 7, Hh signalling starts with the binding of Hh to the transmembrane protein Patched (PTCH). PTCH associates with Smo in the absence of Hh. The binding of

Hh to PTCH leads to the disassembly of the Smo PTCH complex. PTCH is a negative regulator of Smo. After disassembly the receptor Smo is active and antagonises “Suppressor of Fused” (Sufu). This allows the processing of the transcription factors Gli1 and Gli2, whereas Gli3 is no longer processed. Gli1 and 2 are transcriptional activators of Hh target genes, whereas Gli3 acts as an repressor of these genes. So, binding of Hh to PTCH results in the activation of the transcription factors Gli1 and Gli2 and in the inhibition of the repressor Gli3.

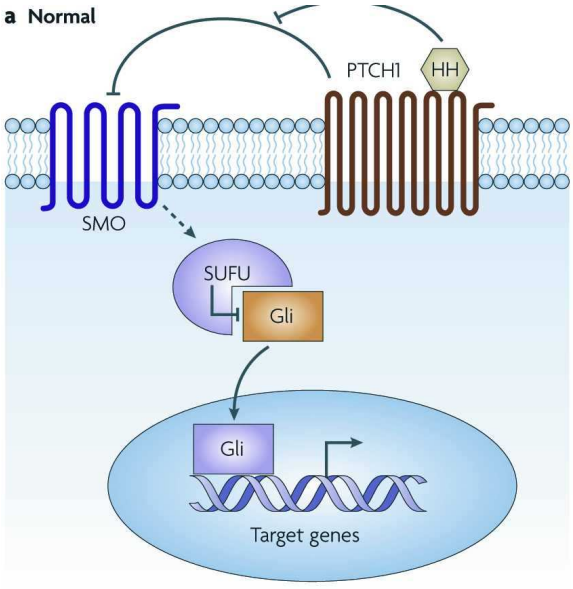

Figure 7. A basic schematic of the Hedgehog (HH) signalling pathway. The extracellular HH ligand binds to patched 1 (PTCH1) receptor. This relieves the inhibition of smoothened (SMO) by PTCHH1, and SMO sends signals by interacting with suppressor of fused (SUFU), resulting in activation of the downstream Gli family of transcription factors. (Epstein, 2008).

First hints for an involvement of the PC in Hh signalling came from studies done in the beginning of 2000 (Andersen et al. 2003; Huangfu et al. 2003). Anderson and colleagues performed a genetic screen in mice to identify genes which, when mutated, cause similar phenotypes as Hh mutants. They were surprised to find mutations in genes coding for IFT88 and IFT172. Additionally, IFT52, Kif3a and the dyneins Dnchc2/Dnchc3 are necessary for Shh signalling (Huangfu et al. 2003; Haycraft et al. 2005; Huangfu and Anderson 2005; Liu et al. 2005). In the absence of these proteins, all modulations of target genes in

response to Hh are blocked and the targets of Gli are not activated in the ventral neural tube of these mice (Huangfu et al. 2003; Liu et al. 2005). The data could be confirmed by the finding that almost all important proteins of the Hh pathway are concentrated at the PC. The Smo receptor must localise to the cilium for normal signalling. Corbit and co-workers demonstrated that ciliary Smo localisation becomes amplified after Hh addition. An inactive form of Smo can not localise to the cilium in the presence of Hh (Corbit et al. 2005). Additionally, the localisation of Smo after Hh addition can be inhibited by the Smo antagonist cyclopamine. Thus, the activity of Smo is correlated with its presence in cilia. Possibly, PTCH might control the localisation of Smo in vertebrates, by inhibiting its transport to the cilium. Interestingly, PTCH localises to the shaft of the cilium and around the base of the cilium (Rohatgi et al. 2007). Addition of an inhibitor of Hh signalling results in an accumulation of PTCH at the cilium (Rohatgi et al. 2007). The idea that Smo localisation to the cilium is suppressed by PTCH is supported by the finding that Smo localised to the cilia in PTCH-/- cells in the absence of Shh. Reintroduction of PTCH into these cells prevented Smo accumulation in primary cilia and suppressed Hh pathway activity. Recently, Kovacs and colleagues (2008) demonstrated that Smo is transported into the PC by β-arrestin and Kif3a. Smo, β-arrestin and Kif3a form a complex and depletion of β-arrestin blocks Smo accumulation in the PC (Kovacs et al. 2008). In contrast, mutation of the gene coding for THM1 (tetratricopeptide repeat containing hedgehog modulator-1), leads to accumulation of Smo in the PC (Tran et al. 2008). This suggests that the THM1 protein is required for the retrograde transport of Smo.

These new findings led to the current model of Hh signalling in vertebrate cells. After addition of Shh, PTCH moves out of the cilium, allowing Smo to enter. The transport of Smo to the cilium is done by the motor protein kinesin II, consisting of Kif3a and Kif2a and β-arrestin. The close vicinity of Smo to the signalling proteins SuFu and Gli allows the activation of the Hh signalling pathway. The signalling can be regulated by the removal of Smo from the cilia. For this retrograde transport the THM1 protein is necessary.

Wnt signalling regulates embryonic development and some key proteins are often mutated in cancer (Moon et al. 2004). There are two Wnt signalling pathways: The canonical Wnt pathway and the noncanonical Wnt-Planar cell polarity pathway (PCP) (Figure 8). The two

different Wnt signalling pathways have different functions: the canonical pathway mediates cell fate and axis formation, whereas the noncanonical regulates gastrulation and differentiation of the cells within the cell plane (Montcouquiol et al. 2006).The canonical pathway leads to the stabilization of β–catenin in response to binding of Wnt3/1 to Frizzled (Fz) and the coreceptor LRP5/6. Subsequently, Dishevelled (Dvl) is phosphorylated. Phosphorylated Dvl inhibits GSK3β. A complex of CK1α kinase, GSK, axin and APC regulates the stability of β–catenin. Active GSK phosphorylates β–catenin and targets it for degradation. After phosphorylation of Dvl, the protein interacts with axin, which destabilizes the inhibitor complex and allows the accumulation of β–catenin. Inhibited GSK3β leads to the accumulation of β–catenin, which is transported into the nucleus and acts as a transcription factor together with TCF/LEF proteins

PCP controls the polarisation of cells within the plane of epithelial cells and thus coordinates the closure of the neural tube and the movement of the cells during gastrulation. The PCP pathway requires the binding of Wnt5a/11/4 to Fz. This leads to the recruitment of Dvl by Vangl to the receptor which then activates small GTPases. The activated GTPases transmit the signal to the JNK cascade (Montcouquiol et al. 2006).

The central protein is Dvl. Both pathways compete on Dvl which suggests that activation of one pathway leads to inhibition of the other.

Recent findings shed new light on how the PC favors the noncanonical Wnt pathway. Previous studies have shown that Invesin inhibits canonical Wnt signalling. Mutations of Invesin causes nephronophthisis characterised by renal cysts (Simons et al. 2005). Inv promotes the degradation of free cytosolic Dvl, which favors the noncanonical signalling. However, Inv not only localises to the PC, making the interpretation of these data less straightforward.

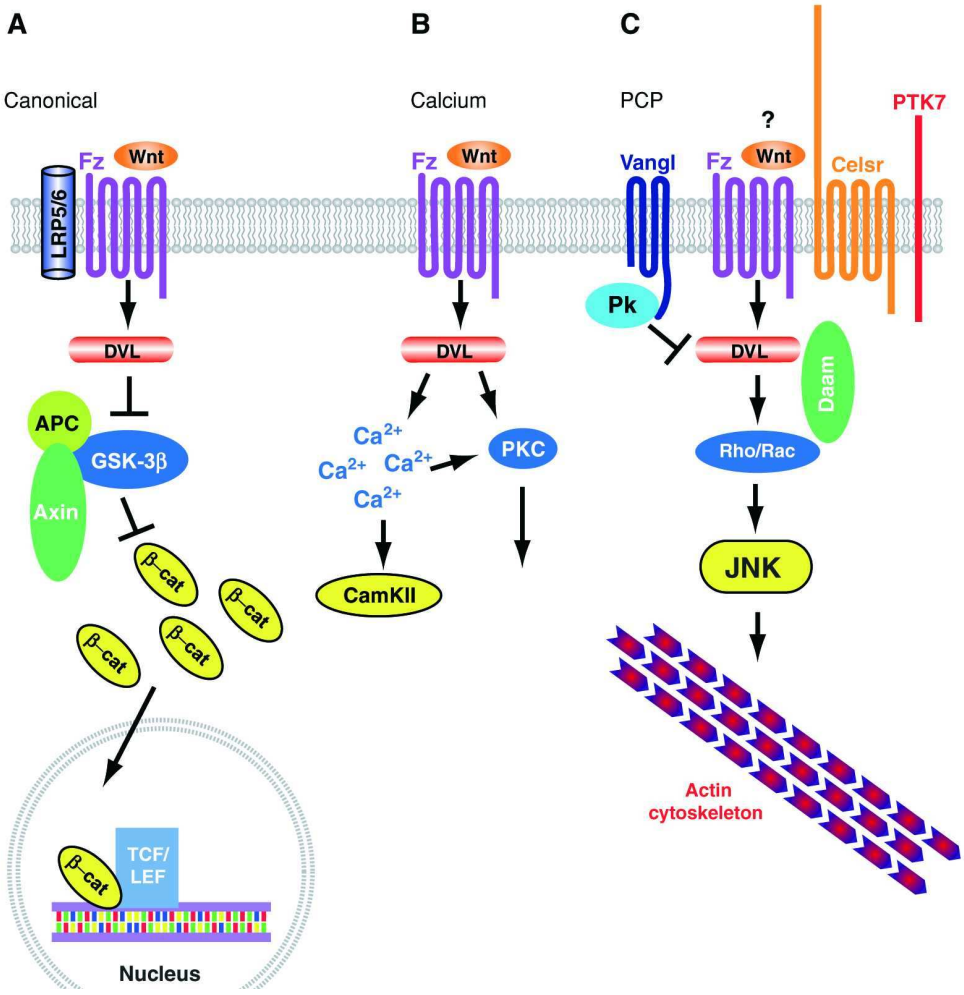

Figure 8. Wnt signalling pathways. (A) The canonical Wnt signalling pathway (B) The Wnt-calcium pathway (C) The Wnt-PCP pathway (adapted from Montcouquiol 2006).

The inhibition of canonical Wnt signalling could be further clarified by recent experiments (Corbit et al. 2008). Corbit and colleagues demonstrated that elimination of the cilia enhances canonical Wnt signalling. SiRNA mediated depletion of Kif3a resulted in enhanced Wnt responsiveness. They also revealed a stronger expression of a β–catenin reporter in Kif3a-/- mice embryos. Similar results were found in cells lacking IFT88 or Odf1, however to a lower extent (Corbit et al. 2008). The exact mechanism however remains elusive. The basal body may inactivate the CK1 α protein kinase required for the activation of Dvl.

It is currently believed that the mechanosensation of the PC is mediated by two proteins, polycystin-1 (PC1) and polycystin-2 (PC2). Both proteins when mutated cause polycystic kidneys. The PC1 and PC2 genes code for a ciliary transmembrane protein and a ciliary Ca^{2+}-channel. Praetorious and Spring demonstrated that bending of the cilium results in an increase of intracellular Ca^{2+} and that removal of the cilium disrupts the response. A bended cilium leads to the activation of the transmembrane protein PC1 (Praetorius and Spring 2001; Praetorius et al. 2003; Praetorius and Spring 2003). This in turn activates PC2 by binding, which results in a Ca^{2+}-influx (Nauli et al. 2003). The signal is further transmitted by the transcription factor Stat6 (Low et al. 2006) and the overall outcome is the regulation of cell proliferation. Faulty regulation is thought to induce cell proliferation and thus promote polycystic kidney disease.

Normal signalling is often necessary for maintenance of differentiated tissues. In most cells, PC formation is closely linked to G0 and growth control (Wheatley 1971). Schneider and colleagues found that activation of cell proliferation is tightly coupled to PC resorption. Induction of cell proliferation by calcium ionophores or addition of PDGF correlate with the disassembly of the PC (Schneider et al. 2005). The receptor PDGFRα is encoded by a growth arrest specific gene and the homodimer PDFGRαα is activated by PDGF-AA. Interestingly, this receptor is targeted to the cilium in G0 and can be activated by the addition of PDGF-AA. These findings could explain how the PC keeps fibroblasts in G0.

3.8 Cep170

Appendage proteins play a role in both in MT anchoring and PC formation (Mogensen et al. 2000; Ishikawa et al. 2005; Graser et al. 2007). Cep170 is a subdistal appendage protein that was originally found in a Yeast-two hybrid screen (Y2H) with the polo box domain (PBD) of Plk1. The C-terminus of Cep170 bound and bundled MT and was phosphorylated by Plk1. Cep170 is displaced from the mother centriole during mitosis, a typical feature of subdistal appendage proteins (Guarguaglini et al. 2005). Cep170 contains a putative FHA domain (aa 23-90) in the amino terminus and a predicted coiled-coil region (aa 1467-1495) in the carboxyl terminus. FHA domains specifically bind phosphorylated proteins and are often found in signalling pathways. Coiled-coil domains are present in structural proteins supporting the formation of permanent protein-protein interactions.

4 Aims of this Project

Cep170 is a centrosomal protein which localises to the subdistal appendages of the mother centriole. Previously studies have uncovered a role of the subdistal appendages in MT anchoring (Mogensen et al. 2000). Particularly, Ninein has been studied in detail. It was found that Ninein anchors the minus ends of the MTs at the subdistal appendages. However, less is known about whether Ninein acts alone or together with other proteins. The aim of this study was to examine the involvement of Cep170 in MT anchoring and its interplay with Ninein.

Recently, it was also discovered that the appendage proteins ODF2 and Cep164 function in ciliogenesis. Thus, the second part of this thesis focused on the question, of which role Cep170 might play in the ciliary life cycle and which proteins interact with the amino terminus of Cep170. Two interactors, IFT81 and PRAX-1, were further characterised. In particular, the role of IFT81 during the assembly of the PC was addressed to explain the function of Cep170 during PC disassembly.

5 Results

In a first series of experiments, we explored the role of Cep170 in MT anchoring and studied its interaction with Ninein. In the second part we examined the function of Cep170 during PC disassembly and the functional relevance of its interaction with the intraflagellar transport protein IFT81.

Cep170 can be divided into an N-terminal half (aa 1-754) and a C-terminal half (aa 755-1460). Although the C-terminal fragment binds to MT and bundles them, it still localises to the subdistal appendages (Guarguaglini et al. 2005). Interestingly, this fragment is also phosphorylated by Plk1, whereas the N-terminal fragment is not phosphorylated (Guarguaglini et al. 2005). The phosphorylation could occur within a serine-rich domain (aa 968-1228). As described below, we could show that the C-terminal half of Cep170 interacts with Ninein and stabilizes MT through binding. Additionally, the C-terminal fragment controls the binding to the subdistal appendages and phosphorylation by Cdk1-cyclin B leads to release from the subdistal appendages.

5.1 Cep170 or Ninein depletion affect MT anchoring

It was known that Ninein is required for the anchoring of MTs at the centrosome (Mogensen et al. 2000; Delgehyr et al. 2005). Because both Ninein and Cep170 localise to the subdistal appendages of the mother centriole we considered it possible that Cep170 has a similar function. To check for defects in MT anchoring in cells lacking Cep170, MT regrowth experiments were performed. COS7 cells (Figure 9) or alternatively A549 cells (Figure 10) were treated with siRNA duplexes specific for Cep170 or Ninein. After 72 h of siRNA treatment MT network was depolymerised by the incubation of cells on ice for 40 min. Afterwards, MT, were polymerised by the addition of 37 °C warm medium to the cells. Cells were fixed after 0 min, 2 min, 4 min, 8 min and 16 min and stained for α–tubulin.

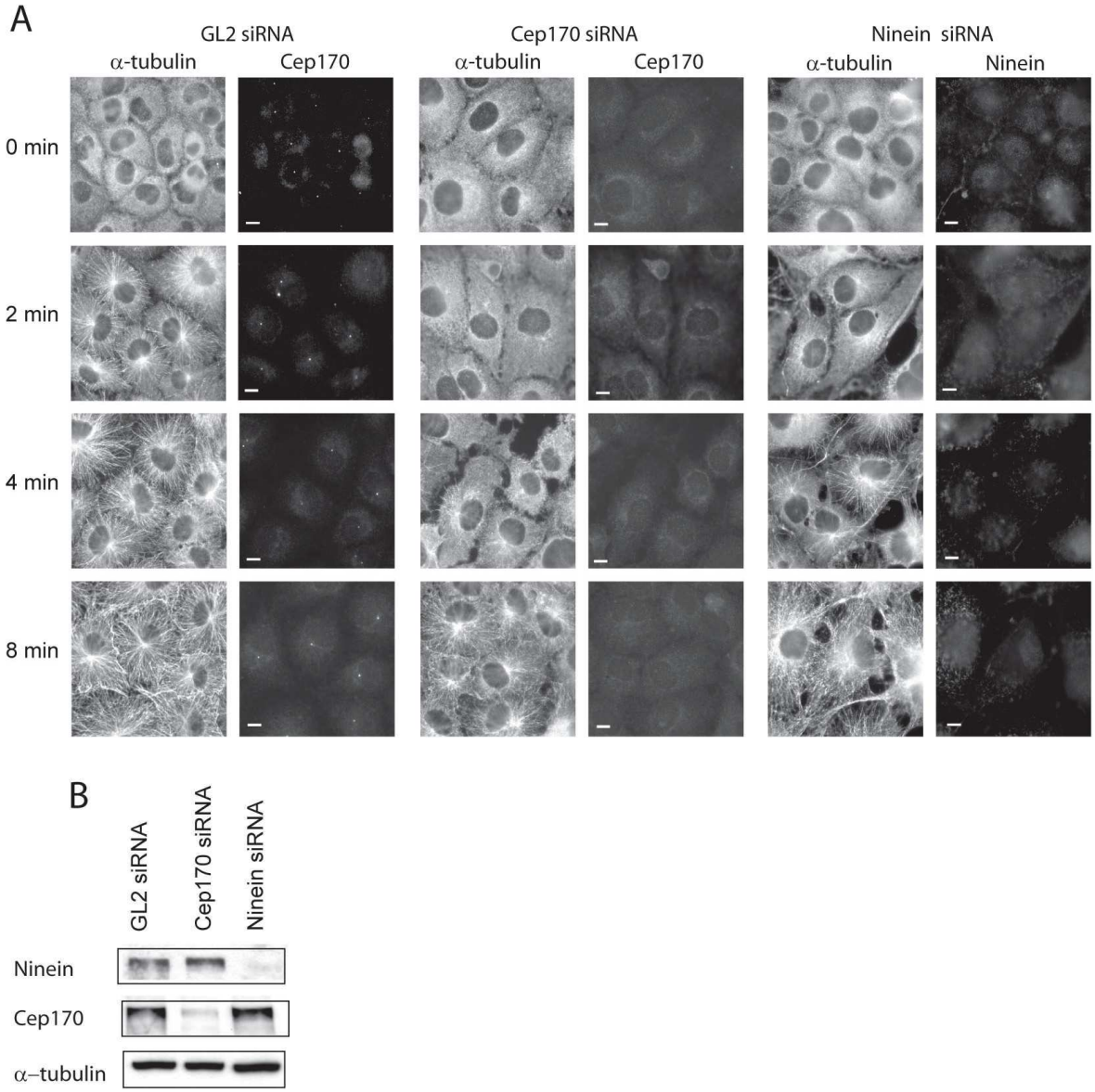

Figure 9. SiRNA mediated depletion of Cep170 and Ninein affects MT anchoring. COS7 cells were transfected for 72 h with control (GL2), Cep170- or Ninein-specific siRNA duplexes. They were then subjected to MT regrowth assays and fixed at the time points indicated. Cep170, Ninein and α–tubulin were visualized with appropriate antibodies. Bars: 10 µm. (B) Depletion efficiency was checked using Western blot analysis.

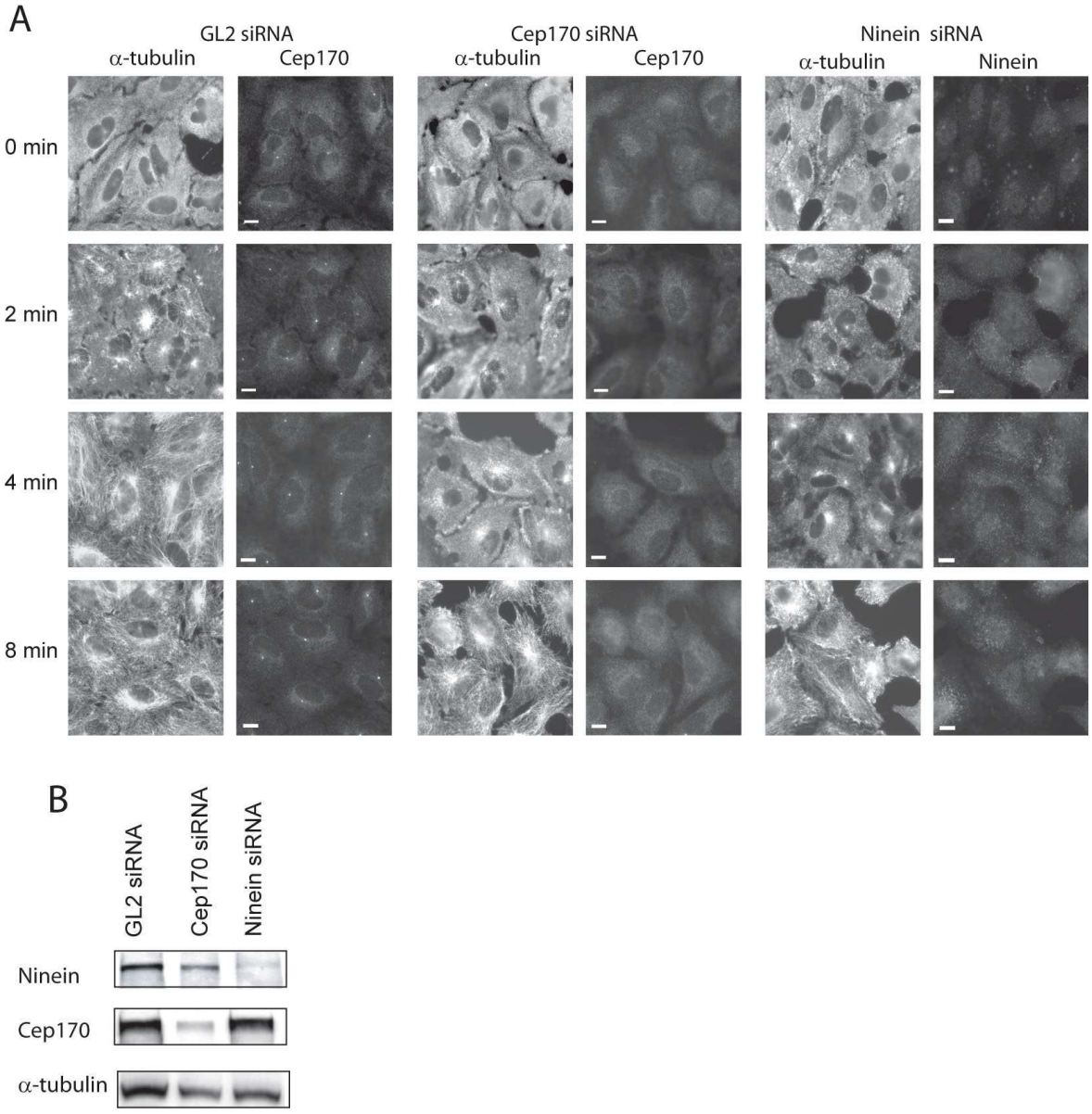

Figure 10. SiRNA mediated depletion of Cep170 and Ninein affects MT anchoring. A549 cells were transfected for 72 h with control (GL2), Cep170- or Ninein-specific siRNA duplexes. They were then subjected to MT regrowth assays and fixed at the time points indicated. Cep170, Ninein and α–tubulin were visualized with appropriate antibodies. Bars: 10 µm. (B) Depletion efficiency was checked using Western blot analysis.

As shown in Figures 9 and 10, depletion of Cep170 or Ninein inhibited the formation of a MT network. Even after 4 min of re-polymerisation the MT array was not completely

formed. These data support the idea that both Ninein and Cep170 are required for MT anchoring. However do they act together?

5.2 The localisation of Cep170 is dependent on Ninein

To find more evidence, for the hypothesis that Ninein anchors MT with the help of Cep170 the following experiments were performed: 1) Colocalisation studies and interdependency experiments using siRNA mediated protein depletion, 2) coimmunoprecipitation experiments of both endogenous proteins and tagged-proteins, 3) overexpression of different Ninein fragments to examine affect on Cep170 localisation and on MT anchoring.

To directly show that Cep170 colocalises with Ninein, U2OS cells were fixed and both proteins detected with specific antibodies.

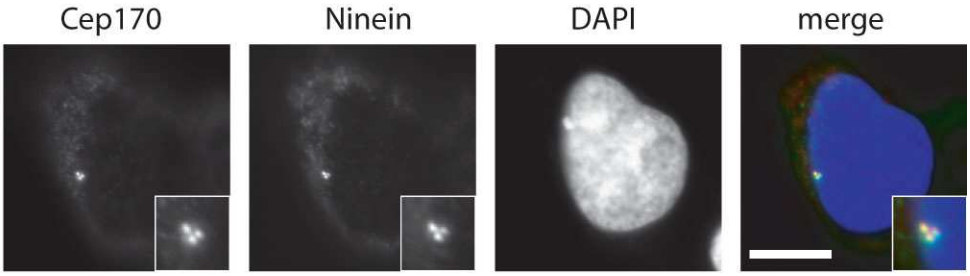

Figure 11. Ninein and Cep170 co-localises on the subdistal appendages. U2OS cells were co-stained with anti-Cep170 antibodies and anti-Ninein antibodies. DNA was stained with DAPI. Bars: 10 µm.

As shown in Figure 11, Cep170 co-localises with Ninein at the subdistal appendages of the mother centriole.

Additionally, the interdependency of Ninein and Cep170 localisation was examined using siRNA mediated protein depletion. U2OS cells were treated with siRNA for 72 h and depletion was confirmed by Western analysis (Figure 12). These interdependency experiments demonstrated that binding of Cep170 to the appendages is dependent on the presence of Ninein (Figure 12A). The reverse was not true. In the absence of Cep170 Ninein remained associated with the subdistal appendages of the mother centriole (Figure 12A). Taken together these findings point to a direct interaction of Ninein with Cep170.

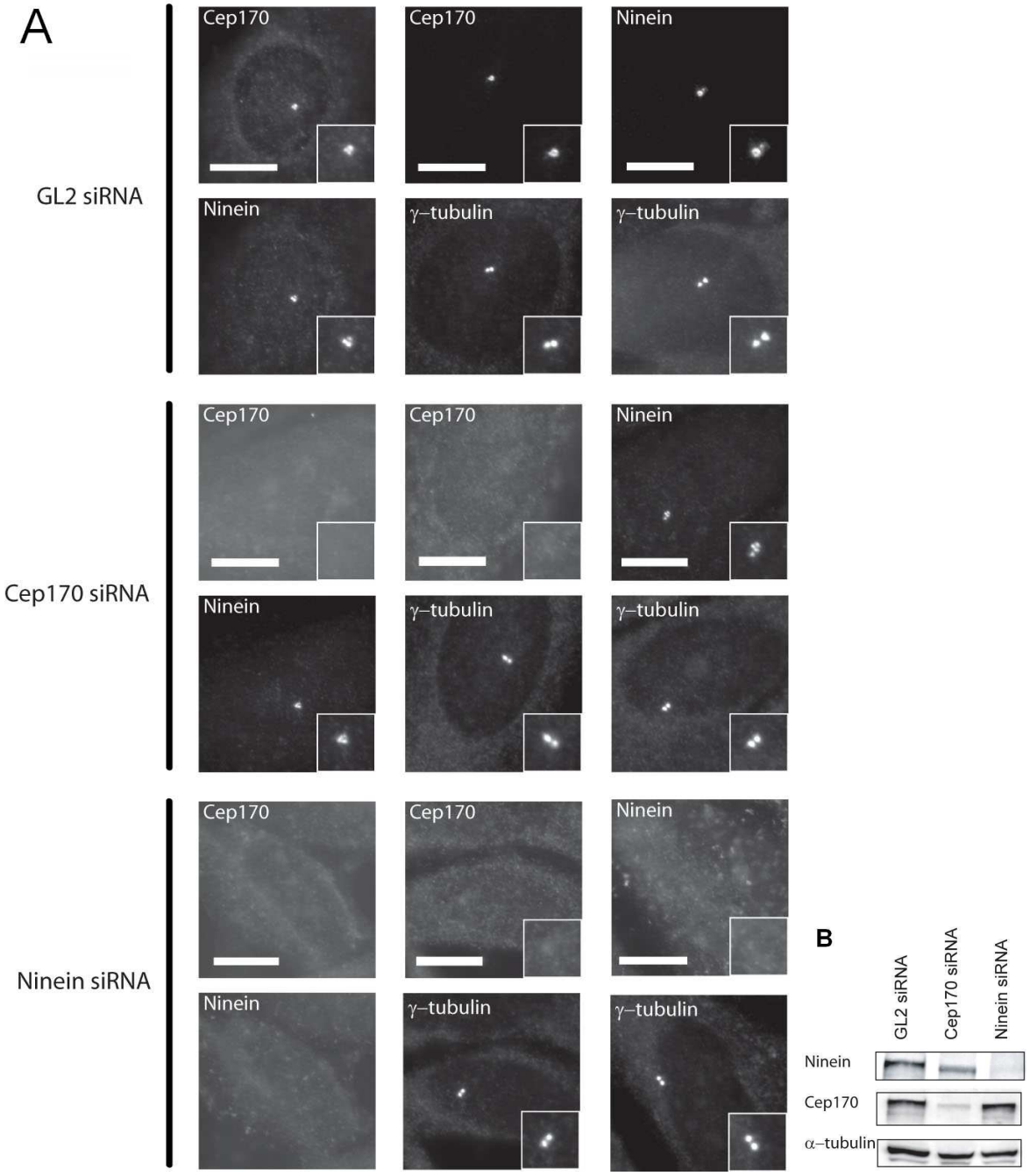

Figure 12. (A) Mutual dependency of Cep170 on Ninein. U2OS cells were transfected for 72 h with siRNA duplexes specific for Cep170, Ninein or with GL2 control siRNA duplexes and then co-stained with antibodies against Cep170 and Ninein (left columns), or Cep170 and γ–tubulin (centre columns) and or Ninein and γ–tubulin (right columns). Bars: 10 µm. (B) Depletion efficiency was monitored using Western blot analysis.

5.3 The C-terminal half of Cep170 interacts with Ninein

To address the question of whether Ninein interacts with Cep170, coimmunoprecipitation experiments were performed. As shown on Figure 13A Ninein could be coimmunoprecipitated Cep170 and vice versa, suggesting a direct interaction between both proteins. To characterise the interaction of Ninein with Cep170 GFP-Cep170 (1-750), GFP-Cep170 (750-1459) and GFP-Cep170 (1-1459) constructs were transiently expressed in 293T cells. After 48 h, cells were lysed and GFP tagged proteins were immunoprecipitated with 1 µg anti-GFP antibody for 1 h at 4 °C. Subsequently, the endogenous Ninein was detected by Western analysis. GFP-tagged full length Cep170 (aa 1-1459) and the C-terminal half of Cep170 (aa 751-1459) precipitated endogenous Ninein (Figure 13B). Additionally GFP tagged fragments of Ninein were expressed in HEK293T cells. In total, three fragments covering full length Ninein were used: an N-terminal fragment (GFP-Ninein (1-719)), a fragment covering a middle part of Ninein (GFP-Ninein (720-1470)) and a C-terminal fragment (GFP-Ninein (1471-2114)). The experimental conditions were the same as described above, except that endogenous Cep170 was detected by Western analysis (Figure 13C). Interestingly, the middle part of Ninein and the C-terminal fragment immunoprecipitated endogenous Cep170 (Figure 13C).

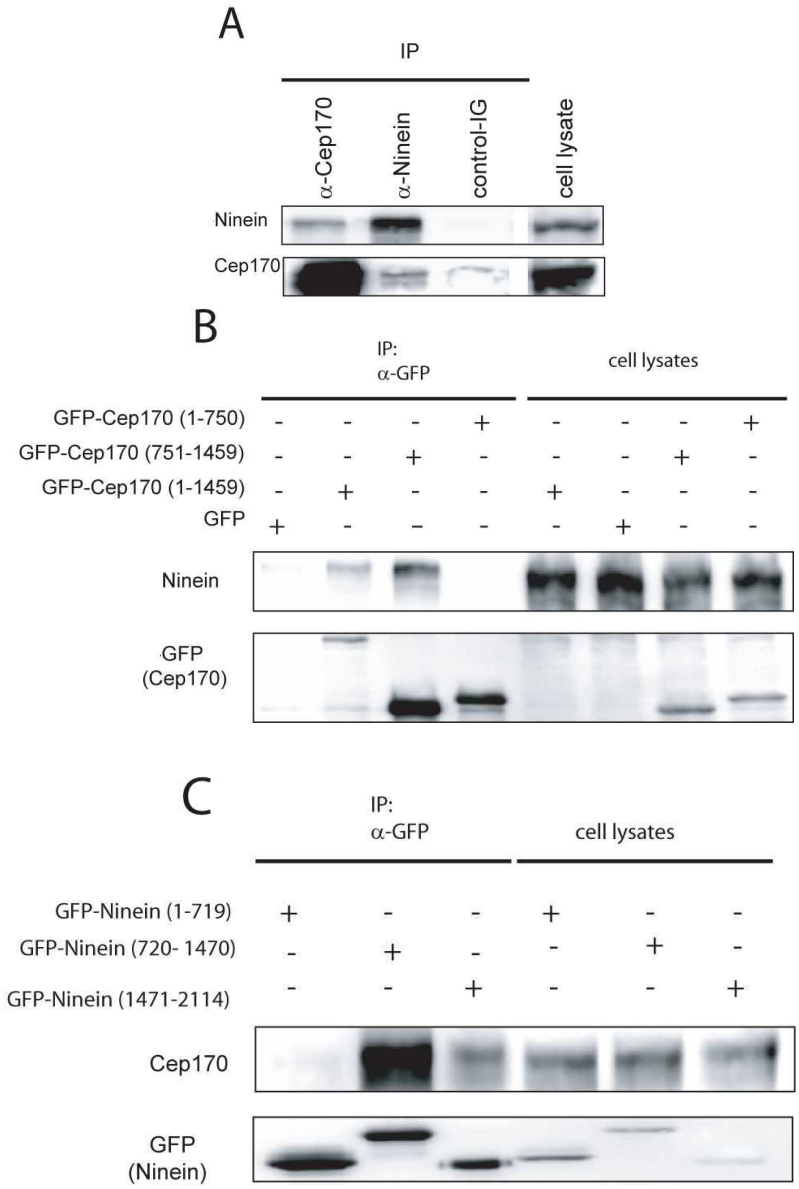

Figure 13. Cep170 interacts with Ninein. (A). Endogenous Cep170 and Ninein were immunoprecipitated from HEK293T cell lysate. Anti-myc antibody was used as control. Immunoprecipitated proteins were then analysed by Western blotting, using the indicated antibodies (B) Ninein interacts with the C-terminal fragment of Cep170 (GFP-Cep170 (751-1459)). Immunoprecipitation experiments were performed after transfection of the indicated plasmids, using anti-GFP antibodies coupled to beads. Immunoprecipitated proteins were then analysed by Western blotting, using anti-Ninein and anti-GFP antibodies. (C) Cep170 interacts with GFP-Ninein (720-1470) and with GFP-Ninein (1471-2114). Immunoprecipitation experiments were performed after transfection of the indicated plasmids, using anti-GFP antibodies coupled to beads. Immunoprecipitated proteins were then analysed by Western blotting, using anti-Cep170 and anti-GFP- antibodies.

To confirm these findings a directed Y2H assay was performed. An N-terminal fragment of Cep170 (Cep170 (1-785) and the C-terminal part (Cep170 (786-1459) were cloned into pFBT (gift from Dr. Francis Barr, Max-Planck Institute of Biochemistry). Different Ninein constructs encoding for an N-terminal, middle part and a C-terminal part of Ninein were already cloned into pAct2 vectors (gift from X. Yan, Max-Planck-Institute of Biochemistry). Because some Ninein constructs were self-activating, 5 mM 3-amino-1,*2*,4-triazole (3-AT) was added to the medium.

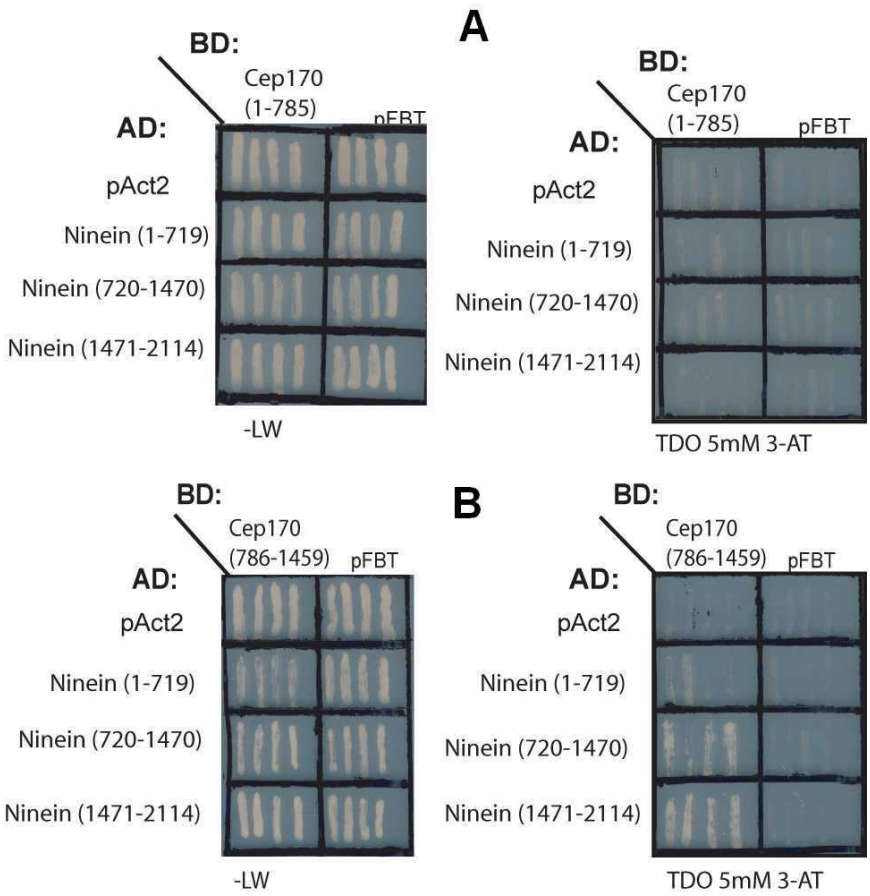

Figure 14. Mapping the interaction region between Cep170 and Ninein. (A)Yeast two-hybrid analyses of the interaction between Cep170 (1-785) and different Ninein fragments. The control panels are on the left side, the selective conditions on the right side. (B) Yeast two-hybrid analyses of the interaction between Cep170 (786-1459) and the indicated Ninein fragments.

In contrast to Cep170 (786-1459), the Cep170 (1-785) fragment did not interact with any of the Ninein fragments. Under selective conditions (H-,W-,L-) the transformed yeast cells could not grow (Figure 14A). Yeast cells harbouring the middle part of Ninein (aa 720-1470) and the C-terminal fragment (aa 1471-2114) were able to grow under selective conditions (Figure 14B). Taken together these results show that the C-terminal half of Cep170 (755-1460) directly interacts with the middle part of Ninein (720-1470) and with the C-terminus of Ninein (1470-2114). All these findings support the idea that Ninein recruits Cep170 via binding to its C-terminal half. The presence of Ninein at the subdistal appendages is clearly required for the targeting of Cep170 to the subdistal appendages, but what is the functional relevance of this interaction?

5.4 Expression of different Ninein fragments affect Cep170 localisation and MT anchoring

Ninein anchors MT at the centrosome and overexpression or depletion of Ninein causes MT anchoring defects (Mogensen et al. 2000; Delgehyr et al. 2005). Delgayr and collegues showed that the transient expression of a C-terminal fragment of Ninein (aa 1874-2113) inhibits the anchoring of the MTs and displaces endogenous Ninein and γ-tubulin. They concluded that the loss of endogenous Ninein caused defects in MT anchoring. Below we will present findings which suggest that Ninein requires Cep170 for the anchoring of the MTs.

To test whether expression of different Ninein constructs displaces Cep170, COS7 cells were transiently transfected with GFP-Ninein (1-719), GFP-Ninein (720-1470) and GFP-Ninein (1471-2114). 24 h after transfection, cells were fixed in methanol and subsequently the localisation of Cep170 was analysed using immunofluorescence microscopy. Additionally, the localisation of γ-tubulin and pericentrin was assayed.

Both transient expression of the middle part of Ninein (GFP-Ninein (720-1470)) and of the C-terminal fragment (GFP-Ninein (1471-2114)) displaced endogenous Cep170 (Figure 15). In line with previous findings the transient expression of the C-terminus of Ninein also displaced γ-tubulin but not pericentrin (Delgehyr et al. 2005). Expression of GFP-Ninein (720-1470) had no effect on γ-tubulin or pericentrin (Figure 15). And finally, expression of

GFP or GFP-Ninein (1-719) had no influence on the localisation of Cep170, γ–tubulin or pericentrin (Figure 15). These results confirm the findings of the interaction studies according to which GFP-Ninein (720-1470) and GFP-Ninein (1471-2114) interact with GFP-Cep170 (750-1459).

To test the contribution of correctly localised Cep170 on MT anchoring, MT regrowth experiments were performed in cells transiently expressing GFP-Ninein (1-719), GFP-Ninein (720-1470) and GFP-Ninein (1471-2114). COS7 cells were transfected with the various Ninein constructs and 24 h later, MT were depolymerised as described previously, followed by repolymerisation for 8 min. After fixation of the cells, the formation of the MT network was detected using specific antibodies for α-tubulin. Localisation of Cep170 was also detected by a specific antibody.

Transient expression of GFP-Ninein (720-1470) or GFP-Ninein (1471-2114) caused MT anchoring defects in COS7 cells (Figure 16). No MT network was formed in cells expressing GFP-Ninein (720-1470) or GFP-Ninein (1471-2114), whereas expression of GFP or GFP-Ninein (1-719) had no effect on MT anchoring (Figure 16).

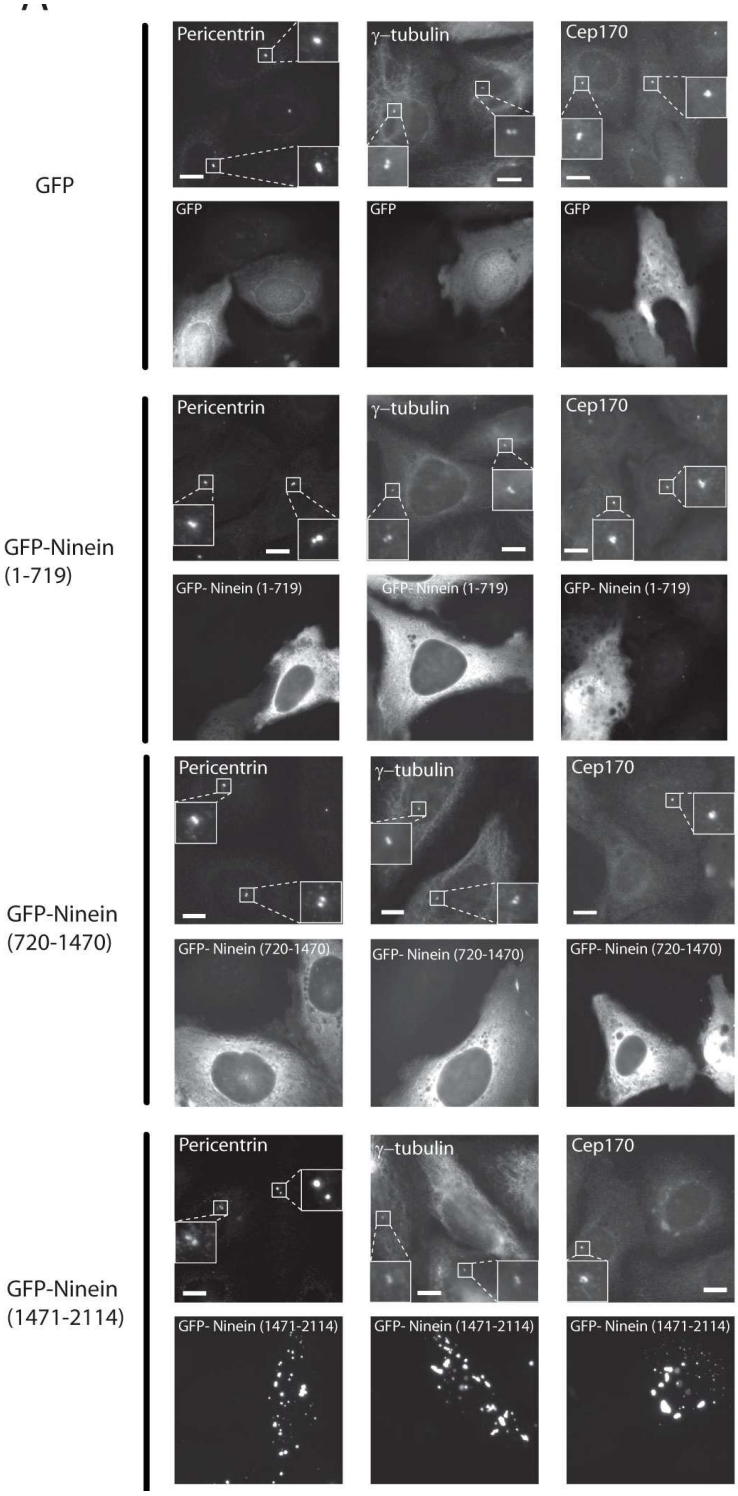

Figure 15. Loss of Cep170 after transient expression of GFP-Ninein (720-1470) and of GFP-Ninein (1471-2114) and loss of γ–tubulin after transient expression of GFP-Ninein (1471-2114). COS7 cells were transfected with the indicated Ninein constructs for 48 h. Cells were stained with antibodies against pericentrin (left column), γ–tubulin (centre column) and Cep170 (right column). Bars: 10 µm.

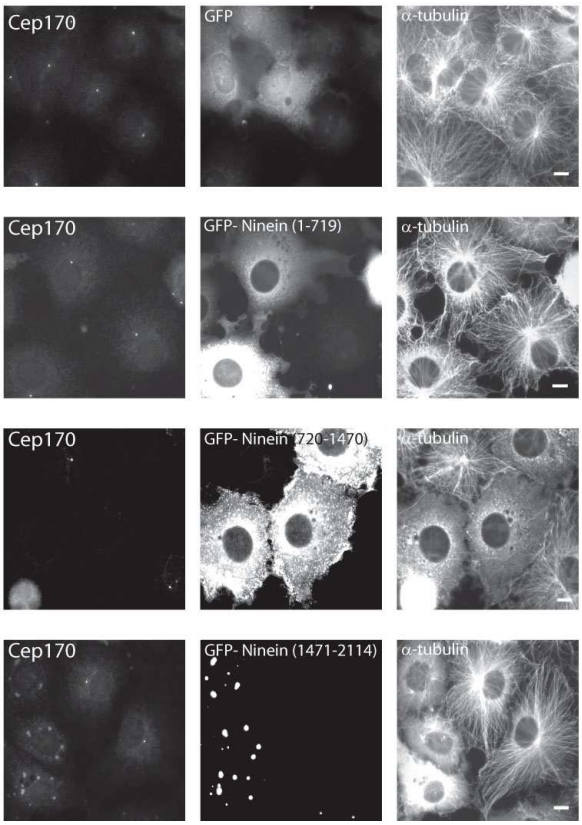

Figure 16. Transient expression of different Ninein constructs affect MT anchoring. COS7 cells were transfected for 48 h with GFP (first row), GFP-Ninein (1-719) (second row), GFP-Ninein (720-1470) (third row) and GFP-Ninein (1471-2114) (bottom row). They were then subjected to MT regrowth assays (8 min incubation in 37 °C warm medium). Cep170 and α–tubulin were visualized with appropriate antibodies. Bars: 10 µm.

To determine how tightly the displacement of Cep170 correlate with MT anchoring defects, three independent experiments were performed and in total 1200 cells were counted.

Four different cell population were distinguished:

1. Cells **with** Cep170 at the mother centriole / **without** MT regrowth defects
2. Cells **without** Cep170 at the mother centriole / **without** MT regrowth defect
3. Cells **with** Cep170 at the mother centriole / **with** MT regrowth defects
4. Cells **without** Cep170 at the mother centriole / **with** MT regrowth defects

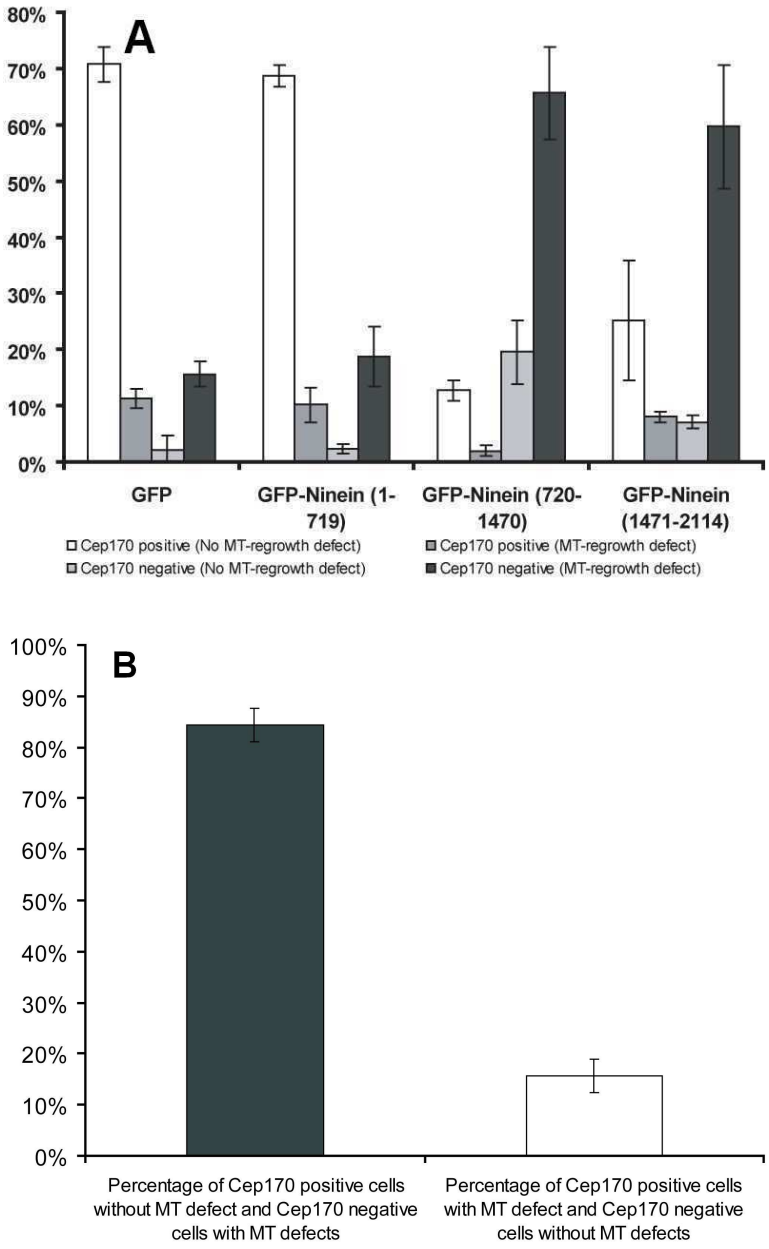

Figure 17. Quantification of the effect of transient Ninein expression on Cep170 localisation and on MT anchoring. (A) COS7 cells were transfected for 48 h with GFP, GFP-Ninein (1-719), GFP-Ninein (720-1470) and GFP-Ninein (1471-2114). They were then subjected to MT regrowth assays (8 min incubation in 37 °C warm medium). Cep170 and α–tubulin were visualized with appropriate antibodies. (B) The following populations of cells were grouped together: Cells with Cep170 at the centriole and without MT anchoring defects plus cells without Cep170 at the centriole and with MT anchoring defect (left bar) or cells with Cep170 at the centriole and with MT anchoring defect plus cells without Cep170 at the centriole and without MT anchoring defects (right bar).

Cells expressing GFP or GFP-Ninein (1-719) showed almost the same distribution of different cell populations. Around 70 % of the cells had a normal MT network with bound Cep170 at the subdistal appendages of the centrioles and only 10 % - 20 % of the cells had no Cep170 at the appendages and defects in MT anchoring (Figure 17A). This distribution changed completely in cells expressing GFP-Ninein (720-1470) or GFP-Ninein (1471-2114). In these cases, most of the cells, around 60 % -70% , showed no Cep170 at the appendages and defects in MT anchoring (Figure 17A).

We thus conclude that expression of GFP-Ninein (720-1470) or GFP-Ninein (1471-2114) resulted in MT anchoring defects, which were associated with the displacement of Cep170 from the appendages.

According to another representation of these data we can distinguish, on the one hand, a population of cells which supports the idea that Cep170 is required for the anchoring of the MTs (Populations 1 and 4) and, on the other hand, a population which does not support this idea (Populations 2 and 3). Around 85 % of all cells belong to population 1 or 4, clearly supporting the conclusion that Cep170 is needed for MT anchoring (Figure 17B).

In summary, the above data clearly demonstrated that Cep170 is required for the anchoring of the MT at the centrosome and that the MT anchoring defect observed in Ninein overexpressing cells can mainly be explained by the displacement of Cep170 from the appendages.

5.5 The C-terminus of Cep170 bundles MT *in vivo* and *in vitro*

In the previous part we could demonstrate that Ninein targets Cep170 to the appendages of the centrosome and that this is required for the anchoring of MTs. So how could Cep170 affect the formation of MT arrays? Of interest in this context, we demonstrated that the C-terminal half of Cep170 was preferentially bound to MT and bundles them (Guarguaglini et al. 2005). Indeed, we could find that high levels of GFP-Cep170 (755-1459) or GFP-Cep170 (755-1407) strongly bundled MT when transiently expressed in U2OS cells for 48 h (Figure 18A).

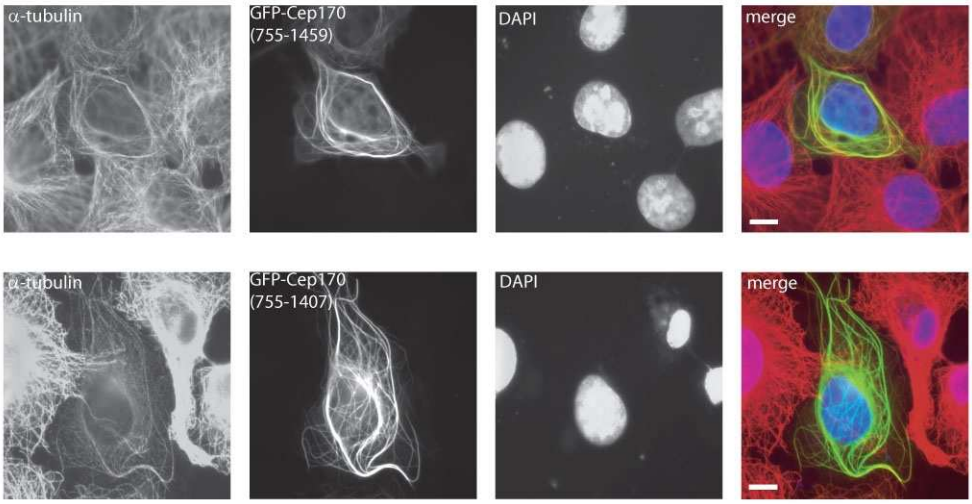

Figure 18. Transient expression of GFP-Cep170 (755-1459) or GFP-Cep170 (755-1407) bundles MTs. U2OS cells were transiently transfected for 48 h with plasmids encoding GFP-Cep170 (755-1459) (upper row) or GFP-Cep170 (755-107) (lower row) 48 h. α–tubulin were visualized with an appropriate antibody and DNA was stained with DAPI. Bars: 10 µm.

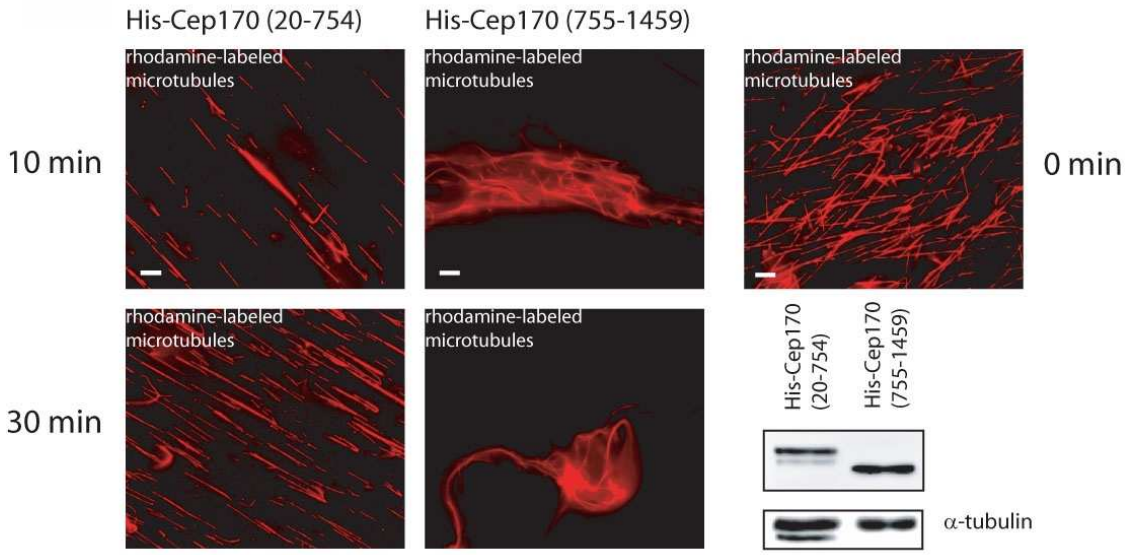

Figure 19. His-Cep170 (755-1459) bundles MTs *in vitro*. Rhodamine labelled MTs were incubated for the indicated time with recombinant His-Cep170 (20-754) (left column) as a control and with His-Cep170 (755-1459) (right column). Bars: 10 µm. The samples were subjected to Western analysis and proteins were detected by anti-His and anti-α tubulin antibodies.

To confirm that Cep170 is able to bundle MTs without a need for additional cofactors, a *in vitro* bundling assay was performed. His-tagged C-term Cep170 (aa 755-1459) and His-tagged N-term Cep170 (aa 1-754) were purified after expression in *E coli*. For *in vitro* bundling assays, 20 µg of rhodamine labelled MTs were incubated at 25 °C with 400 ng human His-Cep170 (20-754) or with His-Cep170 (755-1459). Samples were taken after 0 min, 10 min and 30 min and bundling activity was observed by microscopy. Bundling of MTs could only be observed in the sample containing His-Cep170 (755-1459 (Figure 19). After 10 min almost all MT were bundled, and after 30 min these bundles were further concentrated. His-Cep170 (20-754) did not bundle MT at all (Figure 19). These findings suggest that Cep170 can bundle MT without requiring any additional proteins.

5.6 The MT binding domain of Cep170

Next we asked, which amino acids mediate the binding of Cep170 to the MTs. To address this issue, different truncated versions Cep170 were generated and expressed in COS7 cells for 48 h. Staining of samples with antibodies against α–tubulin allowed the determination of the Cep170 region required for bundling and binding of MTs.

Expression of GFP-Cep170 (755-1429) or GFP-Cep170 (755-1407) strongly bundled MT (Figure 20).When the fragment was further shortened to aa 755-1175, the bundling activity was almost lost, though it was still bound to MTs (Figure 20). Finally, GFP-Cep170 (755-1136) could not bind to MT anymore. Truncations of the N-terminal site decreased MT bundling activity, though the fragment was still bound to MT (GFP-Cep755-1459). Further truncations completely abolished MT (GFP-Cep170 1085-1459) binding (Figure 20). Taken together, these results show that Cep170 binds MTs through a domain comprising aa 1013-1175. Prolongation of the C-terminus increased MT bundling activity (Figure 20). Interestingly, this minimal MT binding domain is rich in arginine and lysines, in contrast to the full length Cep170. Thus it can be speculated that interactions between MT and this basic domain occurs through electrostatical interactions.

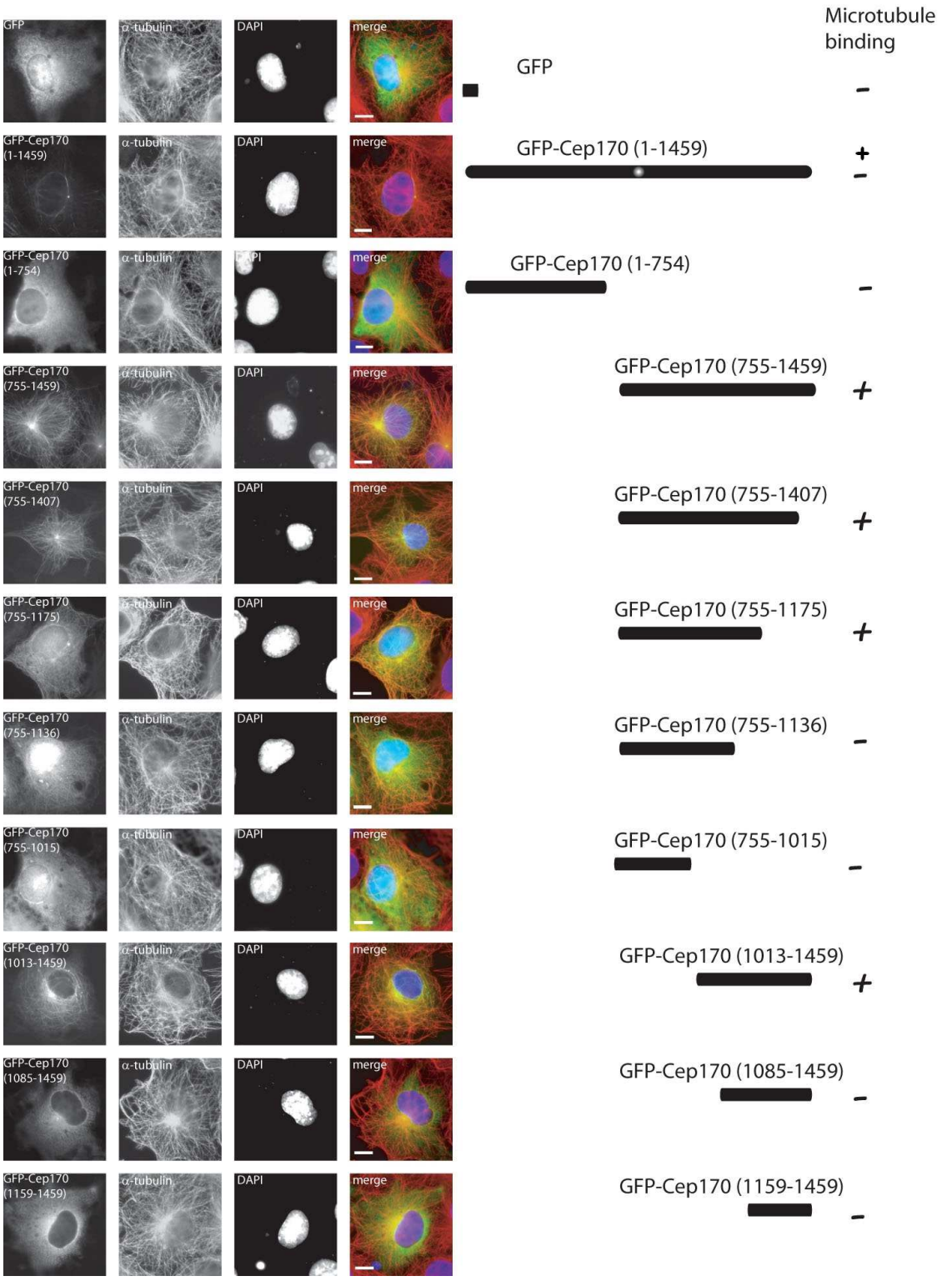

Figure 20. Mapping of the MT binding domain of Cep170. COS7 cells were transfected for 48 h with plasmids encoding different GFP-tagged Cep170 fragments. α–tubulin was visualized with appropriate antibody and DNA was stained with DAPI. Bars: 10 µm.

5.7 Cep170 depletion destabilises the MT network

To test whether Cep170 can stabilise MTs *in vivo* two different experiments were performed. First, the stability of Cep170 induced MT bundles was compared to that of unbundled MTs and second, the stability of the MT network was tested after reduction of Cep170 levels by siRNA mediated protein depletion.

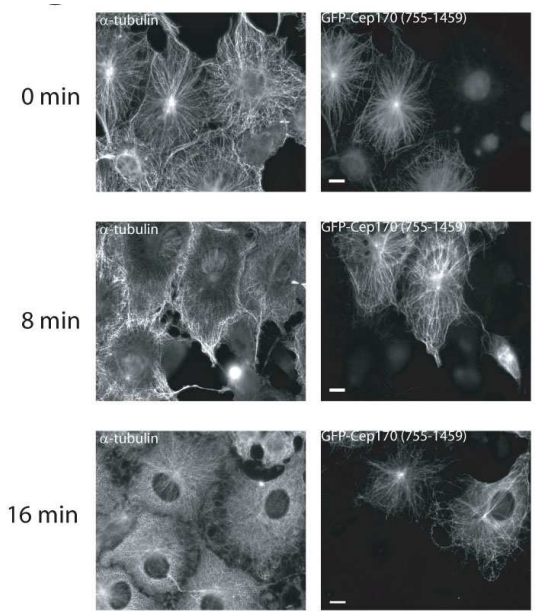

Figure 21. GFP-Cep170 (755-1459) MT bundles are less sensitive to low dose nocodazole treatment. COS7 cells were transfected with the indicated construct for 48 h before cells were treated with 0, 1 µM nocodazole for the indicated time. α–tubulin was visualized with appropriate antibody (left row). Bars: 10 µm.

COS7 cells transiently expressing GFP-Cep170 (755-1459) were treated with 0,1 µM nocodazole for 0 min, 8 min and 16 min and then stained with anti-α-tubulin antibodies. MT-Cep170 bundles were less sensitive to nocodazole treatment than unbundled MTs that could be seen in non-transfected cells (Figure 21). Already, 8 min after nocodazole addition almost all unbundled MT were depolymerised. In contrast, the bundled MT were unaffected. This effect is even stronger after 16 min of nocodazole treatment. The unbundled MT were depolymerised, whereas MT-Cep170 bundles could still be observed (Figure 21).

In a second experiment Cep170 levels were reduced by siRNA-mediated depletion for 72 h. Subsequently, MTs were destabilized by the addition of 0,1 µM nocodazole to the medium for 0 min and 14 min and samples were further processed as described above.

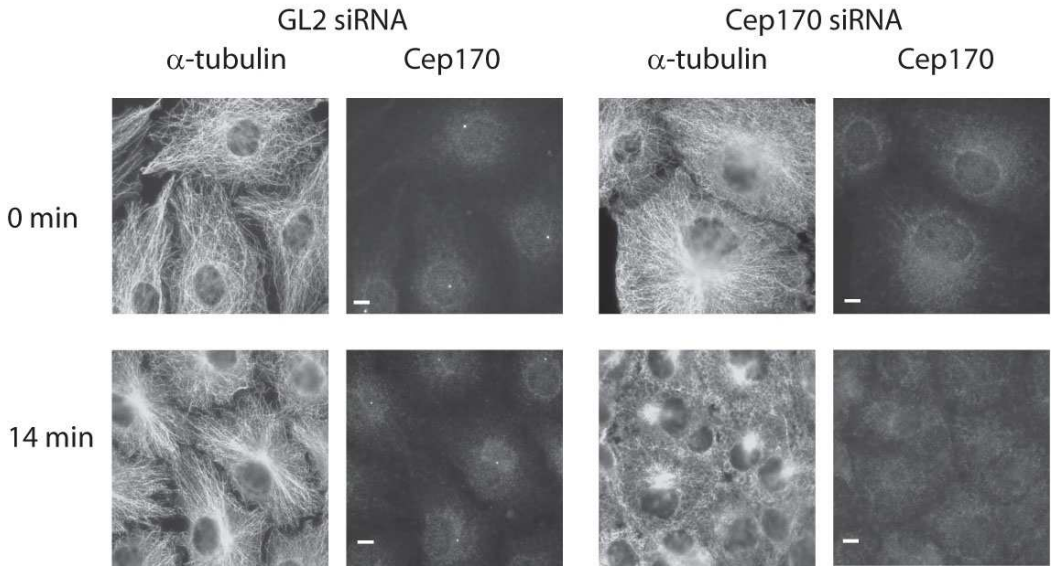

Figure 22. siRNA mediated depletion of Cep170 reduces the stability of MT arrays. COS7 cells were transfected for 72 h with control (GL2) and Cep170-specific siRNA duplexes. They were then treated with 0,1 µM nocodazole for the times indicated. Cep170 and α–tubulin were visualized with appropriate antibodies. Bars: 10 µm.

Depletion of Cep170 reduced the stability of the MT network (Figure 22). MT were depolymerised in cells lacking Cep170, whereas MT in control cells still stable (Figure 22).

In summary, we could show that Ninein requires Cep170 for the anchoring of MTs at the subdistal appendages. Loss of Ninein resulted in delocalisation of Cep170, causing MT anchoring defects. The C-term of Cep170 binds and bundles MTs which results in a stabilisation of MT. Thus we conclude that Cep170 stabilises the MT by bundling them. This in turn supports the formation of a stable interphase MT network.

5.8 Cdk1 regulates the localisation of Cep170

Guarguaglini and coworkers previously showed that Cep170 is phosphorylated by Plk1, but, the functional relevance of this phosphorylation has not been elucidated (Guarguaglini et al. 2005). Besides Plk1, several other kinases control progression through mitosis. In particular, Cdk1-cyclin B is a key regulator of mitosis.

To have a closer look at the possible role of phosphorylation of Cep170, we examined the localisation of Cep170 during nuclear envelope breakdown (NEB). After fixation, U2OS cells were stained with antibodies specific for Lamin A and Cep170.

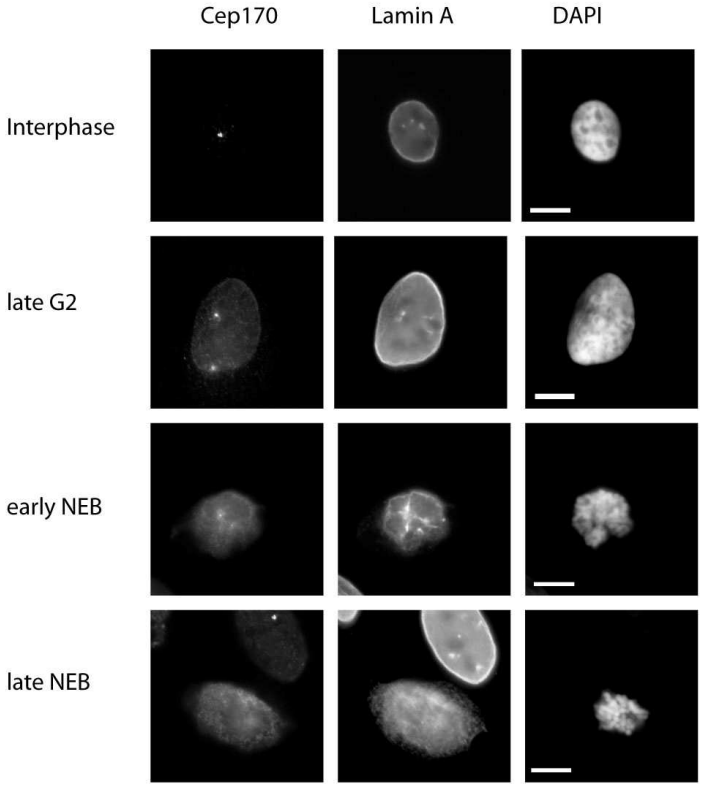

Figure 23. Cep170 is displaced from the centriole at late NEB. U2OS cells were fixed and Lamin A, Cep170 were detected with specific antibodies. DNA was stained with DAPI. Bars: 10 µm.

We found that Cep170 remained associated with the centrosome until late G2 (Figure 23). In G2 cells, both centrioles were Cep170 positive. However, as soon as the nuclear envelope started to break down, the Cep170 signal faded away (Figure 23). Thus, the displace-

ment of Cep170 from the centrosome occurs concomitantly with NEB, a mitotic event which is regulated by Cdk1-cyclin B. This finding suggest that Cep170 might be phosphorylated by Cdk1.

To further explore this possibility, mitotic cells were treated with a Cdk1-cyclin B inhibitor. If the localisation of Cep170 is indeed regulated by phosphorylation, the inhibition of phosphorylation should retarget Cep170 to the centriole. COS7 cells were arrested in metaphase wit 100 nM nocodazole and subsequently treated with 100 µM of the Cdk1 inhibitor roscovitine. In parallel, cells were also incubated with 1 µM of the Plk1 inhibitor TAL. Cep170 localisation was then examined by immunofluorescence microscopy.

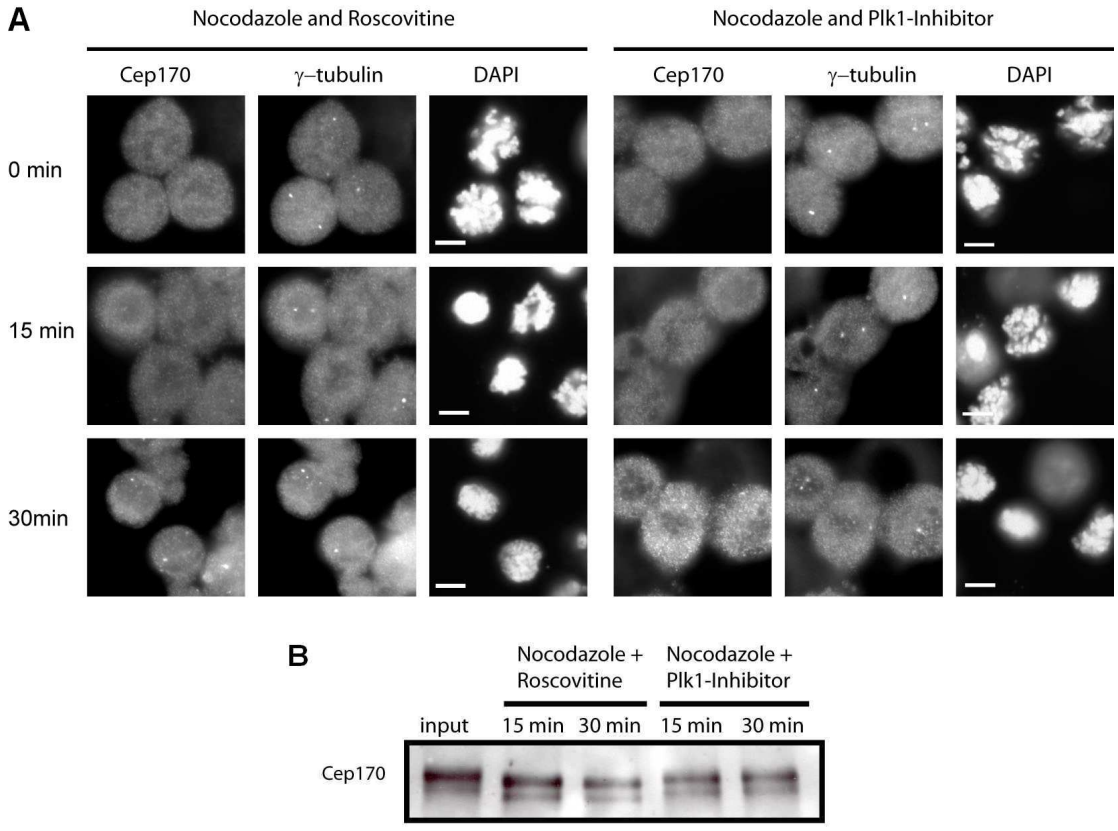

Figure 24. Roscovitine treatment retargets Cep170 to the centrioles. (A) COS7 cells were arrested in mitosis by incubation for 12 h in medium containing 100 nM nocodazole. Then, cells were treated with roscovitine or the Plk1 inhibitor TAL and fixed after 0 min, 15 min and 30 min. Cep170 and γ–tubulin were detected with specific antibodies. DNA was stained with DAPI. Bars: 10 µm. (B) COS7 lysates was analysed with Western analysis. Proteins were separated on a 4 % PAGE gel and transferred to a nitrocellulose membrane. Cep170 was detected with a specific antibody.

Surprisingly, Cep170 was retargeted to the centrioles after 30 min of roscovitine treatment (Figure 24A), whereas Plk1 inhibition for 30 min had no influence on Cep170 localisation (Figure 24A). In parallel, cells were lysed and proteins were separated by gel electrophoresis. After separation in a 4 % polyacrylamid gel, proteins were transferred to a nitrocellulose membrane and Cep170 was detected by antibody (Guarguaglini et al. 2005). In line with previous findings, roscovotine treatment induced a downshift of Cep170 already after 15 min, and the effect was even more pronounced after 30 min. In contrast, inhibition of Plk1 did not change the electrophoretic running behaviour of Cep170. These results suggest that Cdk1 phosphorylates Cep170 and thereby regulates its localisation.

To test whether Cep170 is directly phosphorylated by Cdk1 and dephosphorylated by Cdc14a, an *in vitro* kinase- and phosphatase assay was performed.

GFP-fusion proteins encoding N-term Cep170 (1-755) or C-term Cep170 (755-1460) were *in vitro* transcribed using T7-polymerase and then *in vitro* translated (Promega, *in vitro* translation assay). Afterwards, proteins were precipitated with 1 µg of anti-GFP antibody and washed with kinase buffer (BRB80). Proteins were phosphorylated with Cdk1-cyclin B for 30 min at 30 °C in the presence of ^{32}P-γ-ATP. Reactions were stopped by washing with phosphatase buffer containing EDTA. One half of the reaction mixture was treated with Cdc14a-wt phosphatase and the other with a catalytically inactive Cdc14a mutant for 30 min. Then, the samples were boiled and proteins were separated and transferred onto a nitrocellulose membrane. Phosphorylation was determined by autoradiadiography. Myc-tagged PRC1 was used as a positive control. Fusion proteins were further detected by anti-GFP antibody, anti-Cep170 antibody (specific for C-term Cep170) and by anti-myc antibody (9E10).

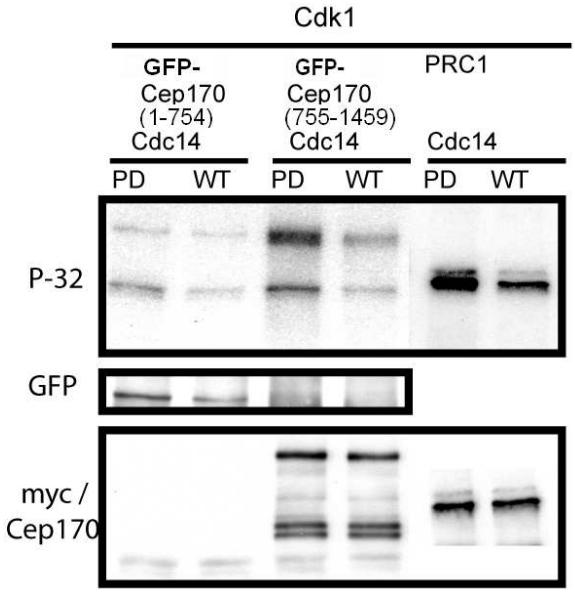

Figure 25. GFP-Cep170 (755-1459) is phosphorylated by Cdk1-cylin B and dephosphorylated by Cdc14a *in vitro*. Plasmids encoding GFP-Cep170 (1-754), GFP-Cep170 (755-1459) and myc-PRC1 as positive control were *in vitro* translated and immunoprecipitated with antibodies coupled to beads. Then, proteins were phosphorylated with Cdk1-cyclin B at 30 °C for 30 min and one aliquot was further treated with Cdc14a phosphatase at 30 °C for 30 min. Proteins were separated on a 10 % PAGE gel and transferred onto a nitrocellulose membrane. Phosphorylation was detected with an X-ray film. Protein amounts were checked with anti-GFP-antibody, anti-Cep170 antibody and anti-myc antibody.

Only GFP-Cep170 (755-1459) was phosphorylated by Cdk1 (Figure 25). GFP-Cep170 (1-754) was not phosphorylated. As expected, PRC1 was an excellence substrate for Cdk1-cyclin B (Neef et al. 2007). Interestingly, addition of Cdc14a phosphatase could revert phosphorylation of Cep170 *in vitro*.

These data suggest that Cdk1 directly phosphorylates Cep170 within its C-terminus (aa 755- 1459) at least *in vitro*. The C-terminus of Cep170 interacts with Ninein and Cep170 and Ninein interaction targets Cep170 to the subdistal appendages of the mother centriole. Phosphorylation of Cep170 by Cdk1-cyclin B within this region might control localisation of Cep170 in mitosis. This phosphorylation could be counteracted by the phosphatase Cdc14a.

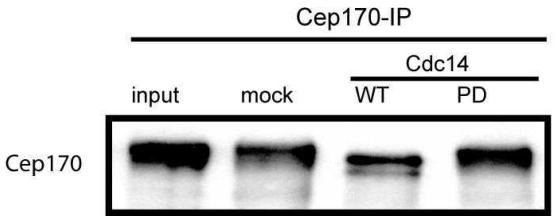

Figure 26. Cdc14a dephosphorylates Cep170, which was immunoprecipitated from mitotic extract. Cep170 was immunoprecipitated by an antibody coupled to beads which were incubated in mitotic HeLaS3 extract. Precipitated Cep170 was incubated with Cdc14a PD ("phosphatase dead" mutant; right row) or with Cdc14a WT (third row from the left) at 30 °C for 30 min. Proteins were separated on a 4 % SDS-PAGE gel and transferred on a nitrocellulose membrane. Cep170 was detected with specific antibody.

This model is further supported by the fact that Cdc14a could dephosphorylate endogenous Cep170 (Figure 26). Endogenous Cep170 was immunoprecipitated from mitotic extract. HeLaS3 cells were arrested in metaphase by 100 nM nocodazole and lysed with lysis buffer. Cep170 was immunoprecipitated using mouse monoclonal antibody (72-372) and treated with Cdc14a WT or PD for 30 min at 30 °C. Afterwards beads were washed and boiled in 2x SDS-gel sample buffer. Protein was separated on a 4 % gel. After transfer onto a nitrocellulose membrane, Cep170 was detected by rabbit-anti Cep170 antibody.

In summary, the above data suggests the following: Cdk1 regulates the binding of Cep170 to the appendages by phosphorylation of the C-term of Cep170. This occurs during NEB when activity of Cdk1-cyclin B rises sharply. Plk1 might phosphorylate Cep170 after Cdk1 phosphorylation and both kinases might then control centriole binding or MT binding. The displacement of Cep170 at the beginning of NEB, then disassembles the subdistal appendages, which in turn may support the formation of a highly dynamic spindle. At the end of mitosis, Cdc14a dephosphorylates Cep170 and thus allows the re-formation of a stable interphase MT array.

5.9 Yeast two hybrid interactors of Cep170

The N-terminus of Cep170 contains a putative FHA domain, a predicted NLS and two putative SH3-ligand domians (aa 545-551; aa 754-751). To find interacting proteins of the N-term Cep170, a Y2H-screen was done. The N-term of Cep170 was cloned into pFBT as a bait (gift from Francis Barr, Max-Planck-Institute of Biochemistry). Plasmids were transfected into yeast strain PJ69-4A and subsequently cotransfected with a cDNA-library from Clontech. The cDNA was derived from HEK293T cells and cloned into pAct2 vector. The transformants were plated onto medium lacking histidine, leucine , tryptohane and adenine. After two weeks at 30 °C, the DNA of the positive clones was isolated, tested for selfactivation and finally sequenced. In total seventy-one positive clones were found on the selective medium and twenty of them were not self activating. Five clones contained a sequence coding for Kiaa0162 and five clones coded for IFT81. Kiaa0162 encodes a 200 kDa protein which was formerly found to interact with the benzodiazepine receptor and thus called peripheral-type benzodiazepine receptor-associated protein 1 or PRAX-1 (Galiegue et al. 1999). IFT81 was identified as a component of the intraflagellar transport complex B. It is a coiled-coil protein which builds a structural core component of this subcomplex, interacting with IFT72 and IFT74 (Lucker et al. 2005). Additionally, when IFT81 is mutated in zebrafish, polycystic kidneys develop (Sun et al. 2004).

5.10 Bioinformatic characterisation of PRAX-1 and IFT81

To analyse both proteins for putative domains, their amino acid sequences were examined using SMART and PFAM algorithms. PRAX-1 is a 200 kDa (aa 1-1857) protein with three predicted SH3 domains, three fibronectin-like domains, one coiled-coil domain and a predicted NLS (Figure 27). The first SH3 (SH3 (1)) locates at the N-terminus (aa 653-720), whereas SH3 (2) and SH3 (3) are at the very end of the C-terminus (aa 1625-1693 and aa 1764-1831). The three fibronectin like domains form a cluster (aa 791-1066) and the NLS (aa 346-350) is located within the N-terminal half. The predicted coiled-coil region locates within the N-terminus (aa 120-520).

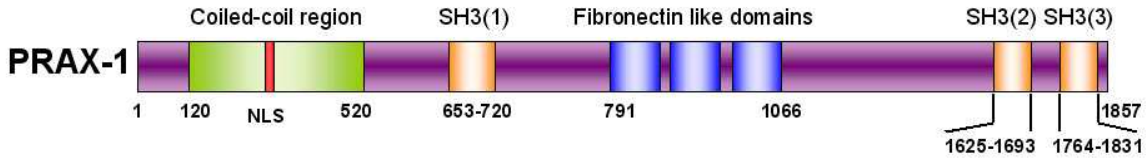

Figure 27. Schematic illustration of PRAX-1. PRAX-1 consists of a N-terminal coiled-coil region, three SH3 domains and a cluster of fibronectin like domains in the centre of the protein.

SH3 domains are protein-protein interaction domains which recognizes proline-rich peptides. They are often found in transient protein complexes and proteins within signalling pathways. In contrast, structural proteins often contain coiled-coil domains allowing permanent protein-protein interactions.

IFT81 is a 80 kDa protein and a pure coil coiled protein (Figure 28). As mentioned before it forms a core component with IFT72/74 for the building of the subcomplex B. IFT81 is required for ciliogenesis and mutations cause polycystic kidneys (Sun et al. 2004; Lucker et al. 2005).

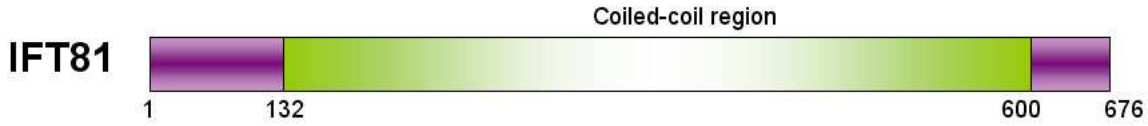

Figure 28. Schematic illustration of IFT81. IFT81 consists of a central coiled-coil region almost covering the whole protein.

5.11 PRAX-1 and IFT81 localise to the mother centriole

To test whether PRAX-1 and IFT81 localise to the mother centriole, both proteins were cloned into a pEGFP vector and expressed for 48 h in U2OS cells. Both proteins (GFP-IFT81 (1-676) / GFP-PRAX-1(1-1875)) localise to one centriole (Figure 29 and Figure 30). To mark centrosomes, antibodies specifically detecting pericentrin or γ-tubulin were used.

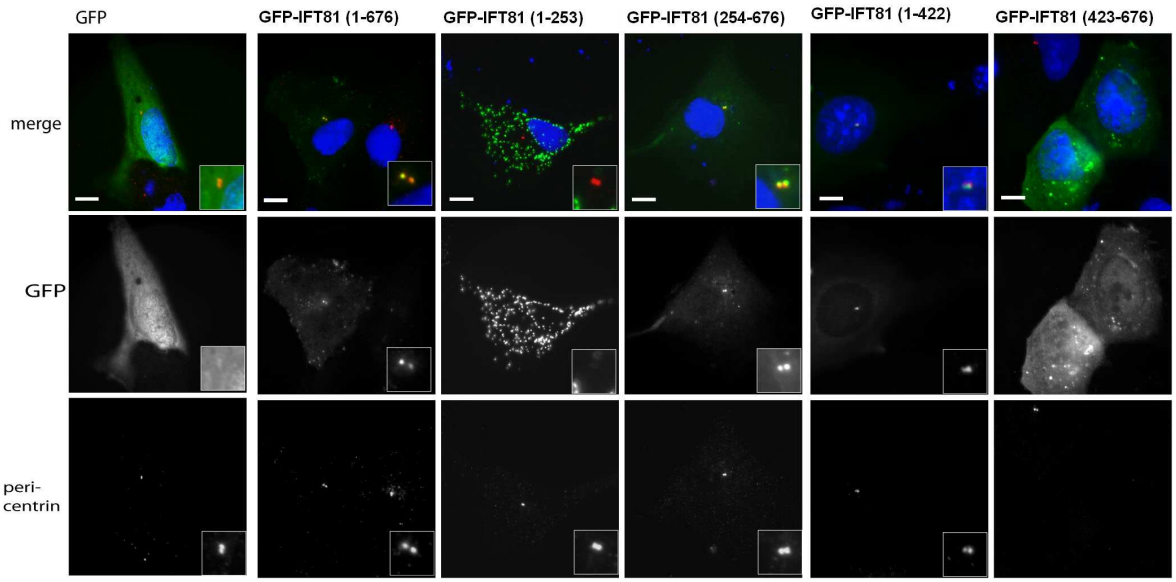

Figure 29. GFP-IFT81 (1-676) localises preferentially to one centriole. U2OS cells were transfected for 48 h with different plasmids encoding the indicated fragments. After fixation of the cells, centrosomes were detected with an antibody specific for pericentrin. Bars: 10 µm.

To map the centrosome targeting domains in the two proteins different constructs were produced and transiently expressed in U2OS cells. Full-length IFT81 (GFP-IFT81(1-676)) only bound to one centriole. This was also true for an N-terminal fragment of IFT81 (GFP-IFT81 (1-422)) (Figure 29). In contrast, GFP-IFT81 (254-676) localised to both centrioles. GFP-IFT81 (1-253) and GFP-IFT81 (423-676) formed insoluble aggregates (Figure 29). This latter phenomenon can often be observed when overexpressing coiled-coil proteins (Andersen et al. 2003). In conclusion, IFT81 needs the N-terminal half to localise to one centriole.

Similar results were observed for the transient expression of full length PRAX-1 (GFP-PRAX-1 (1-1857). Interestingly, FL-PRAX-1 not only bound to one centriole, but it actually formed a star like structure around their centriole. However, this could only be seen at low levels of expression. If FL-PRAX-11 was highly overexpressed, it assembled aggregates and localised to the nucleus (Figure 30).

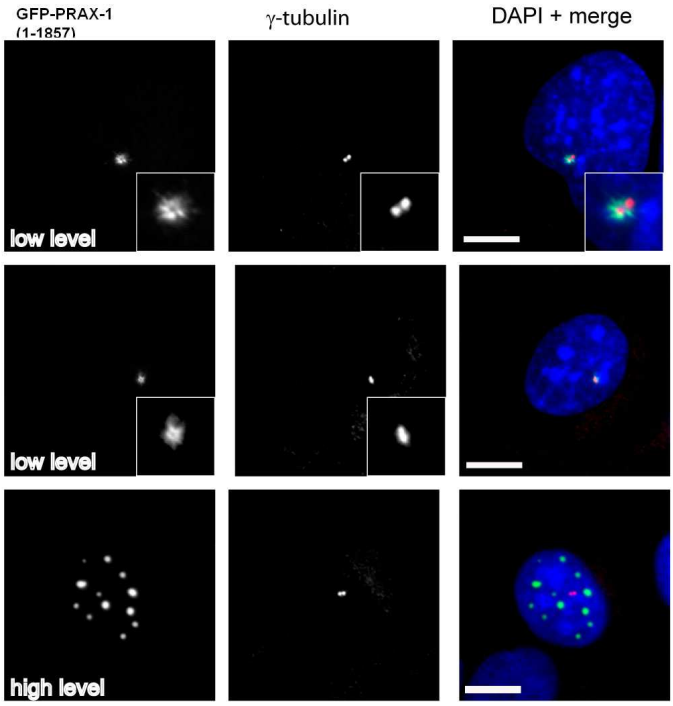

Figure 30. Localisation of GFP-PRAX-1 (1-1857) to the centriole or to the nucleus depends on the expression levels. GFP-PRAX-1 (1-1857) was transiently expressed in U2OS for 48 h. Centrosomes were detected with an antibody specific for γ–tubulin, DNA was stained with DAPI. GFP-PRAX-1-1 (1-1857) is bound to one centriole when present at low abundances; when abundant it localised to the nucleus. Bars: 10 µm.

To demonstrate the binding of PRAX-1 to the mother centriole, U2OS transiently expressing GFP-PRAX-1 (1-1857) were co-stained with an antibody specific for Ninein. The star-like structure of overexpressed PRAX-1 co localised with Ninein, confirming that FL-PRAX binds to the subdistal appendages of the mother centriole (Figure 31).

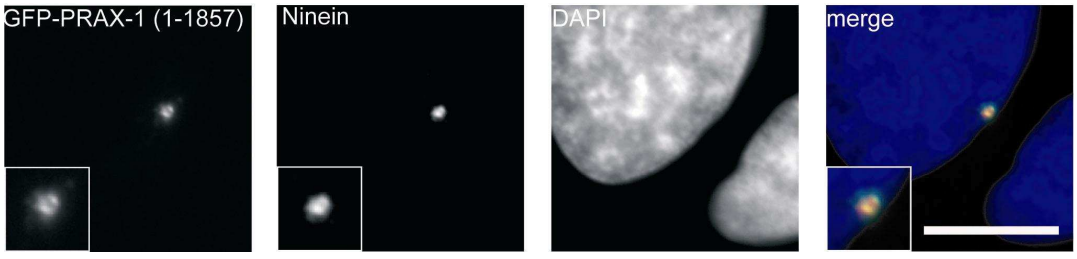

Figure 31. GFP-PRAX-1 (1-1857) co-localises with Ninein. U20S cells were transfected for 48 h with a plasmid encoding for GFP-PRAX-1 (1-1857). After fixation Ninein was detected with specific antibody and DNA was stained with DAPI. Bars: 10 µm.

To further map the domain required to PRAX-1 binding to the mother centriole the following GFP-tagged constructs were produced: fragment missing the last two SH3 domains (GFP-PRAX-1 (1-1459)); an N-terminal fragment comprising aa 1-655 (GFP- PRAX-1(1-655)) and a C-terminal fragment spanning aa 656-1857 (GFP- PRAX-1(655-1857)). These constructs were transiently expressed in U2OS cells for 48 h. After fixation of the cells centrosomes were detected by a specific anti-γ-tubulin antibody (Figure 32).

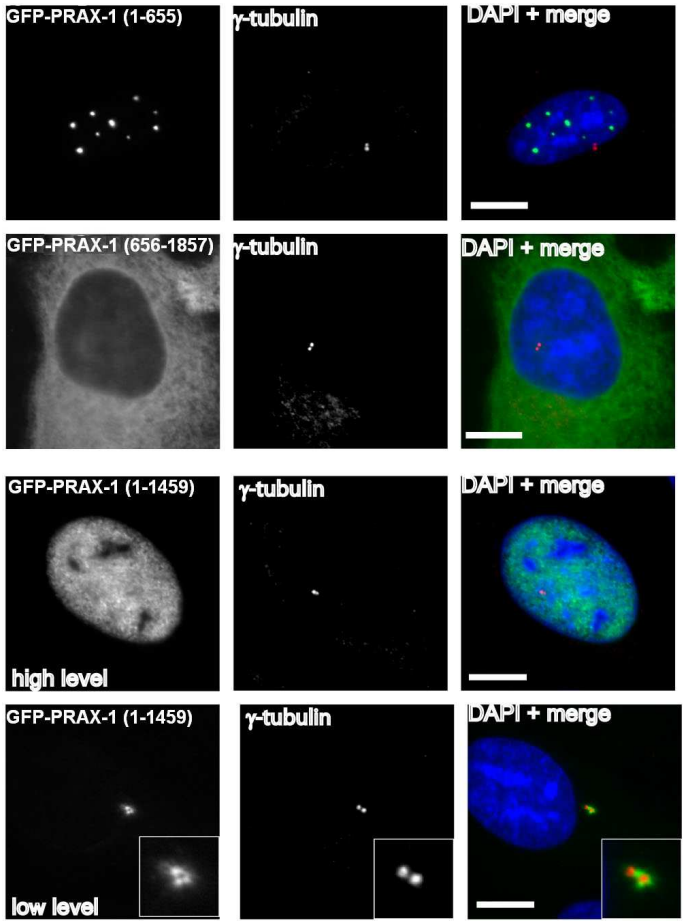

Figure 32. Localisation of GFP-PRAX-1-1 (1-1857) to the centriole or to the nucleus depends on the expression level. GFP-PRAX-1 (1-655) is nuclear and GFP-PRAX-1-1 (656-1857) is cytoplasmic. U2OS cells were transfected with the different constructs for 48 h and after fixation centrosomes were detected with an anti-γ-tubulin antibody. DNA was stained with DAPI. Bars: 10 µm.

Curiously, neither GFP-PRAX-1(1-655) nor GFP-PRAX-1(655-1857) localised to the centrosome. Only GFP-PRAX-1(1-1459) formed star-like structure around one centriole or was localised to the nucleus, depending on protein levels (Figure 32).

To explain these findings it is important to know that the first SH3 domain was destroyed in both the GFP-PRAX-1(1-655) and the GFP-PRAX-1(656-1857) constructs. The boundaries of both fragments lies in the first half of SH3 (1) (aa 653-720), probably explaining why neither of these fragments was able to localise to the centrioles. GFP-PRAX-1(1-655) was found in the nucleus, supporting the presence of an NLS.

5.12 The C-terminus of IFT81 determines localisation to the mother centriole

To map the regions in PRAX-1and IFT81 required for binding to Cep170 immunoprecipitation experiments were performed. GFP-tagged IFT81 and PRAX-1 were expressed in HEK293T cells for 48 h. Cells were lysed and GFP-fusion proteins were immunoprecipitated using of anti-GFP antibody. After separation on a 4-15 % gradient gel and transfer of the proteins to a nitrocellulose membrane, endogenous Cep170 was detected by a rabbit-antibody (Guarguaglini et al. 2005)

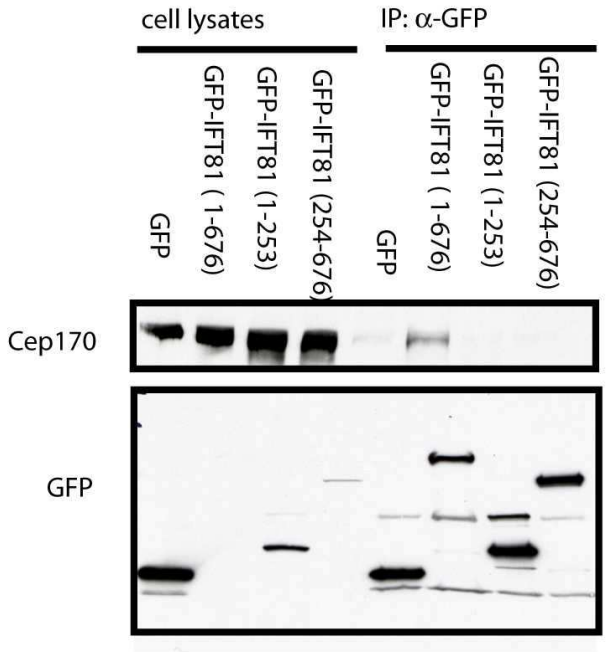

Figure 33. GFP-IFT81 (1-676) interacts with endogenous Cep170. Immunoprecipitation experiments were performed after transfection of the indicated plasmids into HEK293T cells. Anti-GFP antibodies were coupled to beads. Immunoprecipitated proteins were then analysed by Western blotting, using anti-Cep170 and anti-GFP antibodies.

Endogenous Cep170 could only be observed in the immunoprecipitate of FL-IFT81 (GFP-IFT81 (1-676), Figure 33). No Cep170 was precipitated by GFP-IFT81 (1-253) or GFP-IFT81 (254-676). These latter fragments also failed to localise to centrosomes (Figure 29). These results indicate that IFT81 might bind to the subdistal appendages through the interaction with Cep170.

The immunoprecipitation experiments using different PRAX-1 fragments could also confirm previous findings. Neither N-term PRAX-1 (GFP-PRAX-1 (1-655)) nor C-term PRAX-1 (GFP-PRAX-1 (656-1857)) immunoprecipitated Cep170 (Figure 34). In contrast, both FL-PRAX- (GFP-PRAX-1 (1-1875)) and PRAX-1 lacking SH3(2) and SH3(3) (GFP-PRAX-1 (1-1459)) were able to precipitate endogenous Cep170 (Figure 34). Both proteins formed a star-like structure around one centriole. These results indicate that both IFT81 and PRAX-1 might be recruited to the appendages by Cep170.

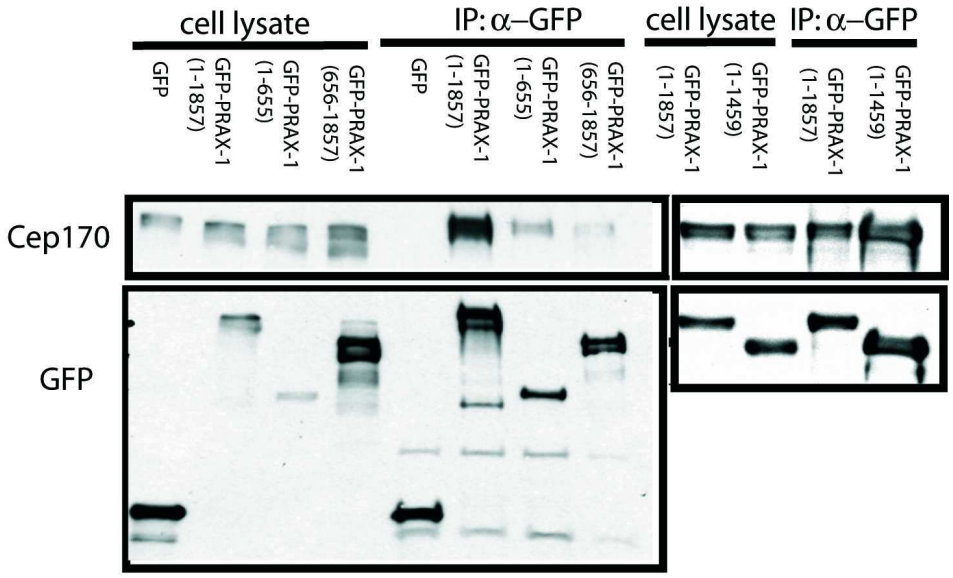

Figure 34. GFP-PRAX-1 (1-1857) and GFP-PRAX-1 (1-1459) interact with endogenous Cep170. Immunoprecipitation experiments were performed after transfection of the indicated plasmids into HEK293T cells. Anti-GFP antibodies coupled to beads were used for precipitation. Immunoprecipitated proteins were then analysed by Western blotting, using anti-Cep170 and anti-GFP antibodies.

5.13 SH3(1) of PRAX-1 determines localisation to the mother centriole

To further address the function of the SH3 domains within PRAX-1 two experiments were performed: First, extended C-term PRAX-1 fragment was constructed to recover the SH3(1) domain and second, GST pull downs were performed.

C-term PRAX-1 was chosen because of it is cytoplasmic localisation after transient expression. As expected, an extended GFP-PRAX-1 (492-1857) localised to one centriole (Figure 35). However, the cytoplasmic levels also remained high. In contrast, a shortened N-term of GFP-PRAX-1 (1-491) localised to the nucleus (Figure 35). So it seems that the first SH3 domain is needed for the binding of PRAX-1 to the mother centriole.

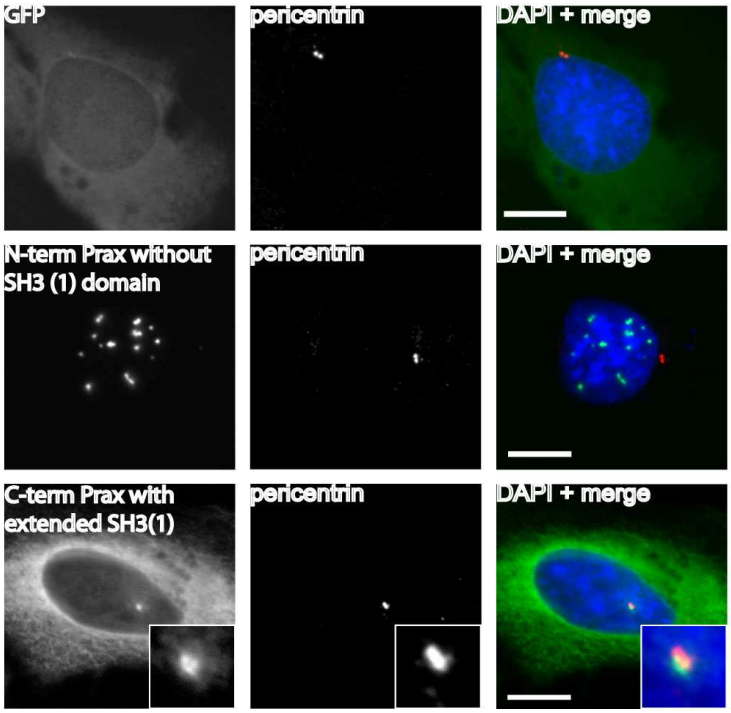

Figure 35. GFP-PRAX-1 (492-1857) localises to one centriole, GFP-PRAX-1 (1-491) is nuclear. U2OS cells were transfected with different constructs for 48 h and, after fixation centrosomes were detected with an anti-pericentrin antibody. DNA was stained with DAPI. Bars: 10 µm.

To address the question of whether SH3(1) might bind to Cep170 all SH3 domains were expressed as GST fusion proteins in *E. coli*. Proteins were purified under native conditions

using the following lysis buffer: 300 mM NaCl, 1 mM DTT, 50 mM Tris pH 7,5, 1 % Triton X-100, and further purified with gluthathione S sepharose.

For the pull downs, 2 µg of GST-tagged protein was incubated in 400 µl cell lysate. This was lysed by lysing HEK293T cells in lysis buffer (150 mM NaCl, 0,7 % NP-40, 40 mM Tris pH7,4, protease and phosphatease inhibitor (Roche)). GST-SH3 fusion proteins were pulled down with gluthathione S sepharose, washed and boiled in Laemmli buffer. After separation of the proteins in a 4-15% gradient gel, endogenous Cep170 was detected with a rabbit antibody (Guarguaglini et al. 2005).

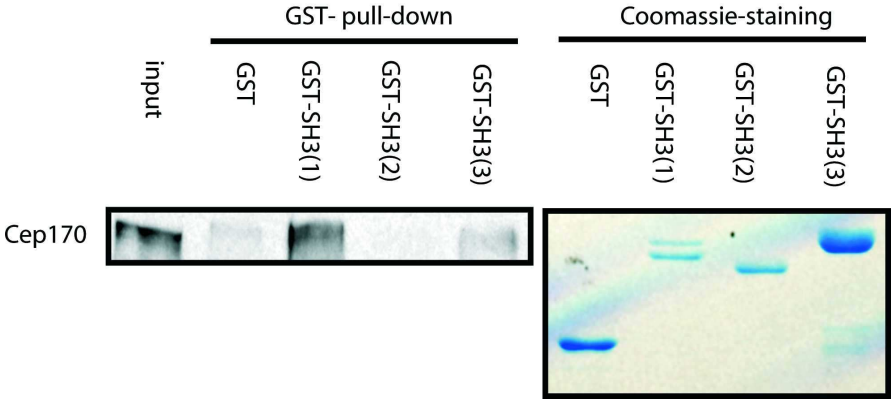

Figure 36. GST-SH3(1) pulls down endogenous Cep170. HEK293T lysate was incubated with 2 µg of GST-SH3(1) / (2) or (3) or with GST as a control. GST-fusion proteins were precipitated with glutathione S sepharose. Proteins were separated by gel electrophoresis and after blotting endogenous Cep170 was detected with a specific antibody.

Interestingly, the first SH3 domain pulled down most endogenous Cep170 (Figure 36). SH3(3) also pulled down some Cep170, however when correcting for the amount of used protein, clearly the SH3(1) had the highest affinity (Figure 36). This result falls in line with the previous findings suggesting that the first SH3 domain of PRAX-1 was required for binding to the mother centriole. Thus we propose that PRAX-1 binds to Cep170 through its SH3(1) domain and that this allows the recruitment to the mother centriole.

5.14 IFT81 in cell cycle

Subdistal appendage proteins are displaced from the mother centriole during mitosis. To determine whether this is also true for IFT81 antibodies were produced by immunization of rats. Subsequently, antibody was affinity purified. Two rats were immunized six-times with 100 µg of GST- IFT81 (1-676). Antibodies were purified on His-FL-IFT81 coupled to Affi-Gel 10 beads (Bio-Rad) and eluted with elution buffer (200 mM glycine, pH 2,7, 150 mM NaCl). Purified antibody was used in a final concentration of 0,2 µg/ml for Western analysis and immunofluorescence. Cell cycle dependency of the localisation of IFT81 was tested by immunofluorescence on hTERT-RPE1 (RPE1) cells. Cells were fixed and IFT81 was detected with the purified rat antibody. Anti-γ–tubulin antibody was used to detect the centrosomal marker γ–tubulin.

IFT81 was present at one centriole in interphase and disappeared from the centrosome in prometaphase (Figure 37A). It remained cytoplasmic throughout mitosis (Figure 37 A).

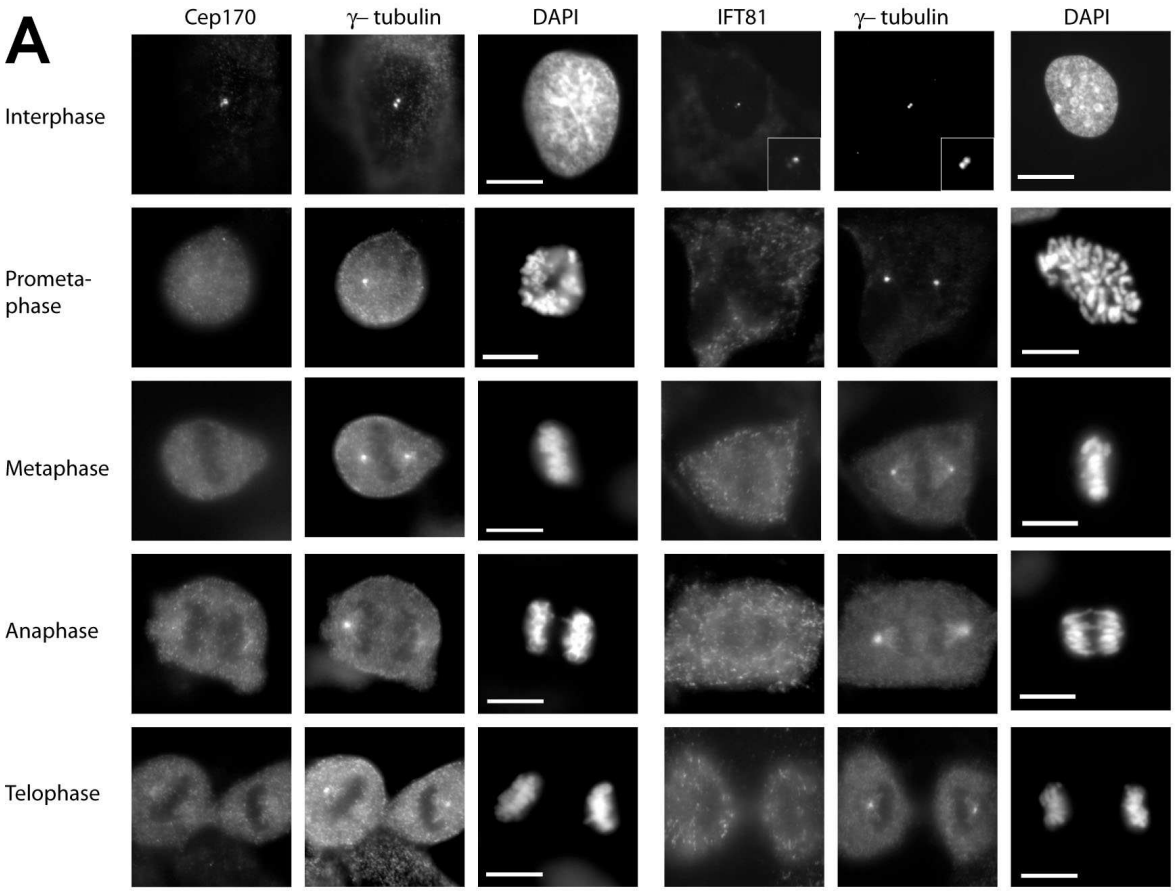

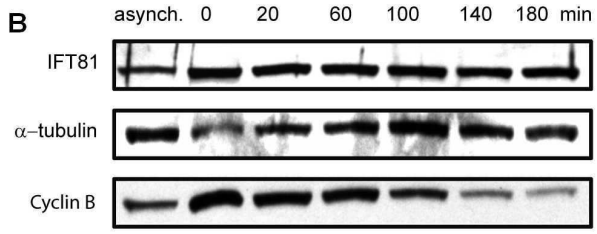

Figure 37. (A) IFT81 is displaced from the mother centriole during mitosis. RPE-1 cells were fixed and stained for IFT81 with affinity purified antibody. Centrosomes were detected with anti-γ-tubulin antibody, the subdistal appendages with anti-Cep170 antibody and DNA was stained with DAPI. Bars: 10 µm. (B) IFT81 levels are not reduced during mitosis. Mitotic HeLaS3 cells were released from nocodazole arrest. Cells were lysed at the indicated time points and proteins were subjected a Western analysis. Progression through mitosis was determined by changes in Cyclin B levels. IFT81, Cyclin B and α-tubulin were detected by antibodies.

We also asked whether the electrophoretic mobility of IFT81 changed during mitosis, due to posttranslational modifications. HeLaS3 cells were arrested in metaphase with 100 nM nocodazole. Then cells were released into PBS and lysed after 0 min, 20 min, 60 min, 100 min, 140 min and 180 min. The progression through mitosis was monitored by the degradation of cyclin B. IFT81 was not up shifted or degraded in mitosis (Figure 37B). Likely, IFT81 is not posttranslationally modified or degraded in mitosis.

5.15 IFT81 is both an appendage protein and a ciliary protein

To show that IFT81 is a appendage protein RPE1 cells were fixed and endogenous Cep170 and IFT81 were detected by immunofluorescence microscopy using specific antibodies.

To demonstrate that IFT81 is a protein in the PC, RPE1 cells were arrested in G0 by incubation with serum-free medium. After 48 h the MT network was depolymerised by incubation on ice for 40 min and cells were fixed. The PC was detected by an antibody specific for acetylated tubulin (T7451).

IFT81 only partially colocalised with Cep170 in normal dividing cells (Figure 38). Cep170 formed a ring like structure around one centriole and IFT81 localised as a tiny dot at the tip of the centriole. Not surprisingly, IFT81 colocalised with the ciliary marker (Figure 38). Additionally, ciliar IFT81 did not colocalise with Cep170 and IFT81 was not equally dis-

tributed within the cilium. It was concentrated at the base and at the tip of the cilium (Figure 38). These are the places in which proteins required for cilium formation are loaded onto or released from IFT particles.

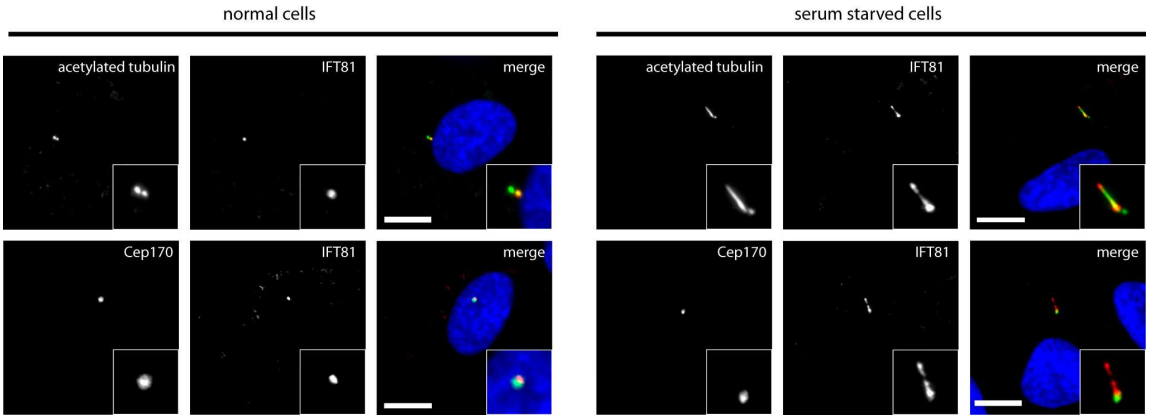

Figure 38. IFT81 co-localises with Cep170 at the centriole but not at the PC. Cycling RPE-1 cells or serum starved (48 h) RPE1 cells were fixed and acetylated tubulin was co-stained with IFT81 (upper row) and Cep170 (lower row). Bars: 10 µm.

To assess whether IFT81 might be more a distal appendage protein, RPE1 cells were also costained for Cep164 and IFT81 with specific antibodies.

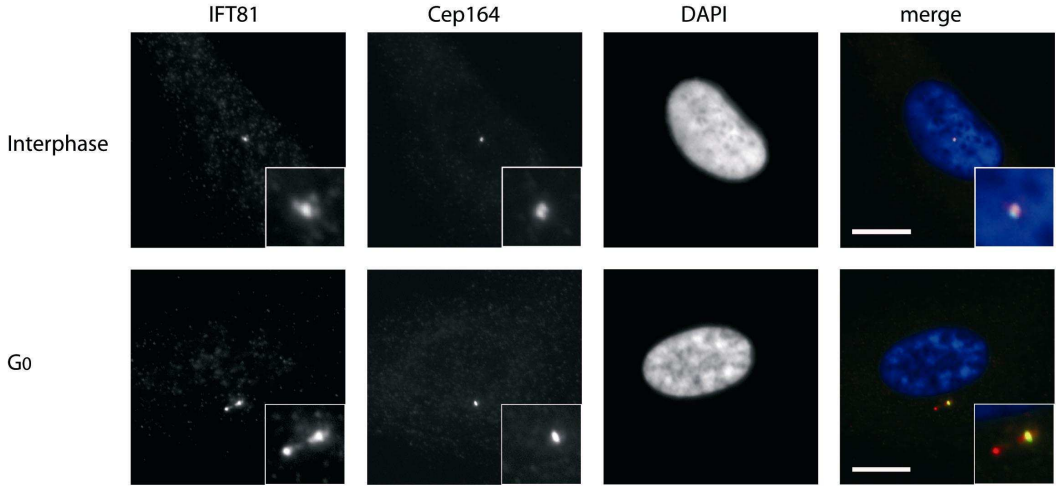

Figure 39. IFT81 co-localises with Cep164 at the base of the PC and at the tip of the centriole. IFT81 was co-stained with Cep164 in interphase RPE1 cells or in serum starved RPE1 cells. DNA was stained with DAPI. Bars: 10 µm.

As seen in Figure 39, IFT81 colocalised with Cep164, suggesting that IFT81 could be a linker of distal and subdistal appendages.

5.16 IFT81 localisation to the centriole is dependent on Cep170

Next we asked whether the localisation of IFT81 depends on the presence of Cep170 or vice versa. To answer this question, U2OS cells were treated for 72 h with siRNA duplexes targeting either and stained for IFT81 and Cep170. For IFT81 depletion two different RNA duplexes and a combination of both duplexes were used. As shown in Figure 40, IFT81 was not bound to the subdistal appendages after Cep170 depletion, depletion of IFT81 had no effect on the localisation of Cep170. These results support the idea that IFT81 is bound to the subdistal appendages of the mother centriole through an interaction with Cep170.

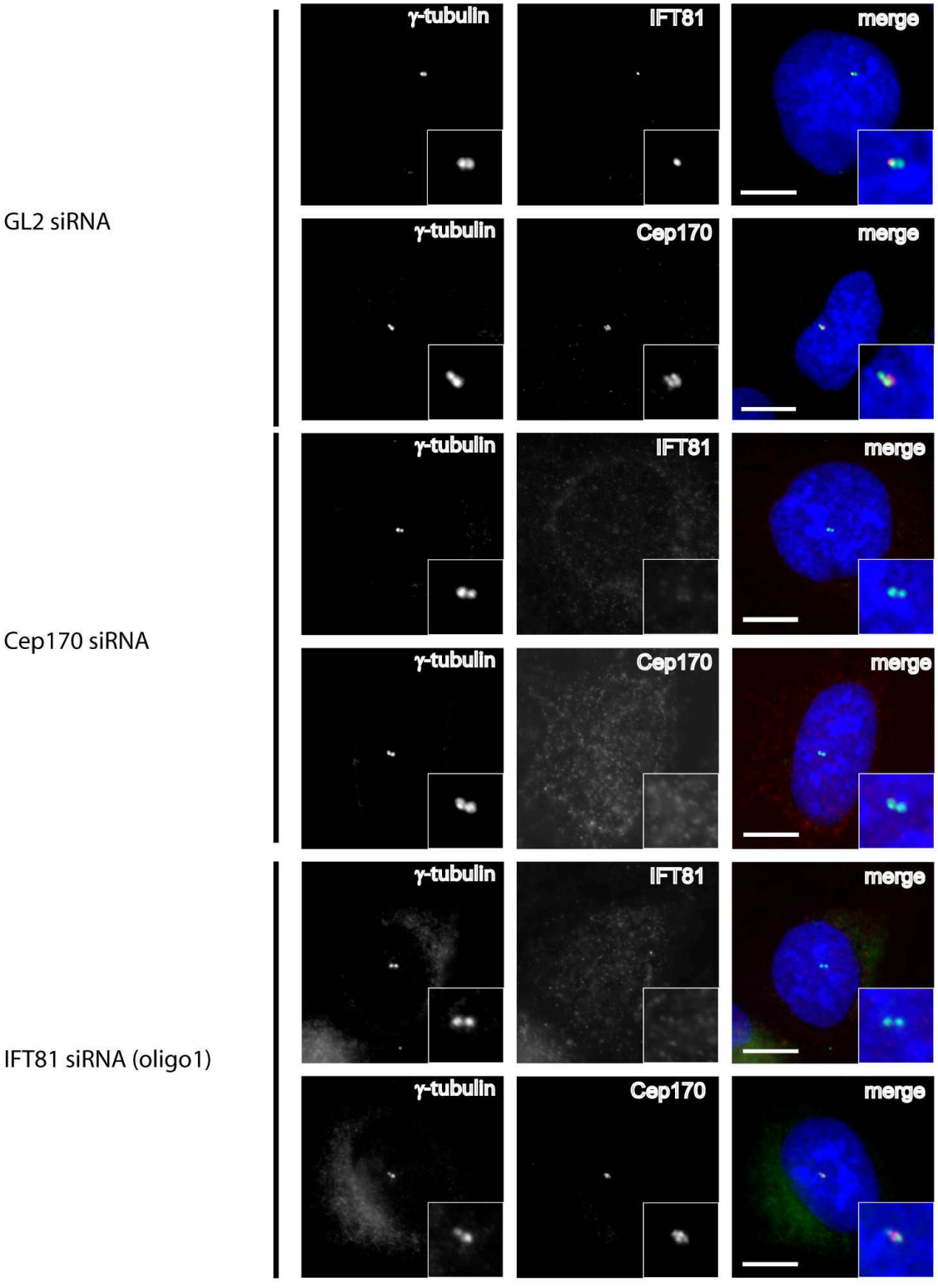
GL2 siRNA
γ-tubulin
IFT81
merge
γ-tubulin
Cep170
merge
Cep170 siRNA
γ-tubulin
IFT81
merge
γ-tubulin
Cep170
merge
IFT81 siRNA (oligo1)
γ-tubulin
IFT81
merge
γ-tubulin
Cep170
merge

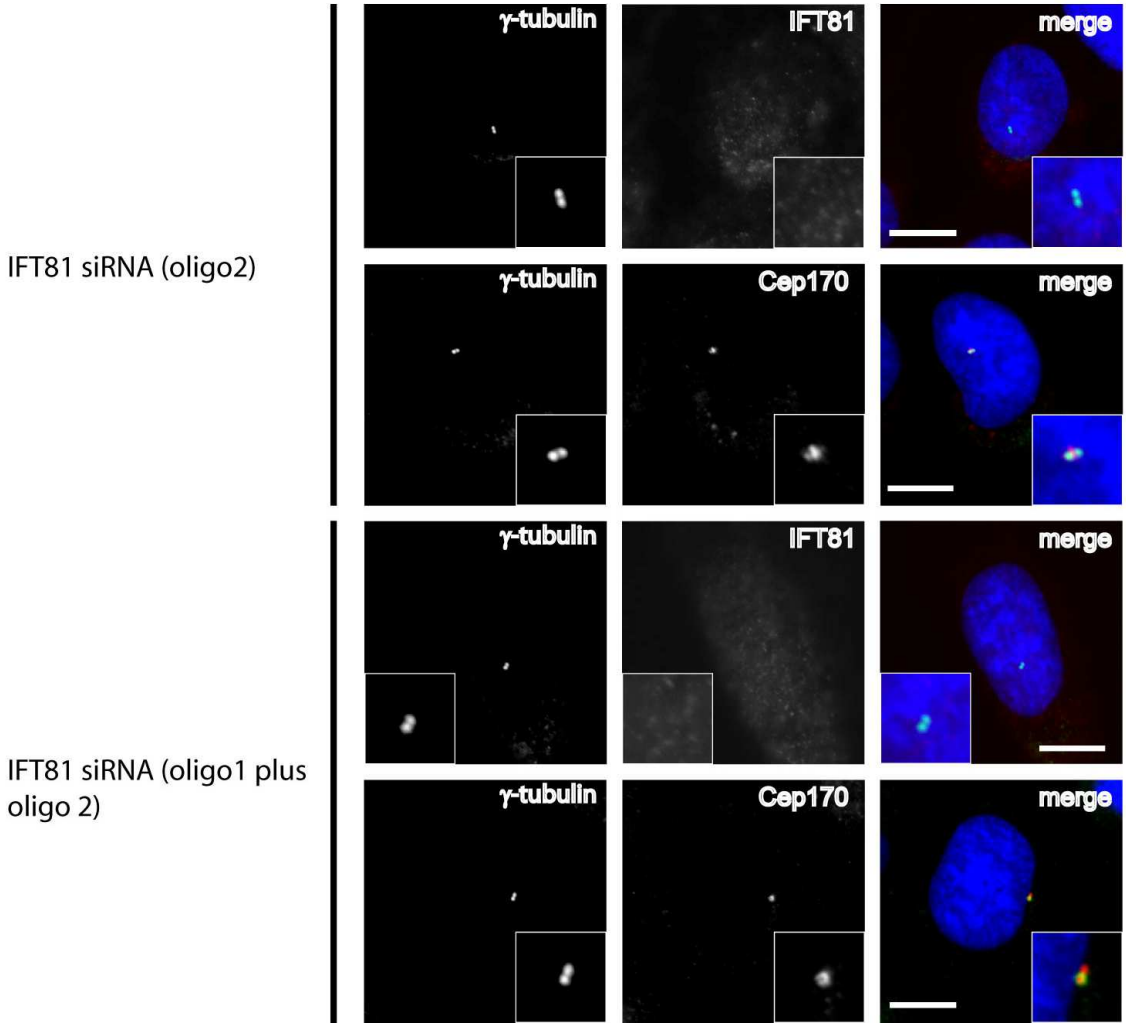

Figure 40. IFT81 binding to the appendages of the centriole is dependent on Cep170. U2OS cells were transfected for 72 h with siRNA duplexes specific for Cep170, IFT81 or with GL2 control siRNA duplexes and then costained with antibodies against γ–tubulin or IFT81 or with antibodies against γ–tubulin or Cep170, as indicated two different siRNA duplexes specific for IFT81 and the combination of both were used. Bars: 10 µm.

5.17 IFT81 depletion inhibits ciliogenesis

To explore the function of IFT81, ciliogenesis was induced in RPE1 cells in the absence of IFT81, Cep170 or Cep164. Cells were treated with the corresponding siRNA duplexes for 72 h to allow efficient depletion of the three proteins. IFT81 was depleted with two different RNA duplexes and a combination of both duplexes was also used. As a negative con-

trol, cells were treated with GL2 duplexes. After siRNA treatment, cells were serum starved to induce ciliogenesis for 48 h, and then processed as described above. Primary cilia were detected by an antibody specific for acetylated tubulin (Figure 41A). Reductions of protein levels were shown by Western blotting (Figure 41B).

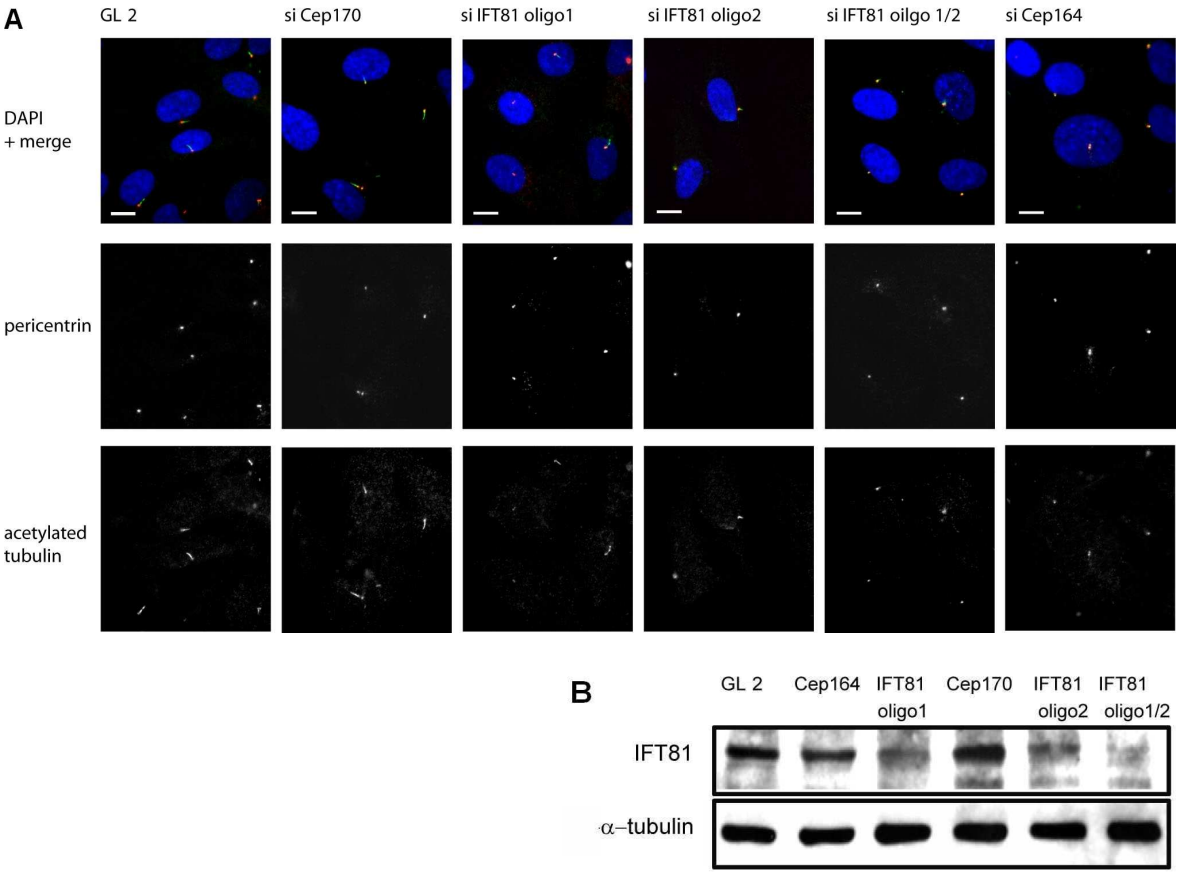

Figure 41. IFT81 is required for PC formation. RPE1 cells were transfected for 48 h with control (GL2) or IFT81, Cep164, Cep170 specific siRNA duplexes, followed by serum starvation to induce PC formation. Then, cells were analysed by immunofluorescence microscopy (A) using antibodies agains acetylated tubulin and pericentrin or by Westen analysis (B). Bars: 10 µm.

Reduction of Cep170 levels had almost no effect on the formation of the PC (Figure 41A). Instead, depletion of IFT81 or Cep164 strongly reduced cilium formation. Since the combination of both IFT81siRNA duplexes resulted in the highest reduction of IFT81 levels (Figure 41B), this combination of both duplexes were further used for subsequent analyses.

To quantify the effects on ciliogenesis, the ratio of cells forming a PC against cells not forming a PC was determined. As above, RPE1 cells were treated with siRNA duplexes for 48 h and subsequently serum starved for 48 h. Three independent experiments were done. In total 900 cells were counted (three hundred cells in each experiment).

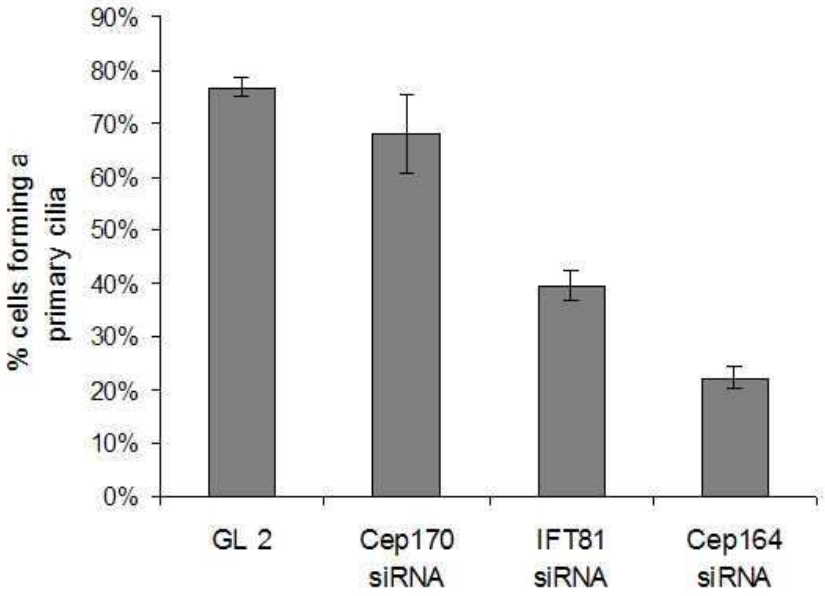

Figure 42. Reduction of PC formation after treatment of RPE1 cells with IFT81 and Cep164 specific siRNA duplexes. RPE1 cells were treated for 48 h with siRNA duplexes, followed by serum starvation for 48 h. For efficient IFT81 depletion, the combination of two duplexes was used.

Results are represented in Figure 42. IFT81 depletion inhibited PC formation. Only 40 % of the IFT81-depleted cells have assembled a PC, compared to 80 % in the control cells (GL2, Figure 42). Only 25 % of the cells with reduced Cep164 levels could form a PC. Surprisingly, the reduction of Cep170 levels only slightly reduced the formation of cilia. 65 % of the cells with reduced Cep170 levels still assembled a PC.

These results show that IFT81 is required for PC formation. However surprisingly, the absence of Cep170, the recruiting factor of IFT81 to the appendages, had no effect on the

formation of PC. This suggests that IFT81 has two different functions, one at the subdistal appendages and another at the PC.

5.18 Cep170 depletion inhibits cilium resorption

In a final series of experiments we asked whether Cep170 might play a role in the life cycle of the PC, or perhaps affecting a step related to maintenance or resorption of the cilium. The PC is disassembled when cells re-enter G1/ S phase (Pugacheva et al. 2007). Re-entry into S phase can be induced by the addition of fetal calf serum.

We further asked whether IFT81 or Cep170 might play any role in this process. To address this question, the levels of Cep170 and IFT81 in RPE1 cells were reduced by siRNA. To induce cilium formation, RPE1 cells were serum starved for 24 h. To disassemble the PC cells were incubated with 10 % serum containing medium for 7 h. After fixation of the cells PC was detected by an antibody specific for acetylated tubulin. Three independent experiments were performed, and in each experiment three hundred cells were counted (Figure 43).

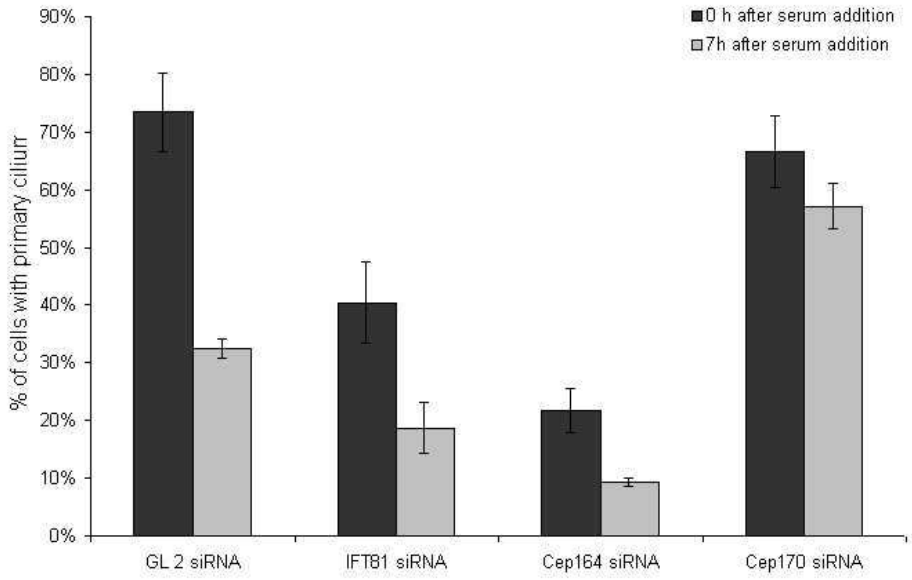

Figure 43. Delay of PC resorption after treatment of RPE1 cells with Cep170 specific siRNA. RPE1 cells were treated for 48 h with siRNA duplexes, followed by serum starvation for 24 h, followed by serum release for 7 h. For efficient IFT81 depletion, the combination of two duplexes were used. Cells were analysed by immunofluorescence microscopy using antibodies against acetylated tubulin as a marker for PC.

As shown on Figure 43, depletion of Cep170 inhibited the resorption of the cilium. Most cells with reduced Cep170 levels (almost 60 %) still had a primary cilia after 7 h of serum treatment. In contrast, in controls only 30 of the cells had a PC (Figure 43). To represent these data in another way, the ratio of cells with PC after 7 h versus 0 h was calculated. This determine the percentage of cells keeping the PC after 7 h of serum treatment. The data are presented in Figure 44. Whereas only 40 % of the cells treated with Cep164 siRNA, IFT81 siRNA or GL2 siRNA their PC, more than 80 % of the cells depleted of Cep170 kept their PC. The data suggests that Cep170 mainly functions in PC disassembly, similar to Aurora A, HEF1 and HDAC6 (Pugacheva et al. 2007).

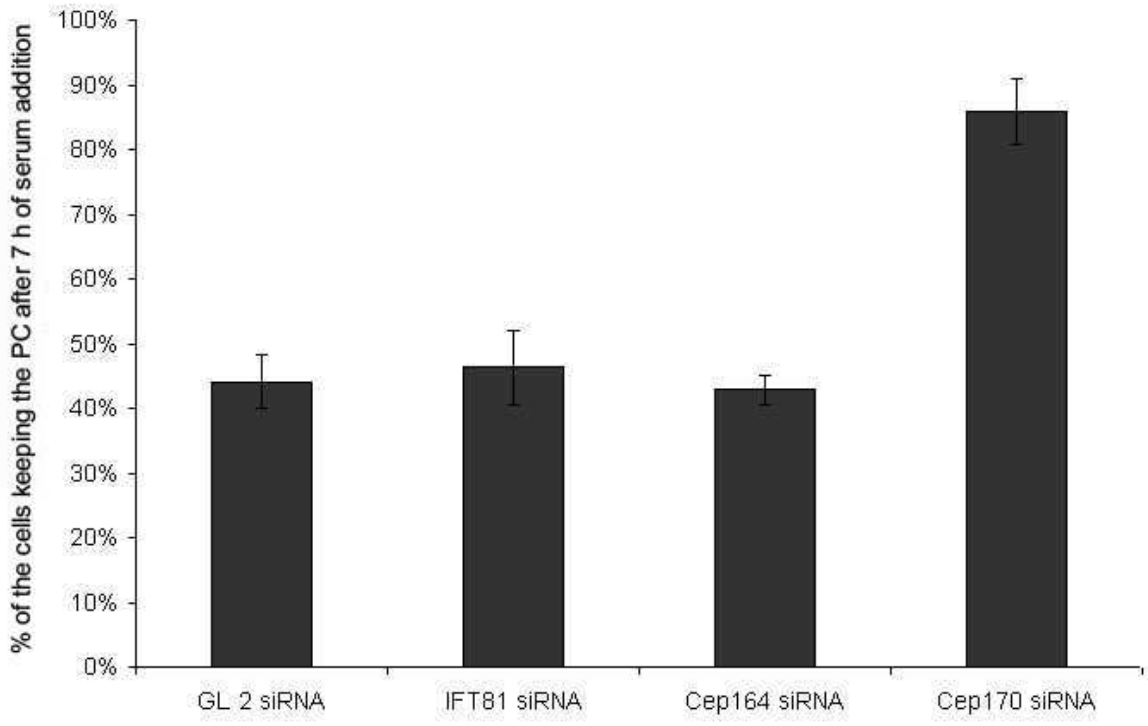

Figure 44. 85 % of the cells with reduced Cep170 levels keep their PC after serum addition. The Figure shows the ratio of cells with PC at time point 0 h relative to cells with PC at time point 7 h.

6 Discussion

The centrosome has two main functions; it organises the MTs and it forms a template for ciliogenesis. Here we could show that the subdistal appendage protein Cep170 plays an important role in both processes.

At the subdistal appendages, Cep170 anchors and bundles MTs. In fact, Cep170 interacts with both Ninein and MT. This supports the formation of the interphase MT array. At the onset of mitosis Cep170 is phosphorylated by Cdk1, which leads to its release from the centrosome, concomitant with the disassembly of subdistal appendages. At the end of mitosis Cdc14a dephosphorylates Cep170 and retargets it to the centrosome, concomitant with the reassembly of the subdistal appendages.

The second important function of Cep170 is its requirement for cilium disassembly. We could show that Cep170 interact with IFT81 and targets it to the appendages. Additionally, we demonstrated that IFT81 colocalises with both Cep170 and Cep164, raising the possibility that subdistal and distal appendages are linked to each other. IFT81 and Cep164 are needed for ciliogenesis and for maintenance of cilia, whereas Cep170 is required for the resorption of the cilium. Below, we discuss how the various proteins might act together.

6.1 Cep170, Ninein and the MTs

Centrosomes organises MT in interphase and during mitosis. Therefore, MTs have to be nucleated and anchored at the centrosome (Mogensen et al. 2000; Luders and Stearns 2007). Centrosomes contain different structures for both functions. The PCM is the main site for MT nucleation, whereas the subdistal appendages of the mother centriole are the main site for permanent anchoring of MTs (Mogensen et al. 2000; Luders and Stearns 2007). Mother centrioles are located in the focus of the MT network, although both centrioles contain similar amounts of MT nucleation sites (Mogensen et al. 2000; Delgehyr et al. 2005). Several subdistal appendage proteins are implicated in MT anchoring. In particular, Ninein was characterised in detail. However it was not clear whether it acts alone or together with other subdistal appendage proteins (Bouckson-Castaing et al. 1996; Mogensen et al. 2000; Delgehyr et al. 2005)

Ninein depletion or overexpression affects anchoring of MTs (Abal et al. 2002; Dammermann and Merdes 2002). Delgehayr and collegues demonstrated that overexpression of different fragments of Ninein caused defects in MT anchoring and MT nucleation (Delgehyr et al. 2005). Moreover, they showed that an overexpressed N-terminal fragment of Ninein (aa 1-373) was cytoplasmic, similar to a fragment comprising the coiled-coil domain (aa 373-1874) which formed aggregates in the cytoplasm. Interestingly, they also showed that transiently expressed C-term Ninein (aa 1874-2113) localised to the centrosome, displaced endogenous Ninein and γ–tubulin and thus caused defects in MT anchoring and MT nucleation. Localisation of other proteins (Pericentrin, AKAP450 and Nlp) implicated in MT organisation to the centrosome was not affected (Delgehyr et al. 2005). The authors suggested that C-term Ninein (aa 1874-2113) displaces endogenous Ninein, however they did not explain how the loss of endogenous Ninein causes defects in MT anchoring.

On the basis of the results described in this thesis, we suggest that Ninein targets Cep170 to the subdistal appendages and that Cep170 is needed for MT anchoring (Figure 45). Cep170 interacts with both Ninein and MT, suggesting that Cep170 is the MT anchor and organiser at the subdistal appendages. This view is supported by several findings:

1) Depletion of Cep170 causes a MT anchoring defect as severe as Ninein depletion
2) Cep170 localisation to the subdistal appendages is dependent on the presence of Ninein
3) Cep170 interacts directly with GFP-Ninein (720-1470) and GFP-Ninein (1471-2114). Overexpression of these Ninein fragments displaces Cep170 and causes MT anchoring defects. Overall, there is a strong correlation between Cep170 displacement and MT anchoring defects.
4) A C-terminal fragment of Cep170 can bind and bundle MTs *in vivo* and *in vitro*
5) Bundled MTs are more resistance to nocodazole treatment than unbundled MTs
6) And, finally, Cep170 depletion destabilises the MT network.

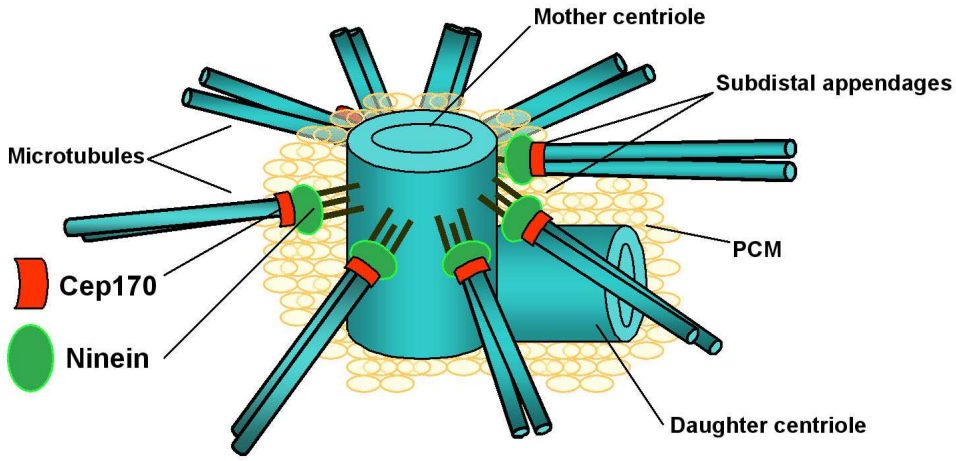

Figure 45. A model for Cep170 function in MT organisation.

These data can explain how the loss of endogenous Ninein causes defects in MT anchoring. Additionally, they can explain why MT were still organised by the mother centriole after low dose treatment with nocodazole and why MTs converge as bundles around the mother centriole. These functions are mediated by Cep170 (Figure 45).

Centrosomes must organise two different MT networks during the cell cycle. A stable interphase MT network and a highly dynamic mitotic spindle. Thus, it is not surprising that centrosomes undergo structural and compositional changes at the onset of mitosis. Additional nucleation sites are recruited and both centrosomes are separated. Interestingly, the subdistal appendages are disassembled, a process which is not well understood.

Here, we can show that disassembly and reassembly is controlled by the action of Cdk1-cyclin B and the phosphatase Cdc14a. This is supported by following findings:

1) Loss of Cep170 occurs during NEB
2) Inhibition of Cdk1-cyclin B retargets Cep170 to the centrosome and down shifts Cep170 in Western analysis.
3) A C-terminal fragment of Cep170 is phosphorylated by Cdk1 and dephosphorylated by Cdc14a
4) Endogenous, phosphorylated Cep170 can be dephosphorylated by Cdc14a

One tentative model would suggest that Cdk1 and Cdc14a control the assembly and disassembly of the subdistal appendages by phosphorylation or dephosphorylation of the C-terminus of Cep170. Interestingly, the C-terminal fragment of Cep170 (aa755-1459) is phosphorylated by Cdk1 and interacts with Ninein. This interaction is required for the localisation of Cep170 to the appendages. Thus, it is likely that Cdk1-cyclin B control the binding of Cep170 to Ninein. Cep170 is also phosphorylated by Plk1 and interacts with the polo-box domain of Plk1 (Guarguaglini et al. 2005). This phosphorylation might regulate the binding or bundling of MTs by Cep170. An important future line of research would be to map the Cdk1- and Plk1 phosphorylation sites and determine their functional relevance. Additionally, the function of the disassembly of subdistal appendages during mitosis could be explored by constructing a Cep170 mutant which is targeted to the centrosomes during mitosis. Either a mutant within the Cdk1 site might remain associated with the centrosome in mitosis or a fusion protein consisting of Cep170 with a centrosomal targeting region (PACT). The permanently targeted Cep170 should have an effect on the mitotic spindle.

Because subdistal appendage disassembly goes hand in hand with formation of the mitotic spindle we speculate that subdistal appendage proteins organise the stable interphase MT network and disassembly of the subdistal appendages at the onset of mitosis allows the formation of the mitotic spindle. Disassembly is regulated by the phosphorylation of Cep170 through Cdk1 and reassembly by dephosphorylation through Cdc14a.

6.2 Cep170, PRAX-1 and IFT81

The PC was long considered as a “rudimentary” organelle, in spite of its presence on almost every cell in the human body. However this view has changed in the last few years, because several diseases were linked to the cilium (Eggenschwiler and Anderson 2007) So, primary cilia are now considered as “antennae” of the cell to sense the environment. The PC is involved in Hh-, Wnt and PDGR signalling (Singla and Reiter 2006). It is built in a process called intraflagellar transport (IFT). IFT requires two subcomplexes IFT-A and IFT-B. IFT subcomplex B proteins form a adapter for the anterograde transports of proteins and membrane components within the cilia (Cole 2003). IFT-B consists of at least eleven IFT proteins. A structural core of IFT proteins is absolutely required for IFT particles assembly. This core is stabilised by tetramers consisting of two copies of IFT81 and the het-

erodimer IFT74/IFT72 (Lucker et al. 2005). Not surprisingly, mutation of IFT81 is linked to ciliary diseases. Additionally, mutations of IFT proteins are associated with changes in Wnt-, Hh- signalling (Badano et al. 2006). The axoneme of the PC consists of extended MTs from the mother centriole. Thus, several mother centriole proteins are required for ciliogenesis. For example, Graser et al. demonstrated that the distal appendage protein Cep164 is needed for cilium formation (Graser et al. 2007). Similarly, Ishikawa showed that Odf2-/- cells could not assemble cilia (Ishikawa et al. 2005). However, mechanistical links to IFT are missing. It is still unknown how proteins at the subdistal or distal appendages are involved in ciliogenesis.

Here, we demonstrated that Cep170 targets IFT81 to appendages of the mother centriole Moreover, Cep170 directly interacts with IFT81. Depletion of Cep170 caused displacement of IFT81 from the centriole and GFP-IFT81 pulled down endogenous Cep170.

IFT81 is absolutely required for ciliogenesis and depletion of IFT81 strongly reduced the formation of the PC. This is not surprising because IFT81 is a structural component of the subcomplex B and depletion of IFT81 should disrupt IFT particle assembly. Interestingly, IFT81 colocalises with Cep164 at the tip of the centriole and at the base of the PC, raising the possibility that the distal appendages are needed for the assembly of the IFT81 particles. This view is supported by the finding that Cep164 is also required for ciliogenesis. We speculate that the distal appendages form a structure to allow the assembly of IFT81 particles.

It may appear surprising that a structural component of the IFT particles localises to the tip of the centriole. IFT81 could be needed for both maintenance and initiation of cilium assembly. Its localisation to the tip of the centriole would favour a role for IFT81 in the initiation of the first steps of cilium assembly. However, it must be further investigated how this initiation is regulated.

Not only the assembly and the maintenance of the PC must be tightly regulated but also its disassembly. When cells disassemble their PC a cascade of HEF1, Aurora A and HDAC6, a tubulin deacetylase, was reported to be activated (Pugacheva et al. 2007). According to their study, the accumulation of HEF1 after serum addition activates Aurora A. Activated

and phosphorylated Aurora A is then targeted to the basal body, allowing the activation of the tubulin deacetylase HDAC6. Depletion of any of these components delayed resorption of PC (Pugacheva et al. 2007). Yet, this study fails to explain how the disassembly of the PC is linked to transport mechanisms within the PC.

Curiously, Cep170 is not needed for cilium formation. Cells without Cep170 can still assemble PC. This raises the question of the functional significance of the Cep170-IFT81 interaction. Perhaps this interaction relates to the observations that depletion of Cep170 inhibits cilium disassembly. Cells without Cep170 cannot disassemble PC.

An attractive model proposes that Cep170 is required for the targeting of IFT81 back to the subdistal appendages during primary cilia disassembly (Figure 46). This would reduce the amount of cycling IFT particles in the PC, which would induce disassembly of the axoneme. It is known that the turnover rate of cargo does not significantly change during cilium assembly and cilium maintenance (Qin et al. 2004). The length of the cilium is kept by a steady state equilibrium, characterised by constant levels of addition and removal of tubulin subunits (Qin et al. 2004). Thus, reduction of this turnover rate by targeting the core component IFT81 back to the appendages would destabilise the axoneme. We speculate that the turnover rate of the cargo is reduced during cilium disassembly and that this is regulated by the retargeting of IFT81 to the appendages of the centriole. Thus, depletion of Cep170 might result in high turn over rates remaining high, which would stabilise the axoneme.

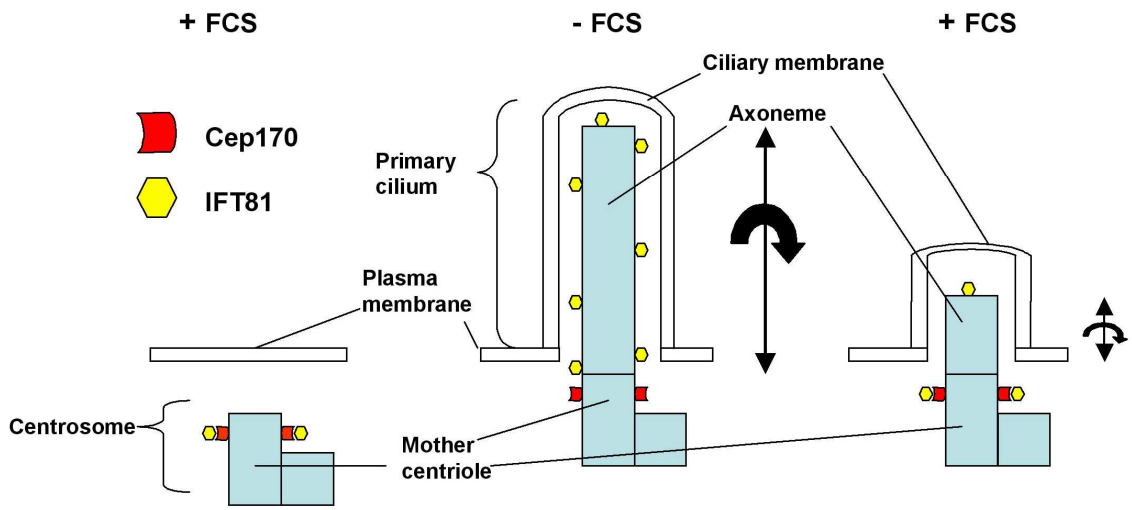

Figure 46. A model for the function of IFT81 and Cep170 in the control of the PC disassembly. Addition of fetal calf serum induces the resorption of the PC characterised by the targeting of IFT81 back to the mother centriole. Lenght (indicated by the arrow) is controlled by the turn-over rate of the IFT.

In summary, our study raises several important questions for future work: How is the interaction IFT81 with Cep170 regulated? Phosphorylation could play a role. Cep170 harbours a FHA domain in its N-terminus, FHA domains bind phosphorylated proteins. Maybe Aurora A phosphorylates IFT81 during cilium resorption which would target IFT81 back to the appendages.

Another open question is the role of IFT81 in the initiation of cilium assembly. Does it interfere with CP110 removal or CPAP transport? A balance of both proteins regulates the length of the centriole and removal of CP110 results in extended centrioles (Tsang et al. 2008). When exactly does assemble IFT81 with IFT72/IFT74 to build the structural core of the subcomplex B? What is the role of IFT81 and Cep164 in cilium maintenance? Do the distal appendages provide a platform for the interchange of IFT particles at the base of the cilium? A closer examination of the role of IFT81 at the base of the cilium might contribute to answer these questions.

The most enigmatic interactor of Cep170 is PRAX-1. PRAX-1is 200 kDa protein containing three SH3 domains. SH3 domains bind to proline rich motifs and are required for transient protein-protein interactions (Galiegue et al. 1999). It is interesting, therefore, that Cep170 contains two putative SH3-ligands (aa 545-551; aa 754-751) in its N-terminus.

Here we could show that transiently expressed PRAX-1 formed star-like structures around the mother centriole. Additionally, PRAX-1 interacts with Cep170 through its first SH3-domain. GST-SH3(1) pulled down endogenous Cep170 and fragments of PRAX-1 with disrupted SH3(1) domain did not localise to the mother centriole. Rescue of SH3(1) retargeted the fragment back to the mother centriole. Interestingly, FL-PRAX-1 and N-terminal fragments were also nuclear proteins. PRAX-1 contains a nuclear targeting sequence KKRKK (aa 346-350) in its N-terminus. Nuclear targeting depends on expression levels. If levels increases PRAX-1 is more and more targeted to the nucleus.

On the physiological role of PRAX-1 we can only speculate. PPAX-1 might synchronise centrosomal processes with nuclear processes. One possibility is the linkage of DNA-synthesis with centrosome duplication. Because of its localisation to the subdistal appendages PRAX-1 might also play a role in ciliary events notably in Hh-, Wnt- or Ca^{2+}-signalling or in the re-entry from G0 into S phase after serum addition. In particular, the occurrence of three SH3 domains required for transient protein-proteins interactions raises the possibility that PRAX-1 is involved in signalling processes. The data presented here provides a starting point for further work, to clarify the contribution of subdistal appendage proteins in cilium biogenesis and resorption, and in cilium dependent signalling.

7 Material and Methods

7.1 Chemicals, materials and antibodies

All chemicals were purchased from Sigma-Aldrich (Seelze, Germany) and Carl Roth (Karlsruhe, Germany). The following antibodies were used for immunofluorescence, Western blot and immunoprecipitation: rabbit serum anti Cep170 N-term (1-755) 1:000 for immunofluorescence, C-term (756-1490) 1:1000 for Western blotting. Mouse monoclonal Antibody against the N-term Cep170 (1-755; (clone number 72-372)) for immunoprecipitation and mouse monoclonal antibody against Ninein (Clone number: (79-160 (16)). Affinity purified anti rabbit Ninein antibody was used at 2 ng/ml. Sheep anti-GFP, mouse monoclonal antibodies to α–tubulin (1:3000), γ–tubulin (1:1000) anti-acetyl tubulin antibody (1:500) were purchased from Sigma-Aldrich. Secondary antibodies: Cy3, Cy2, AMCA donkey anti mouse, anti rabbit (1:1000) were purchased from Dianova. DNA was stained with 4,6-diamidino-2-phenylindole (DAPI, 2 µg/ml). Nocodazole was purchased from Sigma-Aldrich and dissolved in dimethylsulfooxid (DMSO).

7.2 Plasmid preparation

All cloning procedures were performed according to Molecular Cloning, A Laboratory Manual, 2nd edition, Sambrook, J., Fitsch, E.F., Maniatis, T., Cold Spring Harbor Laboratory Press 1989 and Current Protocols in Molecular Biology, Wiley, 1999. Plasmids were cleaved with restriction enzymes as recommended by the suppliers (NEB). Cleaved dsDNA was dephosphorylated with alkali phosphatase (Roche) and ligated with the Fast Ligation Kit (Roche) following the supplier protocol. Plasmids were either extracted from agarose gels or purified from a 2 ml – 50 ml LB overnight culture according to the protocols provided with the kits from QIAGEN. For PCR reactions, Pfu DNA polymerase was used as recommended (Promega) or, alternatively “King of DNA-polymerase” (KOD) were used in the presence of 2 % formamide. All reactions were carried out in a RoboCycler Gradient 96 (Stratagen). PCR products were cloned into Topo vectors according to the manual (Invitrogen). DNA sequences were checked either by sequencing at Medigenomix (Martinsried, Germany) or using the in-house sequencing facility (Martinsried, Germany).

Primers used for PCR reactions are listed in table 1. The PRAX-1 sequence was obtained from Kazusa institute (Japan, Kiaa0162 clone) in pBluescript II SK (-). PRAX-1 Fl was amplified using Expand High Fidelity PCR System (Roche, Penzberg, Germany) and cloned into plasmid pEGPF. Its sequence was confirmed by sequencing.

For the determination of the MT binding sites of Cep170 different constructs were cloned into pEGFP plasmids. IFT81 was cloned into Topo vector and subsequently into pEGFP plasmids.

7.3 Recombinant protein

Recombinant protein was expressed in JEM109 or BL-21 bacteria for 12 hours at 14 °C. To this end a starter culture of transformed bacteria was grown overnight in selective medium and diluted to 1:5 with LB supplemented with antibiotics. The culture was grown until an OD600 of 0,6 was reached. Then the expression of the recombinant protein was induced by the addition of IPTG to a final concentration of 1 mM for 12 h at 14 °C. Cells were pelleted by centrifugation, resuspended in chilled lysis buffer (1 % Triton X-100, 350 mM NaCl, 50 mM Tris-HCl pH 8, EDTA free Protease Inhibitor (Roche, Penzberg, Germany)) and lysed with an airpress. Subsequently, lysates were clarified by centrifugation and then incubated either with Ni-NTA-beads (Qiagen) or glutathione coated beads (Amershan) for 1 h to allow binding of expressed proteins. After several washing steps with lysis buffer, protein was eluted with elution buffer (His-tagged protein: lysis buffer with 50 mM inidazole, GST-tagged protein: lysis buffer with 50 mM glutathione). Purified protein was frozen in aliquots at –20 °C.

IFT81 was cloned into pET28c and pGEX-4T to express a His-tagged or GST-tagged protein in BL21 *E. coli* for 12 h at 14 °C. Cells were lysed with lysis buffer and proteins, respectively, were purified using big preparative 10 % gels. After running protein gels were incubated in KCl and β–mercaptoethanol on ice to precipitate the SDS-protein complex. The expected band at 80 kDa was cut out and gel pieces were crushed after freezing them in liquid nitrogen. Then crushed gel pieces were incubated with 50 ml of 0,5 x running buffer at 4 °C overnight to extract the protein. After centrifugation protein was concentrated using Amicon spinning tubes and dialyzed against PBS 0,5 % Triton X-100. Insolu-

ble protein was further solubilized by the addition of Triton X-100 to a final concentration of 1 %.

7.4 Antibody production

For the production of monoclonal antibodies mice were immunized with either a Cep170 fragment spanning aa 1-754 or 755-1490. Proteins were expressed as poly-histidine-tagged fusion proteins in *E. coli* and purified over a Ni2+-column. 100 µg of protein was injected subcutaneously together with Freund´s (Sigma-Aldrich) or Alu-Gel-8 (SERVA Electrophoresis GmbH) adjuvant. Balb/c mice were immunized every four weeks, to a total of six injections (animal house, Max-Planck Institute for Biochemistry, Martinsried, Germany). After checking for an immune response by immunofluorescence microscopy, the mouse spleens were fused with mouse myeloma cells PAIB3Ag81 using polyethylglycol (PEG 4000; Merck) as described by Kohler and Milstein (Kohler and Milstein, 1975). Fused cells were selected for two weeks in HAT-medium (hypoxanthine/aminopterin/thymidine-medium), followed by selection in HT-medium for the cloning procedure. Supernatants of the fused cells were tested for specific antibodies by ELISA, using GST-tagged N-term Cep170 (aa 1-755) or C-term Cep170 (aa 756-1459). After subcloning of the hybridoma cells, supernatants were further checked for specifity using dot blot assays, immunofluorescence microscopy. Following mouse monoclonal antibodies were produced: 71-413 and 72-372 against C-term of Cep170, 77-416 against N-term Cep170

For production of polyclonal antibodies a poly-histidine-tagged IFT81 protein was expressed in *E. coli* and purified as described above. 100 µg of purified antigen was injected subcutaneously together with Freund´s or Alu adjuvants into rats every four weeks, to a total of seven injections (animal house, Max Planck Institute for Biochemistry, Martinsried, Germany). Subsequently, antibodies were affinity purified using GST-tagged IFT81 protein coupled to AffiGel 10. For immunofluorescence and Western blot 0,2 µg/ml of antibody was used.

7.5 Cell culture and transfection

All cells were grown at 37 °C in a 5 % CO_2 atmosphere. Osteosarcoma cells (U2OS), human embryonic kidney cells (293T) cells, monkey cells (COS7) and human adenocarci-

noma cells (A549) were cultured in Dulbecco´s modified Eagle´s medium (DMEM), supplemented with 10 % heat inactivated fetal calf serum and penicillin-streptomycin (100 i.u./ml and 100 µg, respectively, Gibco-BRL, Karlsruhe, Germany). hTERT-RPE1-cells were cultured in DMEM Nutrient Mixture F12 Ham (Sigma, Munich, Germany), supplemented with 10 % heat inactivated FCS, penicillin-streptomycin (as above), 1 % glutamine (Gibco-BRL, Karlsruhe, Germany) and 0,35 % sodium bicarbonate (Sigma, Munich, Germany). Cells adherent on acid treated glass coverslips were transiently transfected using FuGene (Roche Diagnostics, Mannheim, Germany) or according to the manufacturer´s protocol.

7.6 SiRNA experiments

SiRNA experiments were performed as described previously. The lyophilised and pre-annealed siRNA duplexes were diluted to a stock solution of 20 µM and aliquots were stored at –80 °C. In brief, 0,8 x 10^5 cells were seeded in 2 ml medium containing three glass coverslips. The next day 21 nucleotide siRNA duplexes were transfected using Oligofectamine (Invitrogen, Carlsbad, CA, USA). For a single well of a 6-well plate 3 µl Oligofectamine and 6 µl of 20µM siRNA duplex was added to 80 µl OptiMEM medium (Invitrogen, Carlsbad, CA, USA) in an RNAse-free Eppendorf tube. The mixture was mixed gently and left for 20 min at room temperature. 72 h after addition of the siRNA duplexes cells were fixed with methanol for 10 min or lysed in RIPA-buffer.

7.7 Immunofluorescence microscopy and immunoblotting

Cells on glass coverslips were fixed in cold methanol (-20 °C) for 20 min and rehydrated in phosphate buffered saline. Usually cells were first incubated with 3 % BSA in PBS for 1 hour. Then, the first antibody was diluted with 3 % BSA PBS and cells were incubated for 1 h. After washing with PBS the first antibody was detected with an secondary antibody coupled to different fluorescent dyes. These antibodies were also diluted in 3 % BSA/PBS and incubated with the cells for 1 h at RT. After washing with PBS coverslips were mounted in Moviol.

Immunofluorescens microscopy was performed with a Zeiss Axioplan II microscope equipped with 63x and 100x oil immersion objectives. Photographs were taken with a Mi-

cromax 1300 x 1030 pixel CCD camera (Princton Instruments, Princton, NI) and with Metaview software. Images were processed using Adobe Photoshop software (Adobe systems, San Jose CA).

For Western blotting cells were lysed in RIPA buffer in the presence of EDTA free Protease inhibitor for 20 min on ice. After determination of the protein concentration and addition of gel sample buffer 30 µg were added into the pockets of a polyacrylamide gel. The proteins were separated and transferred onto nitrocellulose using a Hoefer semidry transfer system (Amersham Biosciences, Little Chalfont, UK). For Western blot analysis, membranes were incubated for one hour in blocking buffer (5 % low-fat dry milk in PBS, 0,1 % Tween-20). All antibody incubations were carried out in blocking buffer for 1 hour at room temperature. The protein antibody complexes were detected with a secondary antibody conjugated to HRP. Signals were detected using chemiluminescence and Kodak X-ray films.

7.8 Immunoprecipitation and Pull down assays

For immunoprecipitation experiments and pull down experiments approximately $5x10^7$ HEK 293T cells were lysed in lysis buffer (300 mM NaCl, 1 % Triton X-100, 50 mM TrisHCl pH 7,6, 40 mM NaF, EDTA free Protease inhibitor (Roche), Phosphatase inhibitor cocktail (Roche)). Protein concentration was adjusted to 5 mg/ml. Cep170 was immunoprecipitated using monoclonal antibody 71-372, Ninein was immunoiprecipitated using a specific monoclonal antibody (79-160). GFP tagged protein was immunoprecipitated with 1 µg of rabbit anti GFP (Abcam). The mixtures with the cell lysates were incubated for 1 hour at 4 °C to allow the binding of the antigen to the antibody. After immunoprecipitation the beads were washed four times with lysis buffer and PBS and subsequently boiled in 2x gel sample buffer.

7.9 MT regrowth assays and depolymerization assays

MTs in COS7 or A549 cells were first depolymerized by cold treatment (45 min on ice). For repolymerization of MTs, cells were transferred to 37 °C warm DMEM and fixed after

different time points in methanol (-20 °C) for 20 min and further processed as described above.

For depolymerization assays, COS7 cells were incubated with 0,1 µM nocodazole to destabilize the MTs. Then cells were fixed in methanol (-20 °C) for 20 min and rehydrated with PBS for 1 hour.

7.10 Yeast two hybrid experiments

The coding sequence of N-term Cep170 (aa 1-785) and C-term Cep170 (aa786-1459) was cloned into the bait vector pFBT9 (a version of pGBT modified to encode kanamycin resistance; Clontech Laboratories, Inc.; a kind gift from F. Barr, Max-Planck Institute for Biochemistry, Martinsried, Germany). Ninein (1-719), Ninein (720-1470) and Ninein (1471-2114) were cloned into pACT2 (Clontech Laboratories, Inc., a kind gift of Yan, Xiumin, Max-Planck Institute for Biochemistry, Martinsried, Germany). These plasmids were co-transfected into yeast strain PJ69-4A to test for transactivation. Transformed yeast were plated on selective media lacking leucine, tryptophane and histidine. Medium was supplemented with 5 mM 3-AT and 2 % (wt/vol) glucose as a carbon source (TDO). All results were confirmed by streaking several colonies on selective plates.

For the Yeast two hybrid screen a cDNA-library of Clontech was used. The cDNA wass derived from 293T cells and cloned into the pACT2-vector. As bait N-terminus (aa1-785) of Cep170 was used or ,alternatively, also the C-terminus of Cep170 (aa 786-1460). Transformation conditions were optimized so that at least 10^5 yeast cells were transformed. The transformed yeast cells were plated onto selective medium lacking leucine, tryptophane, histidine and adenine with 2 % (wt/vol) glucose as a carbon source. The plasmids of the positive colonies were isolated and retransformed in yeast to test for selfactivation. Afterwards plasmids were sequenced.

7.11 Cdk1 kinase assays

The substrates for the Cdk1 kinase assay were *in vitro* transcribed and translated using the TNT T7 Quick coupled Transcription/Translation System (Promega, Madison, WI) and following the protocol of the manufactures. Afterwards the GFP-tagged proteins were immunoprecipitated with 1 µg of protein G coupled anti-GFP antibody (Abcam 290) or alter-

natively with protein G anti-myc antibody (9E10). Samples were diluted with immunoprecipitation buffer (150 mM NaCl, 20 mM Tris pH8) and after addition of the antibodies the mixtures were incubated on a rotating wheel at 4 °C for 1 h. Afterwards the beads were washed with immunoprecipitation buffer and BRB80. For phosphorylation the beads were incubated with Cdk1 in BRB80 buffer (80 mM K-Pipes, 1 mM EGTA, 1 mM MgCl2, pH 6,8) and ^{32}P γ–ATP for 30 min and the reaction was stopped by washing with EDTA containing washing buffer

7.12 Cdc14a phosphatase assay

As a substrate either immunoprecipitated protein was used or *in vitro* translated and phosphorylated protein. Samples were washed with phosphatase buffer and Cdc14a was added in 50 mM Pipes pH 4,7. After 30 min of incubation, the activity of the phosphatase was assayed either by the downshift of the immunoprecipitated protein or by reduction of incorporated ^{32}P γ–phosphate.

7.13 MT bundling assays

For MT bundling assays purified and rhodamine-labeled and unlabeled tubulin was used (kind gift from Thomas Mayer, Max Planck Institute for Biochemistry, Martinsried, Germany). For MT polymerisation, 100 µM tubulin was incubated for 40 min at 37 °C with 20 mM GTP in BRB80 buffer containing 50 % glycerol. Subsequently, 35 µM taxol was added to stabilize the polymerised MTs. After 40 min the mixture was centrifugated at 6800 rpm for 30 min at 35 °C. Afterwards, the pellet was resuspended in BRB80 containing 5 µM taxol to a final concentration of 5 µg/µlMT and stored at RT. For *in vitro* bundling assays 20 µg of MTs were incubated with 400 ng human N-term Cep170 or C-term Cep170 for 5 min at 25 °C. Bundling reactions were stopped by the addition of glutaraldehyd and bundling was assayed by microscopy.

7.14 PC growth and resorption assays

For PC outgrowth RPE1 cells were serum starved when confluency was 80 %. Starvation occurred in F12/DMEM containing penicillin for 48 h. Before fixation with methanol for 10 min MTs were depolymerised by cold treatment (40 min, 4 °C).

For resorption assays, serum starved RPE1 cells were seeded onto coverslips at a confluency of 40 %. After addition of medium containing 10 % FCS MTs were depolymerised using the procedure described above. Cells were fixed after 7 h of serum addition in methanol (-20 °C).

Table 1. List of primers

Primer name	**Sequence (5´-3´)**	**Purpose**
M4387	TTGGATCCCGAGTGATCAAATTAAATTCATTATG	IFT81 cloning
M4388	AACTCGAGATCACATTATTAGCCGGTCC	IFT81 cloning
M4364	GGAATTCCCTAGCACTGGACTCTTC	PRAX-1 cloning
M4363	CCGCTGGAGCGGAGCAACTGACAACCC	PRAX-1 cloning
M4658	CATTAGATCTTCCTGCTCCCAGCTGC	SH3(1) cloning
M4659	TTCTCTCGAGCCTACTCTGGAGGGAGGGG	SH3(1) cloning
M4662	TCGAGGATCCCGGTCCCTGCGAGG AG	SH3(2) cloning
M4663	TTCTCTCGAGCCTACTGTCTCCCAGCAGG	SH3(2) cloning
M4664	TCGAGGATCCCGTGTCCAGGCCCCCC	SH3(3) cloning
M3880	TCCCCCGGGCAGCTTAACATCCTGG	Cep170 cloning in pFBT
M3881	CGTCGACGCTAATCCAAAGACTCACTTC	Cep170 cloning in pFBT
M3882	CGTCGACCTGATTCTAGTATGG	Cep170 cloning in pFBT
M3883	CTGCAGTCATTCTTGTACTGTAAC	Cep170 cloning in pFBT

Table 2.List of plasmids

Epitope tags are N-terminal unless otherwise stated.

Name	**Gene**	**Species**	**Insert**	**Vector**	**Tag**
XY163	Ninein	mouse	aa 720-1470	pACT2	AD
XY164	Ninein	mouse	aa 1470-2114	pACT2	AD
MC59	Ninein	mouse	aa 1-719	pACT2	AD
XY189	Ninein	mouse	aa 720-1470	pEGFP-C2	EGFP
XY190	Ninein	mouse	aa 1470-2114	pEGFP-C2	EGFP
MC35	Ninein	mouse	aa 1-719	pEGFP-C2	EGFP
GG8	Cep170	human	aa 20-755	pQE-30	His
GG7	Cep170	human	aa 755-1459	pQE-30	His
GG2	Cep170	human	aa 755-1459	pEGFP-C1	EGFP
GG11	Cep170	human	aa 755-1014	pEGFP-C1	EGFP
GG12	Cep170	human	aa 1015-1459	pEGFP-C1	EGFP
STL1	Cep170	human	aa 2-146;	pGEX-4T	GST
STL2	Cep170	human	aa 2-146; R27D	pGEX-4T	GST
STL3	Cep170	human	aa 2-146	pcDNA3.1 3x myc	Myc
STL4	Cep170	human	aa 2-146; R27D	pcDNA3.1 3x myc	Myc
STL5	Cep170	human	aa 756-1460	pCR II Topo	
STL6	Cep170	human	aa 1-755	pCR II Topo	
STL7	Cep170	human	aa 756-1460	pMalp8His	MBP-His
STL8	Cep170	human	aa 1-155	pMalp8His	MBP-His
STL9	Cep170	human	aa 756-1460	pGEX-p8His	GST-His
STL10	Cep170	human	aa 1-755	pGEX-p8His	GST-His
STL11	GST	human	aa 1-242	pCR II Topo	
STL12	Cep170	human	aa 2-146	pCR II Topo	
STL13	Cep170	human	aa 2-146, R27D	pCR II Topo	
STL14	Cep170	human	aa 2-146	pQE-60	His
STL15	Cep170	human	aa 2-146; R27D	pQE-60	His
STL16	Cep170	human	aa 1227-1460	pCR II Topo	
STL17	Cep170	human	aa 1227-1460	pEGFP-C1	EGFP
STL18	Cep170	human	aa 2-146	pCR II Topo	
STL19	Cep170	human	aa 2-146;R27D	pCR II Topo	
STL20	Cep170	human	aa 1012-1226	pCR II Topo	
STL21	Cep170	human	aa 1012-1226	pEGFP-C1	EGFP
STL22	Cep170	human	aa 1012-1055	pEGFP-C1	EGFP

STL23	Cep170	human	aa 1-785	pCR II Topo	
STL24	Cep170	human	aa 786-1460	pCR II Topo	
STL25	Cep170	human	aa 786-1460	pFBT	BD
STL26	Cep170	human	aa 1-785	pFBT	BD
STL27	Cep170	human	aa 1-1460	pCR II Topo	
STL28	Cep170	human	aa 1-1460	pCR II Topo	
STL29	Cep170	human	aa 2-1460	pcDNA3.1NFlagTo	Flag
STL30	Cep170	human	aa 2-1460	pCFlagTo	Flag
STL31	Cep170	human	aa 2-146	pcDNA3.1 CFLAG	FLAG
STL32	Cep170	human	aa 2-146; R27D	pcDNA3.1CFLAG	FLAG
STL33	Cep170	human	aa 2-247	pEGFP-C1	EGFP
STL34	Cep170	human	aa 248-754	pEGFP-C1	EGFP
STL35	Cep170	human	aa 1-755	pCR II Topo	
STL36	Cep170	human	aa 756-1460	pCR II Topo	
STL37	Cep170	human	aa 1-1460	pCR II Topo	
STL38	Cep170	human	aa 756-1407	pEGFP-C1	EGFP
STL39	Cep170	human	aa 756-1175	pEGFP-C1	EGFP
STL40	Cep170	human	aa756-1136	pEGFP-C1	EGFP
STL41	Cep170	human	aa 756-1093	pEGFP-C1	EGFP
STL42	IFT81	human	aa 2.676	pEGFP-C2	EGFP
STL43	IFT81	human	aa 1-253	pEGFP-C2	EGFP
STL44	IFT81	human	aa 254-676	pEGFP-C1	EGFP
STL45	IFT81	human	aa 1-422	pEGFP-C2	EGFP
STL46	IFT81	human	aa 423-676	pEGFP-C2	EGFP
STL47	IFT81	human	aa 1-676	pGEX-5x-2	GST
STL48	Ninein	mouse	aa 2-372	pEGFP-C1	EGFP
STL49	Ninein	mouse	aa 1875-2114	pEGFP-C1	EGFP
STL50	Ninein	mouse	aa 2-375/1875-2114	pEGFP-C1	EGFP
STL51	Ninein	mouse	aa 2-375	pEGFP-C1	EGFP
STL52	Ninein	mouse	aa 1918-2114	pEGFP-C1	EGFP
STL53	Ninein	mouse	aa 1560-2114	pEGFP-C1	EGFP
STL54	Ninein	mouse	aa 1660-2114	pEGFP-C1	EGFP
STL55	Ninein	mouse	aa 1850-2114	pEGFP-C1	EGFP
STL56	Cep170	human	aa 1085-1459	pEGFP-C1	EGFP
STL57	IFT81	human	aa 1-676	pET28a+	His
STL58	Cep170	human	aa 1085-1460	pCR II Topo	
STL59	Cep170	human	aa 1159-1459	pCR II Topo	

STL60	Cep170	human	aa 1118-1200	pCR II Topo	
STL61	Cep170	human	aa 1160-1200	pCR II Topo	
STL62	Cep170	human	aa 1085-1200	pEGFP-C1	EGFP
STL63	Cep170	human	aa 1159-1459	pEGFP-C1	EGFP
STL64	Cep170	human	aa 1160-1200	pEGFP-C1	EGFP
STL65	PRAX-1	human	aa 1-1857	pEGFP-C1	EGFP
STL66	PRAX-1	human	aa 1-655	pEGFP-C1	EGFP
STL67	PRAX-1	human	aa 656-1857	pEGFP-C1	EGFP
STL68	PRAX-1	human	aa 1-491	pEGFP-C1	EGFP
STL69	PRAX-1	human	aa 492-1857	pEGFP-C1	EGFP
STL70	PRAX-1	human	aa 641-731	pGEX-5x-2	GST
STL71	PRAX-1	human	aa 1611-1700	pGEX-5x-2	GST
STL72	PRAX-1	human	aa 1750-1857	pGEX-5x-2	GST
STL73	PRAX-1	human	aa 1-1459	pEGFP-C1	EGFP

Table 3. List of primary antibodies

number	antigen	made in	dilution	comment	distributor
R154	Ninein	Rabbit	1:1000	Affinity purified	Yan, X
79-160	Ninien	Mouse	1:1000	Hybridoma tissue culture supernatant	Kindly provided by M. LeClech
R113	Cep170	rabbit	1:1000	Serum, immunofluo-rescence	Guarguaglini, 2005
R114	Cep170	rabbit	1:1000	Serum, Western ana-lysis	Guarguaglini, 2005
R172	Cep164	rabbit	1:1000	serum	Graser, 2007
71-372	Cep170	mouse	undiluted	Hybridoma tissue culture supernatant	Lamla, S.
72-413	Cep170	mouse	undiluted	Hybridoma tissue culture supernatant	Lamla, S.
77-311	Cep170	mouse	undiluted	Hybridoma tissue culture supernatant	Lamla, S.
77-416	Cep170	mouse	undiluted	Hybridoma tissue culture supernatant	Lamla, S.
77-419	Cep170	mouse	undiluted	Hybridoma tissue culture supernatant	Lamla, S.
Rat 13	IFT81	rat	0,2 µg /ml	Affinity purified	Lamla, S
9E10	myc	mouse	1:10	Hybridoma tissue culture supernatant	Evan et al., 1985
6-11B-1	Acetylated-	mouse	1:500		Sigma

	tubulin				
Ab4448	pericentrin	rabbit	1 µg/ml		Abcam
Ab290	GFP	rabbit	1:1000		Abcam
DM1A	α-tubulin	mouse	1:5000		Sigma
GTU-88	γ–tubulin	mouse	1:1000		Sigma

Table 4. List of siRNA oligonucleotide duplexes

Gene	Target sequence	Remarks
Ninein	5´-GCGGAGCTCTCTGAAGTTAAA-3	
Cep164	5´-CAGGTGACATTTACTATTTCA-3´	Graser et al., 2007
Cep170	5´-GAAGGAATCCTCCAAGTCA-3´	Guarguaglini et al., 2005
IFT81	´5´-GGATATCAGTGCAATGGAA-3´	
IFT81	´5´-CAGCTCATTAAGAGAGTTGAA-3´	

8 Abbreviations

293T	HEK293T
AA	amino acid(s)
AD	activation domain
ATP	adenosin 5´-triphosphat
BD	binding domain
BSA	bovine serum albumine
Cep	centrosomal protein
DAPI	4´,6-diamidino-2-phenylindole
DTT	dithiothreitol
ECL	enhanced chemiluminescence
EDTA	ethylenediaminetetraacetic acid
EGFP	enhanced green fluorescent protein
EM	electrom microscopy
FCS	Fetal calf serum
GFP	green fluorescent protein
IF	immunofluorescence
IFT	intraflagellar transport
IgG	Immunglobulin G
IP	immunoprecipitation
IPTG	isopropyl-beta-D-thiogalactopyranoside
mAb	monoclonal antibody

MT	MT
Nlp	Ninein-like protein
ODF	outer dense fiber
PBS	Phosphate buffered saline
PC	primary cilium
PCM	pericentriolar material
PCR	Polymerase chain reaction
PD	phophatase dead
Pfam	protein families database
PKD	polycystic kidney disease
Plk1	Polo-kinase 1
Plk4	Polo-kinase 4
PMSF	phenylmethylsulfonyl fluoride
RNA	Ribonucleic acid
RP	retinitis pigmentosa
RPE1	HTERT-RPE1
PRAX	Peripheral-type benzodiazepine receptor-associated protein X
RT	room temperature
SDS-PAGE	Sodium dodecylsulfate polyacrylamid gelelectrophoresis
siRNA	small interfering RNA
WT	wild-type

9 Acknowledgements

First and foremost I would like to thank Prof. Erich Nigg for giving me the opportunity of working in his lab and for invaluable advice and guidance during my stay.

I am thankful to PD Dr. Angelika Böttger for reviewing this manuscript.

I offer my thanks to Dr Andreas Uldschmid for teaching me the intricacies of producing a monoclonal antibody. My greatful thanks must also go to Mikael LeClech and Xiumin Yan for the stimulating and enthusiastic discussions on Cep170 and the centrosome. I wish them both success and best of luck for their future work. I would like to thank Claudia Szalma for technical assistance and Elisabeth Bürgelt for supporting me during the production of the monoclonal antibodies.

Of course the friendship of all people in the department was greatly appreciated. In particular, I thank Eunice Chan, Bin Wang and Shinichiro Yoshimura for support and the shared time not only in science. I am grateful for advices and reagents to Ulf Klein, Tom Gaitanos, Sabine Elowe and Rüdiger Neef.

I would like to thank all those who read and helped with this manuscript.

I am very grateful to Areli for her patience and for sharing her time with me.

My deepest gratidude goes to my parents, Mathilde and Günther Lamla and to my brothers Markus and Gregor for all their support over so many years.

Lastly, I am indebted to all my friends in the lab who lend an understanding ear and with whom I shared this unforgettable time.

10 References

Abal, M., M. Piel, V. Bouckson-Castaing, M. Mogensen, J. B. Sibarita and M. Bornens (2002). "Microtubule release from the centrosome in migrating cells." J Cell Biol **159**(5): 731-7.

Ainsworth, C. (2007). "Cilia: tails of the unexpected." Nature **448**(7154): 638-41.

Aldaz, H., L. M. Rice, T. Stearns and D. A. Agard (2005). "Insights into microtubule nucleation from the crystal structure of human gamma-tubulin." Nature **435**(7041): 523-7.

Andersen, J. S., C. J. Wilkinson, T. Mayor, P. Mortensen, E. A. Nigg and M. Mann (2003). "Proteomic characterization of the human centrosome by protein correlation profiling." Nature **426**(6966): 570-4.

Badano, J. L., N. Mitsuma, P. L. Beales and N. Katsanis (2006). "The ciliopathies: an emerging class of human genetic disorders." Annu Rev Genomics Hum Genet **7**: 125-48.

Bahe, S., Y. D. Stierhof, C. J. Wilkinson, F. Leiss and E. A. Nigg (2005). "Rootletin forms centriole-associated filaments and functions in centrosome cohesion." J Cell Biol **171**(1): 27-33.

Barr, F. A. (2008). "Cilia--the masterplan." J Cell Sci **121**(Pt 1): 5-6.

Barr, F. A., H. H. Sillje and E. A. Nigg (2004). "Polo-like kinases and the orchestration of cell division." Nat Rev Mol Cell Biol **5**(6): 429-40.

Basto, R., K. Brunk, T. Vinadogrova, N. Peel, A. Franz, A. Khodjakov and J. W. Raff (2008). "Centrosome amplification can initiate tumorigenesis in flies." Cell **133**(6): 1032-42.

Beales, P. L., E. Bland, J. L. Tobin, C. Bacchelli, B. Tuysuz, J. Hill, S. Rix, C. G. Pearson, M. Kai, J. Hartley, C. Johnson, M. Irving, N. Elcioglu, M. Winey, M. Tada and P. J. Scambler (2007). "IFT80, which encodes a conserved intraflagellar transport protein, is mutated in Jeune asphyxiating thoracic dystrophy." Nat Genet **39**(6): 727-9.

Berman, S. A., N. F. Wilson, N. A. Haas and P. A. Lefebvre (2003). "A novel MAP kinase regulates flagellar length in Chlamydomonas." Curr Biol **13**(13): 1145-9.

Bettencourt-Dias, M. and D. M. Glover (2007). "Centrosome biogenesis and function: centrosomics brings new understanding." Nat Rev Mol Cell Biol **8**(6): 451-63.

Bettencourt-Dias, M., A. Rodrigues-Martins, L. Carpenter, M. Riparbelli, L. Lehmann, M. K. Gatt, N. Carmo, F. Balloux, G. Callaini and D. M. Glover (2005). "SAK/PLK4 is required for centriole duplication and flagella development." Curr Biol **15**(24): 2199-207.

Bisgrove, B. W. and H. J. Yost (2006). "The roles of cilia in developmental disorders and disease." Development **133**(21): 4131-43.

Bobinnec, Y., A. Khodjakov, L. M. Mir, C. L. Rieder, B. Edde and M. Bornens (1998). "Centriole disassembly in vivo and its effect on centrosome structure and function in vertebrate cells." J Cell Biol **143**(6): 1575-89.

Bobinnec, Y., M. Moudjou, J. P. Fouquet, E. Desbruyeres, B. Edde and M. Bornens (1998). "Glutamylation of centriole and cytoplasmic tubulin in proliferating non-neuronal cells." Cell Motil Cytoskeleton **39**(3): 223-32.

Bouckson-Castaing, V., M. Moudjou, D. J. Ferguson, S. Mucklow, Y. Belkaid, G. Milon and P. R. Crocker (1996). "Molecular characterisation of ninein, a new coiled-coil protein of the centrosome." J Cell Sci **109 (Pt 1)**: 179-90.

Brazelton, W. J., C. D. Amundsen, C. D. Silflow and P. A. Lefebvre (2001). "The bld1 mutation identifies the Chlamydomonas osm-6 homolog as a gene required for flagellar assembly." Curr Biol **11**(20): 1591-4.

Carroll, P. E., M. Okuda, H. F. Horn, P. Biddinger, P. J. Stambrook, L. L. Gleich, Y. Q. Li, P. Tarapore and K. Fukasawa (1999). "Centrosome hyperamplification in human cancer: chromosome instability induced by p53 mutation and/or Mdm2 overexpression." Oncogene **18**(11): 1935-44.

Casenghi, M., P. Meraldi, U. Weinhart, P. I. Duncan, R. Korner and E. A. Nigg (2003). "Polo-like kinase 1 regulates Nlp, a centrosome protein involved in microtubule nucleation." Dev Cell **5**(1): 113-25.

Chang, P., T. H. Giddings, Jr., M. Winey and T. Stearns (2003). "Epsilon-tubulin is required for centriole duplication and microtubule organization." Nat Cell Biol **5**(1): 71-6.

Chang, P. and T. Stearns (2000). "Delta-tubulin and epsilon-tubulin: two new human centrosomal tubulins reveal new aspects of centrosome structure and function." Nat Cell Biol **2**(1): 30-5.

Cole, D. G. (2003). "The intraflagellar transport machinery of Chlamydomonas reinhardtii." Traffic **4**(7): 435-42.

Cole, D. G., D. R. Diener, A. L. Himelblau, P. L. Beech, J. C. Fuster and J. L. Rosenbaum (1998). "Chlamydomonas kinesin-II-dependent intraflagellar transport (IFT): IFT particles contain proteins required for ciliary assembly in Caenorhabditis elegans sensory neurons." J Cell Biol **141**(4): 993-1008.

Corbit, K. C., P. Aanstad, V. Singla, A. R. Norman, D. Y. Stainier and J. F. Reiter (2005). "Vertebrate Smoothened functions at the primary cilium." Nature **437**(7061): 1018-21.

Corbit, K. C., A. E. Shyer, W. E. Dowdle, J. Gaulden, V. Singla, M. H. Chen, P. T. Chuang and J. F. Reiter (2008). "Kif3a constrains beta-catenin-dependent Wnt signalling through dual ciliary and non-ciliary mechanisms." Nat Cell Biol **10**(1): 70-6.

Dammermann, A., A. Desai and K. Oegema (2003). "The minus end in sight." Curr Biol **13**(15): R614-24.

Dammermann, A. and A. Merdes (2002). "Assembly of centrosomal proteins and microtubule organization depends on PCM-1." J Cell Biol **159**(2): 255-66.

Dammermann, A., T. Muller-Reichert, L. Pelletier, B. Habermann, A. Desai and K. Oegema (2004). "Centriole assembly requires both centriolar and pericentriolar material proteins." Dev Cell **7**(6): 815-29.

Delgehyr, N., J. Sillibourne and M. Bornens (2005). "Microtubule nucleation and anchoring at the centrosome are independent processes linked by ninein function." J Cell Sci **118**(Pt 8): 1565-75.

Dictenberg, J. B., W. Zimmerman, C. A. Sparks, A. Young, C. Vidair, Y. Zheng, W. Carrington, F. S. Fay and S. J. Doxsey (1998). "Pericentrin and gamma-tubulin form a protein complex and are organized into a novel lattice at the centrosome." J Cell Biol **141**(1): 163-74.

Doxsey, S. (2001). "Re-evaluating centrosome function." Nat Rev Mol Cell Biol **2**(9): 688-98.

Doxsey, S. J., P. Stein, L. Evans, P. D. Calarco and M. Kirschner (1994). "Pericentrin, a highly conserved centrosome protein involved in microtubule organization." Cell **76**(4): 639-50.

Eggenschwiler, J. T. and K. V. Anderson (2007). "Cilia and developmental signaling." Annu Rev Cell Dev Biol **23**: 345-73.

Epstein, E. H. (2008). "Basal cell carcinomas: attack of the hedgehog." Nat Rev Cancer **8**(10): 743-54.

Fliegauf, M., T. Benzing and H. Omran (2007). "When cilia go bad: cilia defects and ciliopathies." Nat Rev Mol Cell Biol **8**(11): 880-93.

Follit, J. A., R. A. Tuft, K. E. Fogarty and G. J. Pazour (2006). "The intraflagellar transport protein IFT20 is associated with the Golgi complex and is required for cilia assembly." Mol Biol Cell **17**(9): 3781-92.

Fry, A. M., T. Mayor, P. Meraldi, Y. D. Stierhof, K. Tanaka and E. A. Nigg (1998). "C-Nap1, a novel centrosomal coiled-coil protein and candidate substrate of the cell cycle-regulated protein kinase Nek2." J Cell Biol **141**(7): 1563-74.

Galiegue, S., O. Jbilo, T. Combes, E. Bribes, P. Carayon, G. Le Fur and P. Casellas (1999). "Cloning and characterization of PRAX-1. A new protein that specifically interacts with the peripheral benzodiazepine receptor." J Biol Chem **274**(5): 2938-52.

Giet, R., D. McLean, S. Descamps, M. J. Lee, J. W. Raff, C. Prigent and D. M. Glover (2002). "Drosophila Aurora A kinase is required to localize D-TACC to centrosomes and to regulate astral microtubules." J Cell Biol **156**(3): 437-51.

Gorgidze, L. A. and I. A. Vorobjev (1995). "Centrosome and microtubules behavior in the cytoplasts." J Submicrosc Cytol Pathol **27**(3): 381-9.

Graser, S., Y. D. Stierhof, S. B. Lavoie, O. S. Gassner, S. Lamla, M. Le Clech and E. A. Nigg (2007). "Cep164, a novel centriole appendage protein required for primary cilium formation." J Cell Biol **179**(2): 321-30.

Graser, S., Y. D. Stierhof and E. A. Nigg (2007). "Cep68 and Cep215 (Cdk5rap2) are required for centrosome cohesion." J Cell Sci **120**(Pt 24): 4321-31.

Gromley, A., A. Jurczyk, J. Sillibourne, E. Halilovic, M. Mogensen, I. Groisman, M. Blomberg and S. Doxsey (2003). "A novel human protein of the maternal centriole is required for the final stages of cytokinesis and entry into S phase." J Cell Biol **161**(3): 535-45.

Guarguaglini, G., P. I. Duncan, Y. D. Stierhof, T. Holmstrom, S. Duensing and E. A. Nigg (2005). "The forkhead-associated domain protein Cep170 interacts with Polo-like kinase 1 and serves as a marker for mature centrioles." Mol Biol Cell **16**(3): 1095-107.

Gunawardane, R. N., O. C. Martin, K. Cao, L. Zhang, K. Dej, A. Iwamatsu and Y. Zheng (2000). "Characterization and reconstitution of Drosophila gamma-tubulin ring complex subunits." J Cell Biol **151**(7): 1513-24.

Habedanck, R., Y. D. Stierhof, C. J. Wilkinson and E. A. Nigg (2005). "The Polo kinase Plk4 functions in centriole duplication." Nat Cell Biol **7**(11): 1140-6.

Hannak, E., M. Kirkham, A. A. Hyman and K. Oegema (2001). "Aurora-A kinase is required for centrosome maturation in Caenorhabditis elegans." J Cell Biol **155**(7): 1109-16.

Haycraft, C. J., B. Banizs, Y. Aydin-Son, Q. Zhang, E. J. Michaud and B. K. Yoder (2005). "Gli2 and Gli3 localize to cilia and require the intraflagellar transport protein polaris for processing and function." PLoS Genet **1**(4): e53.

Huangfu, D. and K. V. Anderson (2005). "Cilia and Hedgehog responsiveness in the mouse." Proc Natl Acad Sci U S A **102**(32): 11325-30.

Huangfu, D., A. Liu, A. S. Rakeman, N. S. Murcia, L. Niswander and K. V. Anderson (2003). "Hedgehog signalling in the mouse requires intraflagellar transport proteins." Nature **426**(6962): 83-7.

Ishikawa, H., A. Kubo, S. Tsukita and S. Tsukita (2005). "Odf2-deficient mother centrioles lack distal/subdistal appendages and the ability to generate primary cilia." Nat Cell Biol **7**(5): 517-24.

Job, D., O. Valiron and B. Oakley (2003). "Microtubule nucleation." Curr Opin Cell Biol **15**(1): 111-7.

Kleylein-Sohn, J., J. Westendorf, M. Le Clech, R. Habedanck, Y. D. Stierhof and E. A. Nigg (2007). "Plk4-induced centriole biogenesis in human cells." Dev Cell **13**(2): 190-202.

Kovacs, J. J., E. J. Whalen, R. Liu, K. Xiao, J. Kim, M. Chen, J. Wang, W. Chen and R. J. Lefkowitz (2008). "Beta-arrestin-mediated localization of smoothened to the primary cilium." Science **320**(5884): 1777-81.

Kozminski, K. G., K. A. Johnson, P. Forscher and J. L. Rosenbaum (1993). "A motility in the eukaryotic flagellum unrelated to flagellar beating." Proc Natl Acad Sci U S A **90**(12): 5519-23.

Kufer, T. A., H. H. Sillje, R. Korner, O. J. Gruss, P. Meraldi and E. A. Nigg (2002). "Human TPX2 is required for targeting Aurora-A kinase to the spindle." J Cell Biol **158**(4): 617-23.

Lane, H. A. and E. A. Nigg (1996). "Antibody microinjection reveals an essential role for human polo-like kinase 1 (Plk1) in the functional maturation of mitotic centrosomes." J Cell Biol **135**(6 Pt 2): 1701-13.

Lange, B. M. and K. Gull (1995). "A molecular marker for centriole maturation in the mammalian cell cycle." J Cell Biol **130**(4): 919-27.

Leidel, S. and P. Gonczy (2003). "SAS-4 is essential for centrosome duplication in C elegans and is recruited to daughter centrioles once per cell cycle." Dev Cell **4**(3): 431-9.

Leidel, S. and P. Gonczy (2005). "Centrosome duplication and nematodes: recent insights from an old relationship." Dev Cell **9**(3): 317-25.

Liu, A., B. Wang and L. A. Niswander (2005). "Mouse intraflagellar transport proteins regulate both the activator and repressor functions of Gli transcription factors." Development **132**(13): 3103-11.

Low, S. H., S. Vasanth, C. H. Larson, S. Mukherjee, N. Sharma, M. T. Kinter, M. E. Kane, T. Obara and T. Weimbs (2006). "Polycystin-1, STAT6, and P100 function in a pathway that transduces ciliary mechanosensation and is activated in polycystic kidney disease." Dev Cell **10**(1): 57-69.

Lucker, B. F., R. H. Behal, H. Qin, L. C. Siron, W. D. Taggart, J. L. Rosenbaum and D. G. Cole (2005). "Characterization of the intraflagellar transport complex B core: direct interaction of the IFT81 and IFT74/72 subunits." J Biol Chem **280**(30): 27688-96.

Luders, J. and T. Stearns (2007). "Microtubule-organizing centres: a re-evaluation." Nat Rev Mol Cell Biol **8**(2): 161-7.

Marshall, W. F. (2008). "The cell biological basis of ciliary disease." J Cell Biol **180**(1): 17-21.

Mayor, T., U. Hacker, Y. D. Stierhof and E. A. Nigg (2002). "The mechanism regulating the dissociation of the centrosomal protein C-Nap1 from mitotic spindle poles." J Cell Sci **115**(Pt 16): 3275-84.

Meraldi, P., J. Lukas, A. M. Fry, J. Bartek and E. A. Nigg (1999). "Centrosome duplication in mammalian somatic cells requires E2F and Cdk2-cyclin A." Nat Cell Biol **1**(2): 88-93.

Meraldi, P. and E. A. Nigg (2002). "The centrosome cycle." FEBS Lett **521**(1-3): 9-13.

Mogensen, M. M., A. Malik, M. Piel, V. Bouckson-Castaing and M. Bornens (2000). "Microtubule minus-end anchorage at centrosomal and non-centrosomal sites: the role of ninein." J Cell Sci **113 (Pt 17)**: 3013-23.

Montcouquiol, M., E. B. Crenshaw, 3rd and M. W. Kelley (2006). "Noncanonical Wnt signaling and neural polarity." Annu Rev Neurosci **29**: 363-86.

Moon, R. T., A. D. Kohn, G. V. De Ferrari and A. Kaykas (2004). "WNT and beta-catenin signalling: diseases and therapies." Nat Rev Genet **5**(9): 691-701.

Moritz, M., M. B. Braunfeld, V. Guenebaut, J. Heuser and D. A. Agard (2000). "Structure of the gamma-tubulin ring complex: a template for microtubule nucleation." Nat Cell Biol **2**(6): 365-70.

Moritz, M., M. B. Braunfeld, J. W. Sedat, B. Alberts and D. A. Agard (1995). "Microtubule nucleation by gamma-tubulin-containing rings in the centrosome." Nature **378**(6557): 638-40.

Moss, D. K., G. Bellett, J. M. Carter, M. Liovic, J. Keynton, A. R. Prescott, E. B. Lane and M. M. Mogensen (2007). "Ninein is released from the centrosome and moves bi-directionally along microtubules." J Cell Sci **120**(Pt 17): 3064-74.

Nachury, M. V., A. V. Loktev, Q. Zhang, C. J. Westlake, J. Peranen, A. Merdes, D. C. Slusarski, R. H. Scheller, J. F. Bazan, V. C. Sheffield and P. K. Jackson (2007). "A core complex of BBS proteins cooperates with the GTPase Rab8 to promote ciliary membrane biogenesis." Cell **129**(6): 1201-13.

Nagao, K. and M. Yanagida (2002). "Regulating sister chromatid separation by separase phosphorylation." Dev Cell **2**(1): 2-4.

Nakagawa, Y., Y. Yamane, T. Okanoue, S. Tsukita and S. Tsukita (2001). "Outer dense fiber 2 is a widespread centrosome scaffold component preferentially associated with mother centrioles: its identification from isolated centrosomes." Mol Biol Cell **12**(6): 1687-97.

Nasmyth, K. (2002). "Segregating sister genomes: the molecular biology of chromosome separation." Science **297**(5581): 559-65.

Nauli, S. M., F. J. Alenghat, Y. Luo, E. Williams, P. Vassilev, X. Li, A. E. Elia, W. Lu, E. M. Brown, S. J. Quinn, D. E. Ingber and J. Zhou (2003). "Polycystins 1 and 2 mediate mechanosensation in the primary cilium of kidney cells." Nat Genet **33**(2): 129-37.

Neef, R., U. Gruneberg, R. Kopajtich, X. Li, E. A. Nigg, H. Sillje and F. A. Barr (2007). "Choice of Plk1 docking partners during mitosis and cytokinesis is controlled by the activation state of Cdk1." Nat Cell Biol **9**(4): 436-44.

Nigg, E. A. (2002). "Centrosome aberrations: cause or consequence of cancer progression?" Nat Rev Cancer **2**(11): 815-25.

Nigg, E. A. (2007). "Centrosome duplication: of rules and licenses." Trends Cell Biol **17**(5): 215-21.

Oegema, K., C. Wiese, O. C. Martin, R. A. Milligan, A. Iwamatsu, T. J. Mitchison and Y. Zheng (1999). "Characterization of two related Drosophila gamma-tubulin complexes that differ in their ability to nucleate microtubules." J Cell Biol **144**(4): 721-33.

Ou, Y. Y., G. J. Mack, M. Zhang and J. B. Rattner (2002). "CEP110 and ninein are located in a specific domain of the centrosome associated with centrosome maturation." J Cell Sci **115**(Pt 9): 1825-35.

Palazzo, R. E., J. M. Vogel, B. J. Schnackenberg, D. R. Hull and X. Wu (2000). "Centrosome maturation." Curr Top Dev Biol **49**: 449-70.

Pan, J., Q. Wang and W. J. Snell (2004). "An aurora kinase is essential for flagellar disassembly in Chlamydomonas." Dev Cell **6**(3): 445-51.

Pazour, G. J., B. L. Dickert, Y. Vucica, E. S. Seeley, J. L. Rosenbaum, G. B. Witman and D. G. Cole (2000). "Chlamydomonas IFT88 and its mouse homologue, polycystic kidney disease gene tg737, are required for assembly of cilia and flagella." J Cell Biol **151**(3): 709-18.

Pazour, G. J. and G. B. Witman (2003). "The vertebrate primary cilium is a sensory organelle." Curr Opin Cell Biol **15**(1): 105-10.

Pedersen, L. B., S. Geimer, R. D. Sloboda and J. L. Rosenbaum (2003). "The Microtubule plus end-tracking protein EB1 is localized to the flagellar tip and basal bodies in Chlamydomonas reinhardtii." Curr Biol **13**(22): 1969-74.

Pedersen, L. B., M. S. Miller, S. Geimer, J. M. Leitch, J. L. Rosenbaum and D. G. Cole (2005). "Chlamydomonas IFT172 is encoded by FLA11, interacts with CrEB1, and regulates IFT at the flagellar tip." Curr Biol **15**(3): 262-6.

Pelletier, L., E. O'Toole, A. Schwager, A. A. Hyman and T. Muller-Reichert (2006). "Centriole assembly in Caenorhabditis elegans." Nature **444**(7119): 619-23.

Piperno, G., M. LeDizet and X. J. Chang (1987). "Microtubules containing acetylated alpha-tubulin in mammalian cells in culture." J Cell Biol **104**(2): 289-302.

Piperno, G., E. Siuda, S. Henderson, M. Segil, H. Vaananen and M. Sassaroli (1998). "Distinct mutants of retrograde intraflagellar transport (IFT) share similar morphological and molecular defects." J Cell Biol **143**(6): 1591-601.

Poole, C. A., C. G. Jensen, J. A. Snyder, C. G. Gray, V. L. Hermanutz and D. N. Wheatley (1997). "Confocal analysis of primary cilia structure and colocalization with the Golgi apparatus in chondrocytes and aortic smooth muscle cells." Cell Biol Int **21**(8): 483-94.

Praetorius, H. A., J. Frokiaer, S. Nielsen and K. R. Spring (2003). "Bending the primary cilium opens Ca2+-sensitive intermediate-conductance K+ channels in MDCK cells." J Membr Biol **191**(3): 193-200.

Praetorius, H. A. and K. R. Spring (2001). "Bending the MDCK cell primary cilium increases intracellular calcium." J Membr Biol **184**(1): 71-9.

Praetorius, H. A. and K. R. Spring (2003). "Removal of the MDCK cell primary cilium abolishes flow sensing." J Membr Biol **191**(1): 69-76.

Pugacheva, E. N., S. A. Jablonski, T. R. Hartman, E. P. Henske and E. A. Golemis (2007). "HEF1-dependent Aurora A activation induces disassembly of the primary cilium." Cell **129**(7): 1351-63.

Qin, H., D. R. Diener, S. Geimer, D. G. Cole and J. L. Rosenbaum (2004). "Intraflagellar transport (IFT) cargo: IFT transports flagellar precursors to the tip and turnover products to the cell body." J Cell Biol **164**(2): 255-66.

Qin, H., Z. Wang, D. Diener and J. Rosenbaum (2007). "Intraflagellar transport protein 27 is a small G protein involved in cell-cycle control." Curr Biol **17**(3): 193-202.

Quarmby, L. M. and J. D. Parker (2005). "Cilia and the cell cycle?" J Cell Biol **169**(5): 707-10.

Raynaud-Messina, B. and A. Merdes (2007). "Gamma-tubulin complexes and microtubule organization." Curr Opin Cell Biol **19**(1): 24-30.

Rohatgi, R., L. Milenkovic and M. P. Scott (2007). "Patched1 regulates hedgehog signaling at the primary cilium." Science **317**(5836): 372-6.

Rosenbaum, J. L. and G. B. Witman (2002). "Intraflagellar transport." Nat Rev Mol Cell Biol **3**(11): 813-25.

Salisbury, J. L., K. M. Suino, R. Busby and M. Springett (2002). "Centrin-2 is required for centriole duplication in mammalian cells." Curr Biol **12**(15): 1287-92.

Schneider, L., C. A. Clement, S. C. Teilmann, G. J. Pazour, E. K. Hoffmann, P. Satir and S. T. Christensen (2005). "PDGFRalphaalpha signaling is regulated through the primary cilium in fibroblasts." Curr Biol **15**(20): 1861-6.

Scholey, J. M. (2008). "Intraflagellar transport motors in cilia: moving along the cell's antenna." J Cell Biol **180**(1): 23-9.

Signor, D., K. P. Wedaman, L. S. Rose and J. M. Scholey (1999). "Two heteromeric kinesin complexes in chemosensory neurons and sensory cilia of Caenorhabditis elegans." Mol Biol Cell **10**(2): 345-60.

Simons, M., J. Gloy, A. Ganner, A. Bullerkotte, M. Bashkurov, C. Kronig, B. Schermer, T. Benzing, O. A. Cabello, A. Jenny, M. Mlodzik, B. Polok, W. Driever, T. Obara and G. Walz (2005). "Inversin, the gene product mutated in nephronophthisis type II, functions as a molecular switch between Wnt signaling pathways." Nat Genet **37**(5): 537-43.

Singla, V. and J. F. Reiter (2006). "The primary cilium as the cell's antenna: signaling at a sensory organelle." Science **313**(5787): 629-33.

Snell, W. J., J. Pan and Q. Wang (2004). "Cilia and flagella revealed: from flagellar assembly in Chlamydomonas to human obesity disorders." Cell **117**(6): 693-7.

Stolc, V., M. P. Samanta, W. Tongprasit and W. F. Marshall (2005). "Genome-wide transcriptional analysis of flagellar regeneration in Chlamydomonas reinhardtii identifies orthologs of ciliary disease genes." Proc Natl Acad Sci U S A **102**(10): 3703-7.

Sun, Z., A. Amsterdam, G. J. Pazour, D. G. Cole, M. S. Miller and N. Hopkins (2004). "A genetic screen in zebrafish identifies cilia genes as a principal cause of cystic kidney." Development **131**(16): 4085-93.

Takahashi, M., A. Yamagiwa, T. Nishimura, H. Mukai and Y. Ono (2002). "Centrosomal proteins CG-NAP and kendrin provide microtubule nucleation sites by anchoring gamma-tubulin ring complex." Mol Biol Cell **13**(9): 3235-45.

Tam, L. W., N. F. Wilson and P. A. Lefebvre (2007). "A CDK-related kinase regulates the length and assembly of flagella in Chlamydomonas." J Cell Biol **176**(6): 819-29.

Terada, Y., Y. Uetake and R. Kuriyama (2003). "Interaction of Aurora-A and centrosomin at the microtubule-nucleating site in Drosophila and mammalian cells." J Cell Biol **162**(5): 757-63.

Torres-Rosell, J., F. Machin and L. Aragon (2005). "Cdc14 and the temporal coordination between mitotic exit and chromosome segregation." Cell Cycle **4**(1): 109-12.

Tran, P. V., C. J. Haycraft, T. Y. Besschetnova, A. Turbe-Doan, R. W. Stottmann, B. J. Herron, A. L. Chesebro, H. Qiu, P. J. Scherz, J. V. Shah, B. K. Yoder and D. R. Beier (2008). "THM1 negatively modulates mouse sonic hedgehog signal transduction and affects retrograde intraflagellar transport in cilia." Nat Genet **40**(4): 403-10.

Tsang, W. Y., C. Bossard, H. Khanna, J. Peranen, A. Swaroop, V. Malhotra and B. D. Dynlacht (2008). "CP110 suppresses primary cilia formation through its interaction with CEP290, a protein deficient in human ciliary disease." Dev Cell **15**(2): 187-97.

Tsang, W. Y. and B. D. Dynlacht (2008). "sSgo1, a guardian of centriole cohesion." Dev Cell **14**(3): 320-2.

Tsou, M. F. and T. Stearns (2006). "Controlling centrosome number: licenses and blocks." Curr Opin Cell Biol **18**(1): 74-8.

Tsou, M. F. and T. Stearns (2006). "Mechanism limiting centrosome duplication to once per cell cycle." Nature **442**(7105): 947-51.

Varmark, H. (2004). "Functional role of centrosomes in spindle assembly and organization." J Cell Biochem **91**(5): 904-14.

Verollet, C., N. Colombie, T. Daubon, H. M. Bourbon, M. Wright and B. Raynaud-Messina (2006). "Drosophila melanogaster gamma-TuRC is dispensable for targeting gamma-tubulin to the centrosome and microtubule nucleation." J Cell Biol **172**(4): 517-28.

Wang, X., Y. Yang, Q. Duan, N. Jiang, Y. Huang, Z. Darzynkiewicz and W. Dai (2008). "sSgo1, a major splice variant of Sgo1, functions in centriole cohesion where it is regulated by Plk1." Dev Cell **14**(3): 331-41.

Wheatley, D. N. (1971). "Cilia in cell-cultured fibroblasts. 3. Relationship between mitotic activity and cilium frequency in mouse 3T6 fibroblasts." J Anat **110**(Pt 3): 367-82.

Wiese, C. and Y. Zheng (2006). "Microtubule nucleation: gamma-tubulin and beyond." J Cell Sci **119**(Pt 20): 4143-53.

Yan, X., R. Habedanck and E. A. Nigg (2006). "A complex of two centrosomal proteins, CAP350 and FOP, cooperates with EB1 in microtubule anchoring." Mol Biol Cell **17**(2): 634-44.

Yoshimura, S., J. Egerer, E. Fuchs, A. K. Haas and F. A. Barr (2007). "Functional dissection of Rab GTPases involved in primary cilium formation." J Cell Biol **178**(3): 363-9.

Zheng, Y., M. K. Jung and B. R. Oakley (1991). "Gamma-tubulin is present in Drosophila melanogaster and Homo sapiens and is associated with the centrosome." Cell **65**(5): 817-23.

Curriculum Vitae

Stefan Lamla; Date and place of birth: 19th January 1980, Ulm, Germany

Education

11/04-10/08	**PhD thesis** in the Department of Cell Biology at the Max-Planck Institute (MPI) of Biochemistry in Munich. Title: “Functional Characterisation of the Centrosomal Protein Cep170”. Supervisor: Prof. Erich Nigg
10/03-07/04	**Diploma thesis** in the Department of Retrovirology at the Institute of Virology and Immunobiology, University of Würzburg. Title: Role of the Proinflammatory Signal Activity of the Apoptotic Receptors on the Reactivation of HIV in Latently Infected T-cells”. Supervisor Prof. Axel Rethwilm
04/02-09/03	**Study of biology** at the Julius-Maximilians-University of Würzburg, with major in biochemistry, developmental and cell biology, genetics, immunology and virology
10/99-03/02	**Study of biology** at the University of Konstanz
07/99	**High school** degree at the Werkgymnasium in Heidenheim